CELLULAR MECHANISMS UNDERLYING THE CARDIOVASCULAR TOXICITY OF THE HIGHLY ACTIVE ANTI-RETROVIRAL THERAPY ATRIPLA: EFAVIRENZ, EMTRICITABINE AND TENOFOVIR

MARY FALTZ

PhD 2013

Abstract

Highly active anti-retroviral therapy (HAART) has proved very successful in reducing the morbidity and mortality associated with HIV infection. This same lifespan prolongation, however, has also revealed many side effects linked to HAART, including cardiovascular disease. A once daily fixed dose drug combination pill Atripla was hoped to improve compliance and adherence. The HAART components of Atripla efavirenz, emtricitabine and tenofovir are considered to be significantly safer than the conventional reverse transcriptase inhibitors but cardiovascular effects of these drugs have yet to be investigated *in vitro*. The overall objective of this thesis was to examine the effects of the three components of Atripla on cardiovascular cell function.

This project utilised *ex vivo* rat aortic rings and both a cardiac myocyte (H9c2) and endothelial (EA.hy926) cell line for *in vitro* work. Endothelial cell function was assessed by acetylcholine-induced nitric oxide dependent relaxation of aortic smooth muscle. Mitochondrial function was used as a measure of cardiovascular cell viability while morphological techniques were used to determine levels of apoptosis and necrosis. Activation of poly (ADP-ribose) polymerase (PARP) was assessed directly by protein ribosylation or indirectly using a pharmacological inhibitor. The role of endoplasmic reticulum (ER) stress was determined by Western blotting for the protein marker, CHOP.

Efavirenz was the only component of Atripla to cause loss of endothelial cell function, viability and ultimately inducing apoptosis and necrosis via overactivation of PARP. Endothelial function was preserved in female rat endothelial cells following efavirenz-exposure and protection observed with oestrogen in male rat endothelial cells exposed to efavirenz via reduced PARP activity. Similar loss of cell viability and increased cell apoptosis and necrosis was observed in the cardiac cell line following efavirenz exposure, mediated not only by PARP but also by ER stress. Rosiglitazone was shown to protect against the efavirenz-mediated loss of cell viability and cell death in both endothelial and cardiac cells; also protecting endothelial cell function from efavirenz-induced damage. Rosiglitazone was able to attenuate the increase in PARP activation in both endothelial and cardiac cells; however, endothelial cell protection appears to be mediated through PPAR-γ and AMPK activation while in cardiac cells the protection seems to be PPAR-γ-dependent and AMPK-independent.

In conclusion, though the newer HAART drugs may have fewer side effects, cardiovascular complications mediated by efavirenz cannot be ruled out in patients taking Atripla. In the present study, efavirenz-mediated PARP overactivation has been identified as the central mediator of endothelial cell dysfunction, loss of cell viability and increased cell death. Oestrogen-mediated inhibition of PARP may account for the reduced endothelial cell damage observed in efavirenz-exposed aorta from female rats, and explain the reduced cardiovascular side effects of HAART observed in female HIV patients. PARP activation was also found to mediate efavirenz-induced loss of cardiac cell viability and increased cell death, however, alongside PARP activation ER stress was also induced following efavirenz exposure in cardiac cells. Induction of ER stress by HAART drugs in cardiovascular cells suggests a new mechanism by which these drugs increase the risk of cardiovascular complications and disease. Rosiglitazone protects against the efavirenz-mediated cardiovascular cell damage through inhibition of PARP activity and induction of ER stress though the protection appears to be mediated through separate 2nd messenger systems depending on the cell type. The importance of PARP and ER stress in anti-retroviral drug-induced cardiovascular side effects needs further elucidation but may represent a possible screening mechanism for these drug types to identify potential cardiovascular toxicity.

Abbreviations

ACh	acetylcholine
AD	Alzheimer’s disease
AIDS	Acquired immunodeficiency syndrome
AIF	apoptosis inducing factor
AMPK	adenosine monophosphate kinase
AP-1	activator protein 1
ASK-1	apoptosis signal-regulating kinase 1
ATF-4	activating transcription factor 4
ATP	adenosine triphosphate
AZT	zidovudine
BBB	blood brain barrier
CCL-2	chemokine (C-C motif) ligand 2
CCR5	C-C chemokine receptor type 5
CHOP	CEBP homologous protein
cGMP	cyclic guanosine monophosphate
cNOS	constitutive nitric oxide synthase
COX-2	cyclooxygenase 2
CXCR4	C-X-C chemokine receptor type 4
DAG	diacylglycerol
DCF	dichlorofluorescin
ddC	zalcitabine
d4T	stavudine
DMEM	Dulbecco's Modified Eagle Medium
DMSO	dimethyl sulfoxide

ECACC	European collection of cell cultures
ED	endothelial dysfunction
EDRF	endothelium-derived relaxing factor
EDTA	ethylenediaminetetraacetic acid
ELISA	enzyme-linked immunosorbent assay
EMA	European medicines agency
eNOS	endothelial nitric oxide synthase
EPC	endothelial progenitor cells
ER	endoplasmic reticulum
ERK	extracellular signal-regulated kinase
FDA	Food and drug administration
FCS	fetal calf serum
gp120	glycoprotein 120
gp41	glycoprotein 41
GTP	guanosine triphosphate
HAART	highly active anti-retroviral therapy
HAD	HIV-associated dementia
HDL	high-density lipoprotein
HGF	hepatocyte growth factor
HIV	human immunodeficiency virus
HPI	Hoechst / propidium iodide
HRT	hormone replacement therapy
HUVEC	human umbilical vein endothelial cells
ICAM	intercellular adhesion molecule

Iκβα	nuclear factor of kappa light polypeptide gene enhancer in B-cells inhibitor, alpha
IL-1	interleukin-1
IL-6	interleukin-6
IL-8	interleukin-8
iNOS	inducible nitric oxide synthase
IR-β	insulin receptor beta
IRS-1	insulin receptor substrate 1
JAM	junctional adhesion molecule
JNK	jun N-terminal kinase
LDL	low-density lipoprotein
LPS	lipopolysaccharide
MAPK	mitogen activated protein kinase
MDA	malondialdehyde
MEC	mouse endothelial cells
MEF	mouse embryonic fibroblasts
MI	myocardial infarction
MKP-1	MAPK phosphatase 1
NADPH	nicotinamide adenine dinucleotide phosphate
NAD+	nicotinamide adenine dinucleotide
NBT	nitro blue tetrazolium
NEAA	non-essential amino acids

NF-κB	nuclear factor kappa-light-chain-enhancer of activated B cells
Nrf2	NFE2-related factor 2
NRTI	nucleoside reverse transcriptase inhibitor
NtRTI	nucleotide reverse transcriptase inhibitor
NNRTI	non-nucleoside transcriptase inhibitor
NO	nitric oxide
NOS	nitric oxide synthase
p38 MAPK	p38 mitogen-activated protein kinase
PAI-1	plasminogen activator inhibitor-1
PARG	poly (ADP-ribose) glycohydrolase
PARP	poly (ADP-ribose) polymerse
PBS	phosphate buffered saline
PERK	PKR-like endoplasmic reticulum kinase
PI	protease inhibitor
PI3K	phosphatidylinositol 3' - kinase
PKC	protein kinase C
PMSF	phenylmethylsulfonyl fluoride
PPAR-α	peroxisome proliferator-activated receptor alpha
PPAR-γ	peroxisome proliferator-activated receptor gamma

RNS	reactive nitrogen species
RXR	retinoid X receptor
ROS	reactive oxygen species
SDS	sodium dodecyl sulphate
SEM	standard error mean
SOD	superoxide dismutase
TBA	2-Thiobarbituric acid
TBARS	thiobarbituric acid reactive substances
TBS	tris-buffered saline
TCA	trichloroacetic acid
TEMED	tetramethylethylenediamine
TLR-4	toll-like receptor 4
TNF-α	tumour necrosis factor-alpha
UPR	uncoupled protein response
VCAM	vascular cell adhesion molecule
VSV-G	vesicular stomatitis virus-G
ZO	zonula occludens

Table of Contents

Author’s Declaration

I declare that the research contained in this thesis, unless otherwise formally indicated within the text, is the original work of the author. The thesis has not been previously submitted to this or any other university for a degree, and does not incorporate any material already submitted for a degree.

Signed

Dated

Dedication

This thesis is dedicated to Frank, Quentin and Baby Faltz.

List of tables

List of figures

Figure 6.2: Effect of rosiglitazone on efavirenz-mediated loss of cell viability in bend.3 cells after 24 and 48 hours

Figure 6.3: Effect of PPAR-γ antagonist GW9662 on rosiglitazone-mediated protection against efavirenz-induced loss of bEnd.3 cell viability after 24 hours

Acknowledgements

I would like to express my gratitude to my supervisory team including Dr. Jon Mabley and Dr. Charley Chatterjee for their support, encouragement and guidance throughout the realisation of the present project. I also want to thank the whole of the Pharmacology lab in Huxley for welcoming me and making the lab ambience very enjoyable to work in during the past few years. Also, thanks to Dr Pacher for his support.

A special thanks goes to my funding body in Luxembourg, the Fonds national de la recherche, which allowed me to carry out the present study and especially my point of contact, Mrs. Susana Pinto for her efforts throughout the project.

Finally, I would like to acknowledge my husband Frank for everything he has gone through with me in the past years, I wouldn't have been able to complete without him and my little Quentin. A big thanks to my lovely friend Hild Bergin for always being there for me.

Chapter 1

General Introduction

1.1 HIV/AIDS

1.1.1 Statistics

2011 marks the 30th Anniversary of the first occurrence of the deadliest pandemic in recorded recent human history. According to UNAIDS, the joint United Nations Programme on HIV/AIDS, by the end of 2009, the worldwide estimates of HIV infection were nearly 34 million with 3 million new cases diagnosed annually (UNAIDS global report 2010).

It is believed that about 25 million AIDS-related deaths have already occurred since the syndrome was first described in 1981. In the UK, by the end of June 2010, it was estimated that nearly 90,000 people were HIV positive, of whom a quarter were unaware of their infection. Nearly 20,000 people have already died of AIDS in the UK (HPA report 2010).

1.1.2 History

The first cases were described in the United States in 1981, where increasing numbers of a rare pneumonia, caused by pneumocystis pneumonia and Kaposi's sarcoma were seen in homosexual men (Gottlieb, 2006; Montagnier, 2010). The patients had significant immune suppression, facilitating opportunistic infections to ensue and ultimately death to occur (Cadogan and Dalgleish, 2008). Not long after that, two separate laboratories, Montagnier's group in France and Gallo's group in the United States isolated the virus and agreed to name it HIV (Vahlne, 2009).

1.1.3 Socio-economic burden

Besides the significant human suffering, the HIV pandemic has also had an important deleterious impact on socio-economic progress in the most affected societies (Vitoria *et al.*, 2009). According to one study, the average lifetime cost of HIV care in the United States, considering various factors is $385,200, with an estimated life expectancy of 24.2 years from the time of first HIV treatment (Schackman *et al.*, 2006).

Awareness of HIV prevention is therefore crucial in reducing the number of new infections (Gupta *et al.*, 2008). Many interventions aimed at reducing the risk of transmission include antenatal HIV screening, considerably lowering the number of HIV positive newborns (Thorne and Newell, 2005). Sadly, global prevention efforts reach less than 10 % of persons at risk, when development of these efforts could possibly prevent more than half of new HIV infections expected by 2015 and save $ 24 billion in HIV care (Merson *et al.*, 2008).

1.1.4 Viral transmission

Viral transmission mainly occurs via unprotected sexual intercourse, parenterally with contaminated needles, vertically from mother to child and breastfeeding (Petroll *et al.*, 2008; Simon *et al.*, 2006). High-risk groups include homosexual men, intravenous drug users and sex workers (Lyles *et al.*, 2007).

In order to eliminate any risk of transmission, post exposure prophylaxis is in place, especially for people carrying an occupational risk such as healthcare workers (Parkin *et al.*, 2000).

1.1.5 AIDS

The term AIDS is mainly used to refer to the final stages of HIV infection, when life threatening infections including tuberculosis and/or cancers such Kaposi's sarcoma have taken over and the body's immune system is significantly weakened (Barbaro and Barbarini, 2007; Getahun *et al.*, 2010). There is currently no cure or preventive vaccine against HIV infection (Gamble and Matthews, 2010). However, with the introduction of highly active antiretroviral therapy (HAART) in 1996, morbidity and mortality associated with AIDS was dramatically reduced.

People living with HIV have improved quality of life and a similar life expectancy as the general population (Gonzalo *et al.*, 2009; Quinn, 2008). With antiretroviral research evolving rapidly, HIV is no longer a death sentence but has turned into a manageable chronic condition, despite the various obstacles such as drug toxicity and patient adherence (Burgoyne and Tan, 2008; Este and Cihlar, 2010).

1.1.6 HIV diagnosis

Because symptoms of HIV infection are non-specific, diagnosis is sometimes difficult and many patients will have been asymptomatic for a long time before presenting themselves with a compromised immune system (Daar *et al.*, 2008). Early detection of primary HIV infection is not only beneficial for the individual's wellbeing but also for the population at large, since measures can be taken to reduce the risk of spreading the virus (Vogel *et al.*, 2010). The question of treatment initiation of asymptomatic individuals remains debatable to this date (Kitahata, 2010). HIV testing can easily be done by Point-of-care testing, which enables cheap rapid initial diagnosis, which needs to be confirmed by a second test involving ELISA and western blotting (Loubiere and Moatti, 2010; Petroll *et al.*, 2008).

1.1.7 Immunological effects

HIV infects T-helper cells, which form an important component in the immune response, causing a decrease in CD4+ cells (Lane, 2010). A healthy adult will have on average a CD4+ cell count between 800 and 1200 cells/μl (Shete *et al.*, 2010). As mentioned before, there is currently a debate over when to start treatment, with current guidelines suggesting a CD4+ cell count of less than 350 cells/μl (Kitahata, 2010). HIV infection can cause immunodeficiency by three main mechanisms.

HIV can directly kill the infected CD4+ T-cells, cytotoxic CD8 lymphocytes can dispose of them or increased rates of apoptosis can also indirectly cause a drop in CD4+ cell count (Alimonti *et al.*, 2003).

1.2 HIV and cardiovascular effects

HIV positive patients seem to suffer from increased cardiovascular complications, thought to be due to a direct interaction of HIV *per se*, host factors such as smoking and antiretroviral agents (Currier, 2009).

Common cardiac complications seen in HIV positive patients include cardiomyopathy, pericarditis, myocarditis and endocarditis (Table 1.1) (Barbaro and Silva, 2009; Sudano *et al.*, 2006). The mechanism of this morbidity is not fully understood but was initially thought to involve direct infection of the cardiomyocytes by the virus (Currier and Havlir, 2009; Monsuez *et al.*, 2007). HIV also seems to be involved in the development of atherosclerosis by various mechanisms including direct action on cholesterol, infiltration of monocytes and by inducing inflammation (Malvestutto and Aberg, 2010). Further studies have shown that pro-inflammatory cytokines play an important role in the development of heart failure and cardiomyopathy. Tumour necrosis factor alpha (TNF-α), interleukin-1 (IL-1) and interleukin-6 (IL-6) seem to induce inducible nitric oxide synthase (iNOS) in cardiomyocytes through activation of p38 mitogen-activated protein kinase (p38 MAPK) and nuclear factor kappa-light-chain-enhancer of activated B cells (NF-κB) (Barbaro and Silva, 2009; Monsuez *et al.*, 2007).

Condition	Definition	Manifestation/consequence
pericarditis	inflammation of pericardium	chest pain
pericardial effusion	fluid filled pericardial cavity	impairment of heart's pumping ability
cardiac tamponade	rapidly increased effusion	shortness of breath, cough, rapid pulse, chest pain, death
myocarditis	inflammation of myocardium	chest pain, heart failure, death
dilated cardiomyopathy	enlarged portion of heart muscle	impairment of heart's pumping ability
endocarditis	inflammation of endocardium	heart murmurs and congestive heart failure
cardiac neoplasm	cardiac tumor	compromise blood flow, heart block, dysrythmias, death

Table 1.1: Table showing common HIV-linked cardiac complications

1.3 HIV and neurological effects

Blood brain barrier (BBB) disruption by the virus, rather than infection of neurons, has been shown to be an important contributor in the pathogenesis of HIV-associated neurocognitive disorders and HIV-associated dementia (HAD) (Letendre *et al.*, 2010; Lindl *et al.*, 2010). HAD includes cognitive impairment, memory and attention deficit, loss of fine motor control and behavioral symptoms such as indolence and indifference (Anand *et al.*, 2010). Structural and functional changes in the brain vasculature facilitate BBB crossing of infected monocytes and lymphocytes, leading to the progression of HAD (Valcour *et al.*, 2011). There are currently two models suggesting the mechanism of HIV neuropathogenesis.

Firstly, viral proteins released from infected monocytes may directly cause neuronal death and secondly, the inflammatory response initiated by infected and uninfected non-neuronal cells may indirectly cause neuronal death (Lindl *et al.*, 2010).

Figure 1.1: Diagram of an HIV virion

(www.niaid.nih.gov, accessed 16th June 2011)

The viral envelope is made up of an outer lipid membrane including the viral envelope proteins gp120 and gp41 which facilitate fusion of the HIV virion to the host cell. Within the viral envelope lies the matrix which surrounds the capsid, which is made up of the viral protein p24 and incorporates two single strands of HIV RNA. The three structural genes gag, pol and env and six regulatory genes tat, rev, nef, vif, vpr and vpu are needed to produce new mature virus particles able to infect the host cell. The three main HIV enzymes include reverse transcriptase, integrase and protease.

HIV belongs to a subgroup within the retrovirus family known as lentiviruses or 'slow' viruses (Fanales-Belasio *et al.*, 2010). Using the viral enzyme reverse transcriptase, retroviruses convert their viral RNA into viral DNA with the help of the host cell machinery (Figure 1.1) (Teixeira *et al.*, 2011). HIV-1 is the predominant form worldwide, with HIV-2 being more concentrated in Central and Western Africa (Fanales-Belasio *et al.*, 2010).

In order to understand the mechanism of action of the different antiretroviral agents, one must first get an overview of the life cycle of HIV.

1.4 HIV life cycle

1.4.1 Entry of HIV into host cell

The viral surface glycoprotein gp120 attaches itself tightly to the target CD4 receptor, causing a conformational change, which then allows the virus to bind to a second protein known as a chemokine co-receptor, either C-X-C chemokine receptor type 4 (CXCR4) or chemokine receptor type 5 (CCR5) found on immune cells (Figure 1.2) (Mariani *et al.*, 2011).

1.4.2 Fusion

Another viral protein glycoprotein 41 (gp41), fuses the HIV envelope with the host cell membrane, allowing the virus to enter the target cell (Figure 1.2) (Tripathi and Agrawal, 2007).

1.4.3 Reverse transcription

The viral enzyme reverse transcriptase catalyses the conversion of viral RNA into viral double stranded DNA in the host cytoplasm (Figure 1.2) (Teixeira *et al.*, 2011).

1.4.4 Integration

With the aid of a second viral enzyme known as integrase, the viral DNA is randomly integrated into the host cell genome (Figure 1.2) (Teixeira *et al.*, 2011).

1.4.5 Transcription and translation

At this stage, the proviral DNA may remain dormant in the nucleus for months or years or if activated, lead to gene expression and transcription forming viral mRNA, which when translated, produces viral proteins (Figure 1.2) (Mariani *et al.*, 2011).

1.4.6 Assembly and budding

Inside the cell, HIV proteins, enzymes and genomic RNA come together. The precursor proteins are sliced into smaller functional proteins by a third viral enzyme known as protease. The final step consists of a mature virion forming and budding off from the host membrane, using the latter for its outer coat. The virion goes on to infect other cells (Figure 1.2) (Teixeira *et al.*, 2011; Tripathi and Agrawal, 2007).

Figure 1.2: Diagram of the HIV life cycle

(www.niaid.nih.gov, accessed 20th June 2011)

The HIV virion attaches to the host cell CD4 surface receptor with the aid of HIV gp120. HIV RNA, reverse transcriptase, integrase and other viral proteins then enter the host cell, forming viral DNA using the viral reverse transcriptase. The viral DNA is then transported across the nucleus and integrates into the host DNA using the viral enzyme integrase. Using the host cell machinery, new viral RNA is formed and consequently viral proteins, which move to the cell surface forming a new immature HIV virion. Using the viral enzyme protease, a mature virion is created, ready to infect new cells.

1.5 Clinical presentation of HIV infection

1.5.1 Acute infection

Within one to four weeks post viral transmission, the patient might present with mononucleosis- or influenza-like symptoms that can last up to four weeks, most commonly fever, headache, fatigue and a rash (Chu and Selwyn, 2010). During primary infection, HIV levels are estimated to increase rapidly at a rate of 10^{10} new virions daily (Vogel *et al.*, 2010).
A significant drop in CD4+ cell count follows, accompanied with antibody production, seroconverting the patient (Petroll *et al.*, 2008).

1.5.2 Chronic infection

During this second phase of infection, the patient is generally asymptomatic as the virus replicates, causing a chronic state of systemic inflammation. There is a continuous dynamic balance between viral load and immune response, but not powerful enough to fully eradicate the virus (Ford *et al.*, 2009).

1.6 HIV treatment

There are currently 22 antiretroviral agents licensed in the UK for HIV (BNF 61, 2011). The main aim of treatment is focused on decreasing viral load to an undetectable level of less than 50 copies/ml and at the same time increasing the CD4+ cell count, thereby improving the immune function (Gazzard *et al.*, 2008).

Many factors such as co-morbidities and cardiovascular risk need to be considered when initiating treatment. Because HIV treatment is lifelong, patient compliance and adherence are crucial and factors such as tolerability, pill burden and drug toxicity need to be taken into account when developing new antiretroviral agents (Moreno *et al.*, 2010; Negredo *et al.*, 2006; Patel and Patel, 2006). Drug resistance due to genetic mutations is a major problem even in treatment-naïve patients (Johnson *et al.*, 2010). Antiretrovirals can be divided into five main classes, subject to where they act in the replication cycle (Wainberg and Jeang, 2008).

Figure 1.3: Sites of drug targets

(www.biology.arizona.edu, accessed 21st June 2011)

The fusion/entry inhibitors target the attachment of the HIV virion to the host cell surface and prevent its entry. The reverse transcriptase inhibitors inhibit HIV reverse transcriptase and thereby stop the conversion from RNA into viral DNA. The integrase inhibitors target the viral integrase enzyme which is essential for the integration of the new HIV DNA into the host cell DNA. Protease inhibitors inhibit the final step in the replication cycle and block the viral protease enzyme which is required for the production of the final viral functional proteins.

1.6.1 Reverse transcriptase inhibitors

The reverse transcriptase inhibitors can be divided into three types, nucleosides, nucleotides and non-nucleosides.

Nucleoside reverse transcriptase inhibitors (NRTI's) and nucleotide reverse transcriptase inhibitors (NtRTI's) are analogues of deoxynucleotides needed to synthesise the viral DNA (Figure 1.3). By competing with the naturally occurring deoxynucleotides, they act as substrates and incorporate into the growing DNA chain, causing chain termination as they lack a 3'-hydroxyl group (De Clercq, 2009).

Examples of a NRTI and a NtRTI are zidovudine and tenofovir, respectively (Cihlar and Ray, 2010; Tsibris and Hirsch, 2010). Non-nucleoside reverse transcriptase inhibitors (NNRTI's), on the other hand, directly bind to the viral reverse transcriptase enzyme inhibiting its function and thereby causing chain termination. Efavirenz is a commonly prescribed NNRTI (de Bethune, 2010) .

1.6.2 Protease inhibitors

This class of antiretrovirals inhibits the viral enzyme protease, needed to cleave the polypeptide precursors and subsequent production of mature HIV virions (Figure 1.3). Lopinavir belongs to this class of drugs. They are often used in combination with a small dose of ritonavir, inhibiting the metabolism of the protease inhibitor (PI), resulting in higher PI levels and known as 'boosting' (Naggie and Hicks, 2010).

1.6.3 Entry inhibitors

Entry inhibitors bind to chemokine receptors (X4/R5) on host cells, blocking their use as co-receptor for HIV cell entry (Figure 1.3). Currently only an R5 inhibitor called maraviroc is licensed (Gilliam *et al.*, 2011).

1.6.4 Fusion inhibitors

Fusion inhibitors block the viral surface protein gp41 preventing the conformational change required to allow fusion of viral and target cell membranes (Figure 1.3). An example of a fusion inhibitor is enfuvirtide (Tan *et al.*, 2010).

1.6.5 Integrase inhibitors

Integrase inhibitors block the HIV integrase enzyme required to incorporate viral DNA into the host cell DNA (Figure 1.3). Raltegavir is a commonly prescribed integrase inhibitor (Garrido *et al.*, 2010).

1.7 Timeline of HIV treatment

In 1987, the Food and Drug administration (FDA) approved the first antiretroviral agent licensed for HIV treatment. The NRTI zidovudine (AZT) was seen to slow down the course of AIDS, thereby decreasing AIDS-related deaths (De Clercq, 2009). The drug approval process was accelerated in order to facilitate the development of new drugs.

The drug Kaletra (lopinavir/ritonavir) was reviewed and approved within only 3.5 months (FDA website).

In 1992, the first combination therapy, being AZT with the addition of another NRTI zalcitabine (ddC) was seen to reduce problems with drug resistance (FDA press release, 1992). In 1995, the first PI, saquinavir was approved and with this new class, the use of triple therapy has dramatically reduced AIDS-related deaths, transforming HIV infection into a manageable chronic condition (FDA press release, 1995).

In 1996, the first NNRTI nevirapine was approved and patients taking the HAART drug cocktail would have to take as many as 60 pills per day. HAART usually includes 2 NRTI's plus 1 PI or 1 NNRTI (De Clercq, 2009).

In 1998, the first clinical trials for an HIV vaccine 'AIDSVAX' started and the first national guidelines for the use of antiretroviral therapy were issued (McNeil *et al.*, 2004).

In 2006, ATRIPLA, the first fixed dose combination drug, composed of 300mg tenofovir disoproxil fumarate (NtRTI), 200mg emtricitabine (NRTI) and 600mg efavirenz (NNRTI) was approved in the United states and late 2007 in the European community and considered to be an important step forward in combating global HIV pandemic (FDA press release, 2006; EMA assessment report, 2007).

Figure 1.4: Chart illustrating survival from HIV seroconversion in both pre-HAART and HAART periods

(www.otm.oxfordmedicine.com, accessed on 21st June 2011)

Estimated number of individuals surviving from HIV seroconversion in 1986-96 (pre-HAART period) and 1997-2003 (HAART period), with the survival of the latter being significantly better than before the introduction of HAART.

1.8 The cardiovascular system

1.8.1 Endothelial cells

The inner lining of the blood vessels is known as the endothelium (Figure 1.7). Its main function is to regulate blood flow and pressure and provide an antithrombotic surface. It also plays a major role in angiogenesis and vasoregulation, by releasing vasodilators including nitric oxide and prostacyclin and vasoconstrictors such as endothelin and platelet activating factor (Sumpio *et al.*, 2002).

1.8.2 Nitric oxide synthesis

Under normal circumstances, nitric oxide is continually produced, mainly by constitutive NOS (cNOS) and depends on calcium and calmodulin release. Furchgott et al. were first to describe a substance that caused vasodilation in response to acetylcholine (ACh) and thereby opened a new field of research. The group named that substance endothelium derived releasing factor (EDRF), later renamed nitric oxide (NO) (Furchgott and Zawadzki, 1980).

There exist two calcium dependent pathways of nitric oxide synthesis by cNOS. Shear forces caused by regular blood flow stimulate the release of calcium ions and subsequently cNOS production (Figure 1.6).

The second pathway involves receptors in the vascular endothelium that upon binding with a variety of ligands, induce calcium release followed by cNOS increase and nitric oxide production. Endogenous ligands include bradykinin, ACh and substance P.

On the other hand, inducible NOS (iNOS) is only stimulated in the presence of inflammation caused for instance, by pro-inflammatory cytokines such as TNF-α and interleukins. The latter pathway is calcium independent and induces an excess synthesis of nitric oxide.

Figure 1.5: Synthesis of nitric oxide

(www.cvphysiology.com, accessed 1st July 2011)

In the endothelial cell, nitric oxide is produced from the conversion of L-arginine catalysed by iNOS (inducible) or cNOS (constitutive). After the NO synthesis, it binds to guanylyl cyclase in the adjacent vascular smooth muscle cell and GC catalyses the dephosphorylation of GTP to cGMP, causing smooth muscle relaxation.

After its synthesis, NO binds to the heme moiety of hemoglobin in the blood and is quickly broken down. It also binds to and activates the enzyme guanylyl cyclase found in the neighbouring vascular smooth muscle cells. The enzyme catalyses the dephosphorylation of guanosine triphosphate (GTP) to cyclic guanosine monophosphate (cGMP), which acts as a second messenger to signal smooth muscle relaxation (Figure 1.5). cGMP can induce this relaxation by inhibiting calcium entry and reducing intracellular calcium concentration. It can also activate K^+ channels, leading to hyperpolarisation and subsequent relaxation (Michel and Feron, 1997).

Finally, cGMP can induce the release of cGMP-dependent protein kinase leading to the dephosphorylation of myosin light chains followed by smooth muscle relaxation. In the vascular endothelium, NO has several important functions including direct and indirect vasodilation, inhibition of platelet adhesion and an anti-inflammatory effect by inhibiting leukocyte adhesion to the vascular endothelium (Denninger and Marletta, 1999).

Endothelial nitric oxide synthase (eNOS) plays an important role in vasculoprotection. Endothelial nitric oxide produced by eNOS has antithrombotic and anti-atherosclerotic properties, which make eNOS a potential beneficial target for the prevention or treatment of cardiovascular disease. However, under pathological conditions, eNOS may become dysfunctional. ROS may be produced by the uncoupling of eNOS, usually due to a lack of the crucial eNOS cofactor BH_4, the oxidation of which is usually caused by NADPH oxidase-induced oxidative stress (Guzik *et al.*, 2002).

Endothelial dysfunction (ED) can thus occur when NO synthesis and bioavailabilty is inhibited. Many conditions are linked to endothelial dysfunction including atherosclerosis, heart failure, diabetes, hypertension and dislipidaemia. Endothelial function is a key predictor of future cardiovascular events such as stroke and myocardial infarction; therefore maintenance of healthy function is crucial (Cai and Harrison, 2000).

Figure 1.6: The structure of the endothelium

(www.columbia.edu, accessed 1st July 2011)

The illustration of a capillary. The cells are connected by tight junctions. Outside of the basement membrane (BM) lies collagen (C). Pericytes (P) can be seen within the capillary. (M) shows small cytoplasmic marginal folds.

1.9 Atherosclerosis

Atherosclerosis is a widespread condition characterised by an accumulation of lipid substances such as cholesterol in medium and large arteries, forming ‘plaques’. The latter can cause the arteries to thicken, narrow and lose elasticity, reducing blood flow to the target tissues.

Chronic inflammation is caused by the infiltration of macrophages and LDL-cholesterol with HDL failing to effectively remove fat and cholesterol from the macrophages. Standard risk factors for the development of atherosclerosis include hyperlipidaemia, diabetes, hypertension and tobacco smoking. They can all contribute to changes in the endothelium causing it to become ‘sticky’ (Kher and Marsh, 2004; Munro and Cotran, 1988).

The expression of adhesion molecules as well as chemokines on the surface lead to infiltration of monocytes and T-lymphocytes into the blood vessel. They then accumulate cholesterol and turn into foam cells, leading to endothelial disruption followed by platelet adhesion. Vascular smooth muscle cells move to the site of the foam cells and atherosclerotic plaques form, which can become larger and cause ‘hardening’ of the blood vessel affected. The plaque is mainly composed of a fibrous cap enclosing cholesterol, cell remains and tissue factors from macrophages (Figure 1.7) (Reape and Groot, 1999). The narrowing of the blood vessel causes inadequate blood flow to the affected organ, especially in instances of high demand such as physical exertion and therefore can lead to chest pain for example if the coronary artery is affected.

When plaques rupture and travel to smaller blood vessels, an embolus is formed, which can shift to other organs e.g. lungs (pulmonary embolism), heart (myocardial infarction) or brain (stroke).

Figure 1.7: Illustration of a normal human artery and an artery narrowed by atherosclerotic plaque

(www.clivir.com, accessed 7th July 2011)

On the right picture, the endothelium lining the blood vessel can easily be seen. The left picture illustrates the damaged endothelium due to foam cells, lipids, calcium and cellular debris as well as a fibrous cap, globally known as atherosclerotic plaque, causing a narrowing of the artery.

1.10 The Blood brain barrier

The brain vasculature is far more complex than the blood vessels in the rest of the body. The cellular structure known as the blood brain barrier not only forms a physical protective obstruction to unwanted molecules but also provides the brain with essential nutrients. The BBB was first described by Paul Ehrlich as being an interface between brain tissue and circulating blood (Ehrlich and Cserr, 1978). The brain endothelial cells are connected via tight junctions, with high transendothelial electrical resistance, forming an efficient barrier. Another distinct feature of the brain blood capillaries is that they are enclosed by the end feet of the astrocytes and thus contributing to partial permeability (Figure 1.8) (Abbott *et al.*, 2010).

Only lipid soluble molecules including oxygen, anesthetics and alcohol can penetrate the lipid membranes. Therefore, in order to target HIV in the brain, drugs need to be made more lipid soluble. Water-soluble molecules such as glucose and amino acids need to cross the BBB via carrier mediated transport mechanisms in the cell membrane. In addition, enzymes sited in the brain capillaries also break down unwanted molecules and efflux pumps contribute to selective permeability by transporting molecules back into the systemic circulation (Figure 1.8) (Glynn and Yazdanian, 1998). Unlike other body tissues, where extracellular fluid is made by leakage from capillaries, the BBB secretes its own extracellular fluid at a constant rate, which is very important in order to maintain a controlled brain volume.

The intercellular tight junctions are formed by claudins, occludin and junction associated molecules (JAM's), connected by scaffolding proteins of the zonula occludens (ZO) to the actin cytoskeleton (Kniesel and Wolburg, 2000).

Commonly studied efflux transporters include the multidrug resistance associated proteins, breast cancer resistance protein and the ATP binding Cassette like p-glycoprotein (Abbott *et al.*, 2006).

Figure 1.8: Illustration of the blood brain barrier

Diagram of a cerebral capillary enclosed in astrocyte end-feet. Features of the blood-brain barrier are shown: (1) tight junctions that close the crossing between the capillary (endothelial) cells; (2) the lipid nature of the cell membranes of the capillary wall which prevents water-soluble molecules from crossing; (3), (4), and (5) represent some of the carriers and ion channels; (6) the 'enzymatic barrier ' which removes molecules from the blood; (7) the efflux pumps which extrude fat-soluble molecules that have crossed into the cells.

Any disruption of the intercellular tight junction proteins, increasing the permeability of toxins and drugs to the brain may be important in the neuropathogenesis seen in HIV patients (Kanmogne *et al.*, 2005).

1.10.1 Dementia

BBB disruption has been associated with conditions including dementia, Parkinson's disease, stroke and multiple sclerosis, of which HAD is most commonly seen in HIV patients (Wang *et al.*, 2008). Dementia is marked by a gradual decline in cognitive function and its incidence usually rises with age. Not only cognitive features such as learning, language, memory and attention are affected, but also personality and behavioral changes may be observed. The most widespread form of dementia seen in the developed world is Alzheimer's Disease (AD), marked by a slow onset and gradual loss of short-term memory (Anand *et al.*, 2010). The exact etiology of AD is somewhat still unclear but is thought to involve the progressive accumulation of proteins in the brain and therefore its diagnosis is solely based on cognitive tests rather than laboratory results (Valcour *et al.*, 2011).

Many factors can increase the risk of developing dementia, including trauma, infections such as HIV and vascular complications such as cerebrovascular accident and atherosclerosis. Unlike AD, the latter causes are seen to be of rapid onset and progression (Anand *et al.*, 2010).

1.11 HAART toxicity

The success of HAART in reducing morbidity and mortality associated with HIV/AIDS was overshadowed by significant toxicities linked to antiretroviral agents (Burgoyne and Tan, 2008). Beside the widely known side effects reported with long term antiretroviral use, including dyslipidaemia, lipidostrophy and diabetes, increased cardiovascular risk seems to be on the rise, although females are less affected than males, as oestrogen seems to have a poly (ADP-ribose) polymerase (PARP)-mediated protective effect (Mabley *et al.*, 2005).

1.11.1 HAART cardiovascular toxicity

1.11.1.1 Endothelial cells

Endothelial dysfunction plays a major role in the development of atherosclerosis. Increased expression of adhesion molecules, loss of anticoagulant activity, increased release of cytokines and chemokines and reactive oxygen species (ROS) are all associated with vascular dysfunction (Heitzer *et al.*, 2001; Shimokawa, 1999). By assessing endothelial function, one can predict the risk of cardiovascular events such as stroke and myocardial infarction (Heitzer *et al.*, 2001). Many studies have linked endothelial dysfunction to HIV infection and antiretroviral therapy (de Gaetano *et al.*, 2003; Francisci *et al.*, 2009).

Since the different antiretroviral agents are rarely given as monotherapy, it is difficult to determine which drug causes cardiovascular toxicity, commonly ascribed to NRTI's, NNRTI's and PI's. Endothelial function can be measured by flow-mediated dilatation (Pyke and Tschakovsky, 2005).

NRTI's are thought to cause endothelial dysfunction by inhibiting DNA polymerase-gamma (DNA pol-γ), which is crucial for mitochondrial replication and repair and thereby reducing mitochondrial levels or disrupting the electron transport chain (Lewis *et al.*, 2003). Many studies, however, have concluded that the vascular toxicity caused by NRTI's may be attributed to an increased level of oxidative stress (Lewis *et al.*, 2001). Indeed, treatment of cultured endothelial cells with AZT was shown to cause apoptosis-independent cell dysfunction within 24 hours (Jiang *et al.*, 2007). The mitochondria seem to be the main target of NRTI-mediated cytotoxicity involving changes in transmembrane potential and a reduction in ATP levels (Lund *et al.*, 2004).

Many studies have proposed that ROS may be the main culprit in the vascular side effects associated with the use of HAART. Future work, however, need to further investigate the effects of HAART on endothelial cells, as the mechanism of toxicity is not conclusive.

Cardiovascular side effects reported include atherosclerosis, myocarditis, endocarditis, pericardial effusion, congestive heart failure and dilated cardiomyopathy (Barbaro, 2002).

The pathophysiological link of these metabolic disturbances with a prolonged inflammatory state has been shown to be a major factor in endothelial dysfunction and atherosclerosis. Hurwitz et al. found that although HIV did independently increase inflammatory markers, PI's in particular increased the risk of myocardial infarction (MI) in the next ten years by 56 % compared to those not on PI's (Hurwitz *et al.*, 2004).

The D:A:D study (Data Collection of Adverse effects of Anti-HIV Drugs Study) started in 1999 and mainly focused on cardiovascular toxicity, including increased risk of MI caused by the nucleoside analogues. This class of drugs includes stavudine, zidovudine, lamivudine, didanosine and abacavir (Friis-Moller *et al.*, 2003).

With the HIV population living longer, people with underlying cardiovascular risk similar to the general population have more pronounced long-term effects. The standard reversible cardiovascular risk factors include smoking, hyperlipidaemia, hypertension, diabetes mellitus and visceral fat accumulation. Non-reversible risk factors include male gender; age over 40 years and family history of cardiovascular disease. The lifestyle of HIV positive patients can also increase the likelihood of developing cardiovascular problems (Friis-Moller *et al.*, 2003).

1.12 Toxicity mechanisms

1.12.1 DNA polymerase-γ hypothesis

The DNA polymerase-γ hypothesis has always been a suggested explanation for the damage mediated by antiretrovirals (Lewis *et al.*, 2003), but it is now apparent that the etiology is far more complex, involving multiple mechanisms as well as an effect by HIV *per se*, infection of cardiac myocytes, cytotoxicity of HIV proteins, immune cell interactions in cardiac tissues and opportunistic infections among others (Fiala *et al.*, 2004; Martinez *et al.*, 2009).

In order to be active, the nucleoside analogues first need to be phosphorylated by cell kinases to tri-phosphate moieties, which resemble the endogenous nucleotides and competitively inhibit the viral reverse transcriptase. Because they lack a 3'-OH group, they subsequently terminate chain elongation. The DNA pol-γ hypothesis assumes that the NRTI-triphosphate incorporates into the mitochondrial DNA, inhibiting new synthesis, thereby causing mitochondrial depletion in the affected cell. In addition, the hypothesis suggests that mutations in mtDNA may be involved in disrupted oxidative phosphorylation and consequent electron leakage from the mitochondria (Lewis *et al.*, 2003).

1.12.2 Oxidative stress

Oxidative stress seems to play a major role in the early stages of mitochondrial pathogenesis. It has been extensively studied and linked to the pathophysiology of endothelial dysfunction, including that mediated by HAART (Mondal *et al.*, 2004). Oxidative stress can be defined as the imbalance between the formation of reactive oxygen species and cellular antioxidant capacity. ROS are generated as byproducts of several cellular metabolic activities and in instances of Redox disturbance; they can cause damage to cellular components including lipids, proteins and DNA. The DNA damage is often key to the long-term effects caused by ROS. Examples of ROS include the superoxide anion, hydrogen peroxide and hydroxyl radical (Kowaltowski and Vercesi, 1999).

Reactive nitrogen species (RNS) are also of importance as they are caused by the combination of nitric oxide and superoxide anion to form peroxynitrite, which can be very detrimental to the cell and is known as nitrosative stress (Eu *et al.*, 2000).

Under normal physiological circumstances, the generation of ROS is kept under control by counteraction of antioxidants. When this balance is disturbed, however by more severe oxidative stress, the cell enters an ATP-depleting cycle, inhibiting apoptosis and dies in the process of necrosis (Sies, 1997). There are various cellular sources of ROS generation including organelles and enzymes.

During oxidative phosphorylation, highly activated electrons can leak from the mitochondria and go on to form ROS. Enzymes that may generate ROS include xanthine oxidase found in the mitochondria and cytoplasm, nicotinamide adenine dinucleotide phosphate (NADPH) oxidase in the plasma membrane and cyclooxygenases located in the cytoplasm. Exogenous sources of ROS include cigarette-smoking, ionizing radiation, bacterial and viral infections (Andersen, 2004; Bernhard and Wang, 2007; Cai and Harrison, 2000).

Oxidant	Formation	Feature
superoxide ($O_2^{\cdot}$)	auto-oxidation/Electron transport chain	not very reactive but can release Fe^{2+}, can form H_2O_2 and precursor for $OH^{\cdot}$ formation
hydrogen peroxide (H_2O_2)	dismutation of $O_2^{\cdot}$	lipid soluble, hence can penetrate membranes
hydroxyl radical ($OH^{\cdot}$)	Fenton reaction/decomposition of $ONOO^-$	very reactive and damages most cellular components
hypochlorous acid (HOCl)	from H_2O_2 by myeloperoxidase	very reactive, lipid soluble, damages protein structures.
peroxynitrite ($ONOO^-$)	reaction between $O_2^{\cdot}$ and NO	very reactive, lipid soluble, can form $OH^{\cdot}$

Table 1.2: Table showing common oxidants and their effects which can contribute to oxidative stress

1.12.3 Oxidative stress and cardiovascular effects

Superoxide and hydrogen peroxide (Table 1.2) are the main oxidants generated in vascular cells by various enzymes including NADPH oxidase, nitric oxide synthase (NOS) and xanthine oxidase.

If there is an imbalance between superoxide levels and antioxidant levels such as superoxide dismutase (SOD), the reaction continues to produce the highly reactive peroxynitrite from superoxide and nitric oxide (Table 1.2). This consequently causes nitric oxide depletion, further forming oxidants (Zalba *et al.*, 2000). The cell loses its vasodilating ability due to the drop in nitric oxide bioavailability and this in itself contributes to cardiovascular dysfunction (Griendling *et al.*, 2000).

Endothelial cell derived-ROS may further induce smooth muscle cell hypertrophy and apoptosis dependent vascular cell death. Many studies have shown that free radical scavengers and antioxidants reversed HAART-mediated endothelial cell dysfunction, thus implying an involvement of oxidative stress (Mondal *et al.*, 2004). The latter has been closely linked to an important cytoprotective mechanism known as the endoplasmic reticulum stress, which has been shown to play a significant role in the pathogenesis of many conditions including atherosclerosis and diabetes (Malhotra and Kaufman, 2007; Yoshida, 2007).

1.12.4 Endoplasmic reticulum stress

The endoplasmic reticulum (ER) consists of an advanced luminal network in which proteins are synthesised, folded and transported to the secretory pathway. The network includes ER chaperones that facilitate protein folding and are in a way responsible for ‘quality control’, only allowing correctly folded proteins to exit the ER (Oyadomari and Mori, 2004).

Any disruption to normal ER function due to oxidative stress, viral infection or chemical insults may lead to endoplasmic reticulum stress. Normal function of the chaperones is highly calcium dependent and significant changes in calcium homeostasis can lead to ER stress as part of a cytoprotective mechanism (Kaufman, 1999). The unfolded protein response (UPR) is triggered by ER stress due to the accumulation and aggregation of misfolded or incompletely folded proteins. If ER homeostasis can't be restored due to significant damage such as high oxidative insult, the cell triggers a pro-apoptotic process (Szegezdi *et al.*, 2006).

1.12.5 Cell Death (Apoptosis/Necrosis)

Severe oxidative stress may lead to cell death either by apoptosis or necrosis, influenced by the intensity of the strain. Apoptosis is defined as being a mechanism of programmed cell death, whereby the cell 'commits suicide'. The process is energy dependent and occurs in response of various stress inducers including toxins, radiation, infections or oxidative stress (Chandra *et al.*, 2000). A nuclear enzyme PARP may play an important role in regulating this process (Pieper *et al.*, 1999).

Necrosis on the other hand is often described as the uncontrolled form of cell death, whereby the cell swells and releases its contents, thus affecting neighboring cells and is more detrimental to the cell than apoptosis (Majno and Joris, 1995).

Overactivation of PARP is believed to be involved in the pathogenesis of many conditions, including myocardial infarction, inflammatory diseases and neurodegenerative disorders (Tentori *et al.*, 2002). PARP is associated with the regulation of inflammatory mediators including iNOS, intercellular adhesion molecule (ICAM) and TNF-α (Cuzzocrea, 2005).

1.12.6 PARP

PARP is a 116 kDa chromatin bound DNA repair enzyme found in the nucleus of the cell. PARP-1 is the most abundant and commonly studied isoform, thought to be responsible for over 80 % of all PARP activity. Its structure exhibits three major domains, the N-terminal DNA binding domain with its two Zn fingers, the automodification domain and the C-terminal catalytic domain (Figure 1.9) (Pacher and Szabo, 2007).

Figure 1.9: PARP-1 protein domains

(www.activemotif.com/parp1.html (accessed 27th June 2011)

PARP displays a carboxyl-terminal domain in which poly (ADP-ribosyl)ation occurs using NAD^+molecules as a donor of ADP-ribose groups. ' There is also an amino-terminal DNA binding domain holding three zinc finger motifs, a nuclear localization signal, and an automodification domain that functions as the target of covalent auto-poly (ADP-ribosyl)ation, Thanks to these domains, PARP-1 can interact with genomic DNA and chromatin, poly(ADP-ribosyl)ate different nuclear target proteins and contribute to the regulation of nuclear functions.

PARP-1 is thought to have a variety of functions, including DNA repair, DNA metabolism, gene transcription and genomic integrity. PARP-1 also seems to play a major role in apoptosis (Herceg and Wang, 2001).

When moderate single- or double strand DNA breaks occur in response to endogenous and exogenous insults, PARP detects the damage and becomes activated. It binds to the DNA via its second zinc finger domain, forms homodimers and catalyses the cleavage of nicotinamide adenine dinucleotide (NAD^+) into nicotinamide and ADP-ribose polymers. The latter are covalently bound to nuclear acceptor proteins such as histones, but also PARP itself (automodification).

For a long time, it was thought that glutamic acid residues in the acceptor proteins were the target of poly (ADP-ribosyl)ation, however, recent studies have shown that lysine residues were more involved (Pacher *et al.*, 2002a; Szabo, 2002). When there is extensive DNA damage, PARP becomes overactivated and triggers an energy consuming cycle, depleting NAD^+ and ATP and eventually resulting in cell dysfunction and death by apoptosis or necrosis depending on cell type, stress severity and duration. In the scenario of apoptosis, PARP is inactivated by caspases, generating two fragments and preserving cellular energy in the form of NAD, required for apoptosis to proceed, also known as programmed cell death. Necrosis on the other hand, is a more uncontrolled mechanism of cell death that may also affect neighbouring cells (Figure 1.10) (Pieper *et al.*, 1999).

Figure 1.10: The effects of PARP

(http://uts.cc.utexas.edu accessed 27th June 2011)

Many factors influence PARP activity, including DNA damage, caspases and intracellular NAD^+ concentration. The inactivation of PARP by caspase-3 cleavage is one of the main events of apoptosis, while PARP overactivation can lead to NAD^+ and ATP depletion and lead to necrosis.

PARP cleavage is therefore considered to act as a molecular switch between the two routes of cell death (Figure 1.10). Recently, another caspase-independent form of cell death only associated with PARP was described, known as parthanatos. The mechanism is still unclear but is thought to involve pro-apoptotic mitochondrial apoptosis inducing factor (AIF), translocating to the nucleus and triggering chromatin condensation and DNA fragmentation, resulting in cell death (Yu *et al.*, 2009).

The short *in vivo* half-life of the polymer and another enzyme poly (ADP-ribose) glycohydrolase (PARG) indicate that poly (ADP-ribosyl)ation is a rapid energetic process. PARG is required for degrading PARP into free ADP ribose and AMP (Kraus and Lis, 2003).

There seems to be a controversy between research groups as to the role of PARP in the described cell death pathways. The conflict, however, seems to be overcome by more or less accepting that the intensity of DNA damage and metabolic state of the cell determine the fate of the cell (Ha and Snyder, 1999).

Previous reports have shown that impairment of cardiovascular function in diseases such as diabetes thought to be mediated by PARP overactivation might be reversed using one of the most potent and selective PARP inhibitors, PJ-34 (Figure 1.11). This water-soluble phenanthridinone derivative has been shown to maintain endothelial function in vascular rings following high glucose levels. Most PARP inhibitors impede the binding of NAD^+ to the catalytic domain of PARP. In addition, they may bind to DNA itself, thereby preventing detection of the DNA nicks by PARP and subsequent overactivation (Pacher *et al.*, 2002b).

PJ-34

Figure 1.11: The chemical structure of the PARP inhibitor PJ-34 (www.chemicalbook.com, accessed 27th June 2011)

There are opposing reports of PARP playing a central role in facilitating integration of the HIV genome into the host genome. On the one hand, Ha et al. showed that integration of a vesicular stomatitis virus glycoprotein (VSV-G) pseudotyped molecular clone of HIV-1 was significantly inhibited in mouse embryonic fibroblasts (MEF) originating from PARP -/- mice, concluding that PARP is essential in the HIV integration process (Ha and Snyder, 1999).

On the other hand, using the same type of cells as well as human PARP knockdown cells, Ariumi et al. suggested that PARP is not required for successful integration of HIV (Ariumi *et al.*, 2005). In accord with the latter study, another group also suggested that PARP is certainly not indispensable for the infection of murine cells by retroviruses as both wild type and PARP deficient MEF cells got infected by two separate HIV derived VSV-G pseudotyped lentivirus vectors (Siva and Bushman, 2002).

Before activation, NF-κB is held in the cytosol in an inactive form with its inhibitor, nuclear factor of kappa light polypeptide gene enhancer in B-cells inhibitor, alpha (IκBα). Once activated by cytokines, IκBα becomes phosphorylated and separates from NF-κB, rendering it active followed by translocation to the nucleus where it binds to elements in the promoter of many genes in order to modulate their expression (Karin, 1999), such as promoters expressing tight junction proteins preventing their expression (Aveleira *et al.*, 2010). The activation of NF-κB is thought to contribute to the development of cardiovascular disease by its pro-inflammatory, pro-oxidant and pro-adhesion gene transcription (Donato *et al.*, 2009).

1.13 ATRIPLA

With the introduction of Atripla, marketed by Bristol-Myers Squibb Co. and Gilead Sciences Inc. in the US in 2006 (FDA press release 2006) and in Europe in late 2007 (EMA assessment report, 2007) compliance and adherence problems seen with HAART were hoped to be resolved, as patients only need to take one pill in the morning. The benefit of being a single pill regimen is that it has improved adherence to such an extent that 80 % of treatment naïve patients in the USA are started on it (Julg and Bogner, 2008).

Previous fixed dose drug combinations only contained NRTI's, whereas ATRIPLA combines drugs from three different antiretroviral classes.

Figure 1.12: The chemical structure of the ATRIPLA components, efavirenz, emtricitabine and tenofovir

(www.rxlist.com/atripla-drug.htm, accessed 24th June 2011)

Adherence is important as missing doses is the most significant cause of treatment failure from viral resistance and multi-pill regimens had proved difficult to maintain (Chesney, 2003). The once-daily pill has not been thoroughly investigated with regards to cardiovascular side effects. The pill was considered to have considerably less cardiovascular side effects than its predecessors.

Preliminary data show that at least one of the drugs efavirenz, has significant adverse effects on endothelial cell function and viability (previous own data).

Contrary to NRTI's, efavirenz does not interfere with DNA-polymerase-γ and thus the cardiotoxicity is unlikely to be justified using the DNA pol-γ hypothesis. As the triple pill is relatively young, little is known about long-term side effects.

As previously stated, this cytotoxicity is believed to be mediated by oxidative stress causing increased DNA single strand breaks with subsequent overactivation of the repair enzyme PARP resulting in decreased cellular NAD^+ and ATP levels and eventually resulting in cell death either by apoptosis or necrosis. PARP has played a major role in cardiovascular dysfunction caused by diabetes, MI, sepsis and now perhaps that induced by HAART (Pacher *et al.*, 2002a).

HIV *per se* is known to cause cardiovascular side effects, however, this project focuses on drug-related cardiovascular dysfunction only.

1.14 Potential protective strategies

1.14.1 Rosiglitazone

A suggested protective strategy against HAART- mediated cardiovascular toxicity is rosiglitazone (Figure 1.13). This antidiabetic drug, belonging to the thiazolidinediones, was shown to confer cardioprotection against ischaemia/reperfusion injury in animal models (Yue *et al.*, 2008).

Ironically, in 2010, rosiglitazone was withdrawn from the UK market due to suspicion of cardiotoxicity in diabetic patients, especially those with co-morbidities and a high cardiovascular risk (Cohen, 2010)(EMA assessment report, 2010).

The drug is still prescribed in the United States (Woodcock *et al.*, 2010). Rosiglitazone is thought to sensitise adipose tissue to insulin by activating peroxisome proliferator-activated receptor gamma (PPAR-γ) and thus conferring its glucose lowering effect. The mechanism of cardioprotection is still unclear and needs further research (Palee *et al.*, 2011). Cardiomyocytes express all three isoforms of PPAR (Huang *et al.*, 2011) and peroxisome proliferator-activated receptor alpha (PPAR-α) agonists such as fibrates, commonly used in dislipidaemia may offer similar cardioprotection to rosiglitazone (Bulhak *et al.*, 2009). The anticipated protective effect by rosiglitazone was hypothesised to involve activation of PPAR-γ and/or AMP-activated protein kinase (AMPK).

rosiglitazone

Figure 1.13: The chemical structure of rosiglitazone

(www.rxlist.com/avandia-drug.htm, accessed 27th June 2011)

1.14.1.1 The PPAR-γ pathway

PPAR-γ is a nuclear ligand-activated transcription factor that regulates the target gene expression. It forms a heterodimer with a second receptor known as retinoid X receptor (RXR), which upon binding with the ligand causes a conformational change, recruiting transcriptional co-activators such as activator protein-1 (AP-1) and NF-κB, leading to gene transcription (Figure 1.14) (Ryan *et al.*, 2004). PPAR-γ is predominantly expressed in adipocytes but is also found in heart, liver and kidney (Huang *et al.*, 2011; Nicholls and Uno, 2012).

Figure 1.14: The PPAR-γ pathway

(www.ppar.cas.psu.edu, accessed 30th June 2011)

Upon binding with the ligand, the retinoid X receptor undergoes a conformational change, recruiting transcriptional co-activators such as NF-κB leading to gene transcription. Adipo, adipocyte; ADRP, Adipocyte differentiation-related protein; aP2, adipocyte Protein 2; CBP, cAMP response element-binding protein; C/EBP, cytidine-cytidine-adenosine-adenosine-thymidine-enhancer binding protein; COX-2, cyclooxygenase-2; ERK, extracellular signal regulated kinases; IL-1, interleukin-1; JNK, c-Jun N-terminal kinases; L, ligand; LPL; lipoprotein lipase; MKP, mitogen-activated protein kinase phosphatase; NF-κB, nuclear factor kappa-light-chain-enhancer of activated B cells; p300, nuclear co-activator; PGJ_2, prostaglandin J2; PPRE, PPAR response element; RXR, retinoid X receptor; SRC-1, steroid receptor co-activator-1.

The thiazolidinediones have also been shown to have AMPK involvement when sensitising the cells to insulin (Ceolotto *et al.*, 2007).

1.14.1.2 The AMPK pathway

AMPKs play a major function in cellular energy homeostasis and act in response to cellular stresses that deplete ATP, such as low glucose or hypoxia in view of activating ATP replenishing pathways (Figure 1.15).

AMPK is a heterotrimeric complex made of three subunits, a catalytic alpha and two regulatory beta and gamma subunits (Hardie, 2008; Mitchelhill *et al.*, 1997).

Figure 1.15: The AMPK pathway in heart ischemia

(www.card.ucl.ac.be, accessed 30th June 2011)

When activated as in the case of myocardial ischemia, AMPK switches on ATP generating pathways such as glycolysis as well as switching off ATP-consuming pathways such as protein synthesis. LKB-1 was shown to play an important role in AMPK activation. AMP, adenosine monophosphate; AMPK, adenosine monophosphate-activated protein kinase; ATP, adenosine triphosphate; LKB1, liver kinase B1.

1.15 Aims and objectives

The overall aim of this study is to determine the effects of the Atripla components, tenofovir, efavirenz and emtricitabine, on cardiovascular cell function and investigate potential protective strategies.

Elucidation of the mechanisms of toxicity and protection is crucial for the development of future potential therapies counteracting HAART-mediated cardiovascular dysfunction and thereby reducing mortality associated with HIV cardiovascular toxicity.

Chapter 2

Materials and Methods

Materials

2.1 List of chemicals

Acetic acid

Acetylcholine

AICAR

Albumin

Ammonium persulfate (APS)

Anti-Actin

Anti-CHOP

BAY

Beta-mercaptoethanol

Bis-acrylamide

Bradford reagent

Bromocresol powder

Compound C

Dimethyl sulfoxide (DMSO)

Dulbecco's Modified Eagle Medium (DMEM)

Efavirenz

Emtricitabine

Enhanced chemiluminescence (ECL)

Ethanol

Ethylenediaminetetraacetic acid (EDTA)

EUK-134

Fetal calf serum (FCS)

Glucose

Glutamine

Glycine

Growth medium

GW1929

GW9662

Hoechst 33342 dye

Laemmli sample buffer

Magnesium sulphate

Malondialdehyde standard (TBA)

Methanol

Milk (5 %)

Nitro blue tetrazolium (NBT)

Non-essential amino acid (NEAA)

Oestrogen

Penicillin/streptomycin

Phenylmethanesulfonylfluoride (PMSF)

Phenylephrine

Phosphate buffered saline (PBS)

Pioglitazone

PJ-34

Potassium chloride

Potassium hydrogen phosphate

Potassium hydroxide (KOH)

Propidium iodide

Protease inhibitor cocktail

Quinazoline (QNZ)

Rosiglitazone

SP600125

Sodium bicarbonate

Sodium chloride

Sodium dodecyl sulphate (SDS)

Sodium hydroxide

Sodium pyruvate

Succinic acid

Tenofovir

Tetrazolium dye (MTT)

Tetramethylethylenediamine (TEMED)

Tris (pH 7.4)

Tris-buffered saline (TBS)

Tris-HCl buffer (pH 6.8)

Triton-X

Trizma base

Trichloroacetic acid (TCA)

Trypsin

Tween 20

Versene

^{3}H-NAD

2.2 List of suppliers

Abcam (Cambridge, UK)

Axxora (Nottingham, UK)

BioRad (Hertfordshire, UK)

Calbiochem (Nottingham, UK)

European Collection of Cell Cultures (ECACC)

Innotech (Boston, USA)

Lonza (Slough, UK)

Oxoid (Basingstoke, UK)

Santa Cruz Insight Biotechnology, Wembley, UK

Sequoia Research (Pangbourne, UK)

Sigma Aldrich (Poole, Dorset, UK)

University of Sussex (Brighton, UK)

Upstate Biotechnology, UK

Western Blotting Detection System (Amersham, Buckinghamshire, UK)

Methods

2.3 *In vitro* studies

In order to determine the effects of the Atripla components on the cardiovascular system, three model systems were used in the form of H9c2, EA.hy926 and bEnd.3 cell lines as well as *ex vivo* studies on rat aortic rings to further elucidate the effects on endothelial function.

2.3.1 Cell culture

Cells were cultured in growth medium Dulbecco's modified Eagle medium (DMEM), supplemented with heat inactivated 10 % fetal calf serum (FCS), 2mM glutamine, 1% non-essential amino acids (NEAA), 1 mM sodium pyruvate and 1% penicillin/streptomycin.

Growth conditions were maintained in a humidified incubator (Haraeus) at 37 ºC, 5 % carbon dioxide and 95 % air. For the *in vitro* studies, cells were plated in supplemented DMEM with 3 % fetal calf serum.

Consumables for cell culture were obtained from Fischer Scientific (Loughborough, Leicestershire, UK). The initial stock was stored in liquid nitrogen in a mixture of growth medium and DMSO 10 %.

2.3.1.1 H9c2

The established H9c2 cell line was obtained from the European Collection of Cell Cultures (ECACC catalogue no 88092904). The cells were obtained as split sub-confluent cultures (70 – 80 %) seeded at 1-3x 10,000 cells/cm^2 using 0.25 % trypsin/EDTA and incubated at 37°C and 5 % carbon dioxide. H9c2 cells of passage number 5-40 were used in this study.

2.3.1.2 EA.hy926

The EA.hy926 cell line was obtained from the European Collection of Cell Cultures (ECACC catalogue no CRL-2922). EA.hy926 cell passages number 3-60 were used in this study. This cell line comparable to HUVEC is derived from human umbilical vein and was first established and described by Dr. C.-J. s. Edgell in 1983. By fusing human umbilical vein endothelial cells with an established cell line A549 that originated from a human lung carcinoma, this new cell line has proved to be very beneficial in endothelial toxicity studies. Many characteristics also found in primary endothelial cells could be preserved, including endothelin activity.

2.3.1.3 bEnd.3

The bEnd.3 cell line is derived from a mouse SV129 brain endothelioma (ECACC catalogue no 96091929). The cells were obtained as split sub-confluent cultures (70-80 %) seeded at 4 x 10,000 cells/cm^2 using 0.25 % trypsin/EDTA and incubation at 37 °C and 5 % carbon dioxide.

bEnd.3 cells of passages up to number 40 were cultured in growth medium DMEM, supplemented with heat inactivated 10 % FCS, 2mM glutamine, 1 % NEAA, 1 mM sodium pyruvate, 1 % penicillin/streptomycin and 5µM of 2-mercaptoethanol.

2.3.2 Cell passaging

When the cells reached subconfluency, they were passaged every 2-3 days to prevent differentiation. The cells in the 75 cm^2 Nunc culture flasks were treated with a trypsin/versene (0.1 %/0.02 % w/v) solution for five minutes at 37 °C. Once the cells were detached from the flask surface, the trypsin was neutralised with 10 % FCS containing culture medium and the mixture transferred to a centrifuge tube. This solution was then centrifuged at 500g for five minutes (Haraeus Multifuge 3s Centrifuge).The supernatant was aspired and the formed pellet was resuspended in 12 ml of culture medium and disrupted using a 10 ml pipette in order to get a uniform solution. This was then equally distributed between 4 flasks, maintained in the incubator and the media replaced every 2 days. The cells were plated in 6-, 12-, 24- and 96 well plates according to the different experiments' requirements.

For cell counting, after centrifugation, the pellet was resuspended in 5 ml of culture medium, an aliquot of 20 µl was taken and using a haemocytometer, the cells were counted in the grid, an average taken, expressed in unit of cells/ml with the aim of plating 25,000 cells per well.

The plating of cells was done 24 hours prior to the individual experiment and held in the quarantine incubator. All consumables used in the various experiments were purchased from Sigma-Aldrich (Poole, Dorset, UK), unless stated otherwise. The Atripla components efavirenz, emtricitabine and tenofovir DF were obtained from Sequoia Research and rosiglitazone came from Axxora (Nottingham, UK).

Initial experiments consisted of determining the effect of the individual Atripla components. Cells were treated with increasing concentrations (3, 10, 30 and 100 μM) of the three drugs efavirenz (Mw 315.68), emtricitabine (Mw 247.25) and tenofovir disoproxil fumarate (Mw 635.51) and incubated for 24 and 48 hours. Preparation of the different drug solutions was carried out by weighing out 5 grams of the drug powder and dissolving it in 1 ml of DMSO, since the water solubility of all three drugs is relatively poor.

2.4 Cell viability measurements

2.4.1 MTT assay

Cell viability was assessed using the MTT assay, which is a colorimetric assay, commonly used in cytotoxicity studies. This assay measures the reduction of yellow MTT tetrazolium salt (3-(4,5-Dimethylthiazol-2-yl)-2,5-diphenyltetrazolium bromide) to purple water - insoluble formazan by mitochondrial succinate dehydrogenase.

By adding an organic solvent (DMSO) to the cells, the formazan reagent exhibits the purple color in different degrees of intensity, which can be quantified using a spectrophotometer at an absorbance of 540 nm. Because this reduction takes place in the mitochondria of metabolically active cells, it is a relative marker of cell viability. In most experiments, the cells were allowed to cultivate in 96-well plates, 24 hours prior to the individual experiments. This assay has the advantage of being rapid, reliable and cost-effective.

The results are expressed as a percentage of mitochondrial function as cells that are damaged by the various treatments decrease the reduction of MTT to formazan. Following incubation of the drug treated cells for 24 hours, the solutions were removed from all the wells, replaced with 100 μl of a 0.5mg/ml MTT (in DMEM) solution and incubated for 45 minutes until a purple tint could be seen.

The MTT solution was aspired from the wells and replaced with 100 μl of DMSO, which produced varying degrees of intensity of a purple colour, according to the level of cell viability. Using an Oasys UVM 340 spectrophotometer (Digiread software), the absorbance could be measured at a wavelength of 540 nm and results expressed as a percentage of untreated control cells. Using Excel, the absorbance values of each drug treatment were converted to percentages of untreated control cells by dividing each value with the mean absorbance value of the control and multiplying this by 100.

2.4.2 Cell death assessment (Hoechst/propidium iodide staining)

This assay is important in order to determine whether the cell toxicity induced by the different drugs can be attributed to apoptosis or necrosis. As mentioned before, apoptosis consists of a regulated energy dependent cell death process known as ‘cell suicide’.

When the cell degrades by apoptosis, it shrinks and dies from the ‘inside’, hence preventing leakage of noxious substances that could affect surrounding cells. Necrosis on the other hand is the uncontrolled mode of cell death, whereby the cell swells, ruptures and eventually releases its contents, which can be detrimental to neighboring cells. Because propidium iodide is water-soluble, it can’t penetrate the lipid bilayer of the cell membrane under normal conditions. If the cell membrane is damaged as in necrosis, the dye can easily penetrate the cell and stain it pink. Hoechst 33342 dye can penetrate intact plasma and nuclear membranes and thus stains both living and apoptotic cells blue.

Using an inverted fluorescent microscope (Axiovert 25) and a 4’, 6-diamidino-2-phenylindole (DAPI) filter, one could easily distinguish viable, apoptotic and necrotic cells. Under the microscope, live cells appeared blue with an intact membrane, apoptotic cells also looked blue but with small apoptotic bodies, post-apoptotic cells exhibited apoptotic bodies but pink/red, necrotic cells appeared pink/red. HPI staining constitutes a rather subjective and ‘artificial’ method of evaluating apoptosis and necrosis as it uses a small number of cells and it can be unwillingly biased by the operator.

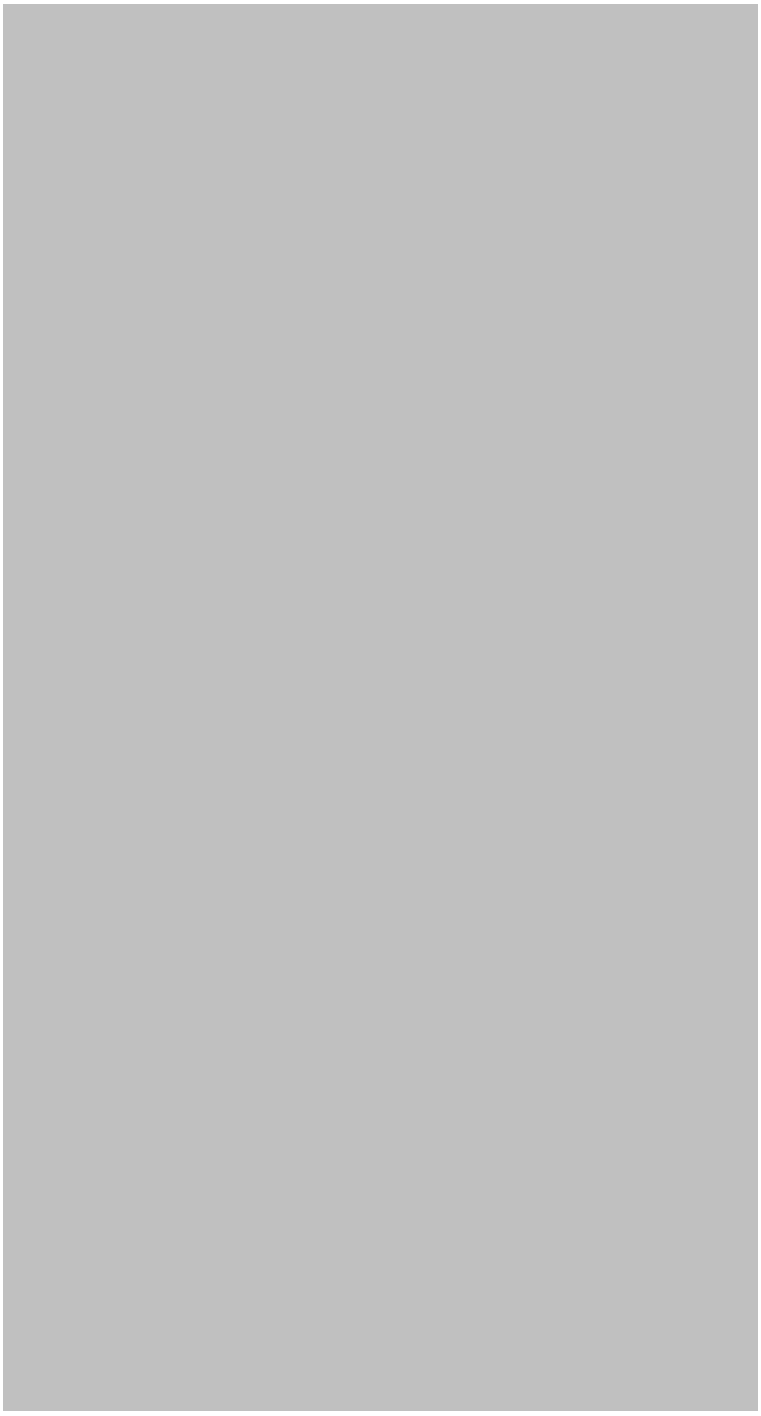

Figure 2.1: Hoechst/propidium iodide images. (A) living cells (B) apoptotic cells (C) necrotic cells (D) post-apoptotic cells.

Apoptotic cells show nuclei which contain condensed DNA and therefore take up more of the Hoechst dye, staining blue, while necrotic cells lose the integrity of their plasma membrane and stain pink due to propidium iodide. Post apoptotic necrotic nuclei stain pink but because they maintain apoptotic bodies inside of them.

For cell death experiments, cells were grown in 24-well plates 24 hours prior to treatment and counted 24 hours post treatment. The day of the cell counting, the appropriate drug solutions were removed from the wells and replaced with 100 µl/well of a solution containing 50 µl Hoechst dye (1µg/ml), 50 µl propidium iodide (2µg/ml) and 900 µl of DMEM. The cells were then incubated for 10 minutes and examined under the fluorescent microscope. The settings on the microscope were the following: excitation wavelength 365 nm and emission wavelength 420 nm and magnification was 32 X. Five random fields of visualization were taken in each well in order to obtain a reliable count. The cells were scored as being live, apoptotic and necrotic according to color and morphology (Figure 2.1) and expressed as percentages of the total count in each well. Using a Sony camera attached to the microscope, pictures of each category could be taken.

2.5 Cellular oxidative stress measurement

In order to determine the involvement of oxidative stress in the cellular damage induced by efavirenz, the nitroblue tetrazolium (NBT) and thiobarbituric acid reactive substances (TBARS) assays were carried out.

2.5.1 NBT assay

The NBT assay is based on the reduction of the yellow nitrotetrazolium salt by superoxide anions to the blue water insoluble formazan product. By measuring the absorbance spectrophotometrically at a wavelength of 700 nm, this assay can provide a relatively reliable indication of oxidative stress generation in the treated cells.

24 hours prior to the experiment, the cells were grown in 12-well plates and treated with 900 μl of efavirenz for 2, 4 and 6 hours. In order to get the final concentration of 25 μg/ml in each well, 100 μl of an NBT solution was added to each well including the control wells that contained 900 μl of DMEM.

Following incubation (37 °C and 5 % CO_2) for 2, 4 and 6 hours, the solutions were removed from the wells and the cells were washed with 1ml of 70 % methanol for ten minutes. Following further washes with 100 % methanol, the cells were left to air dry and 400 μl of a 5ml KOH/6ml DMSO solution was added to each well and left at room temperature for ten minutes.

Prior to reading the absorbance at 700 nm (Oasys UVM 340 spectrophotometer, Digiread software), the cells were transferred in aliquots of 100 μl into a 96 well plate. The intensity of the blue colour was correlated with the level of oxidative stress generated with each drug treatment and expressed as percentages of the control.

2.5.2 TBARS (MDA) assay

Oxidative stress generates highly unstable lipid hydroperoxides, the decomposition of which produces malondialdehyde (MDA), which is a reliable indicator of lipid peroxidation.

The cells were subconfluently cultured in 6 well plates and exposed to 3, 10 and 30 μM of efavirenz for 24 hours. The cells were lysed using 150 μl of cold 0.1 M Tris-HCl buffer at pH 6.8, containing 1 % (w/v) SDS and 1 % (v/v) Protease inhibitor cocktail.

The lysate was then made clear by centrifugation at 15000 g at 4 °C for 15 minutes. The aliquot of 125 μl clear lysate was mixed with 50 μl of 10 % (w/v) SDS and 250 μl of 20 % (v/v) acetic acid followed by the addition of 750 μl of 0.67 % (w/v) TBA in a test tube. The mixture was then incubated in a water bath at 100 °C for one hour, allowed to cool and 500 μl of water added to each test tube followed by centrifugation. The absorbance was measured spectrophotometrically at a wavelength of 532 nm using an Oasys UVM 340 spectrophotometer (Digiread software) and the results expressed as a percentage of untreated control cells (Figure 2.2).

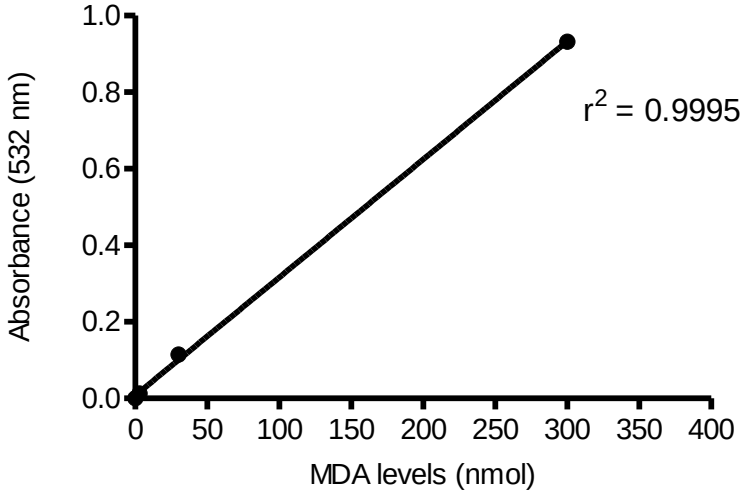

Figure 2.2: A representative MDA standard curve

2.6 Immunoblot

2.6.1 Protein extraction

Cells were incubated in dishes and allowed to grow until they reached confluency. The radio immunoprecipitation assay (RIPA) buffer was made up containing 150 mM sodium chloride, 50 mM tris at pH 7.4, 1 mM EDTA, 1 % triton-X, 0.1 % SDS, 1 mM PMSF and 1 ml protease inhibitor cocktail. The cells were washed with cold PBS for five minutes followed by the addition of a 10 ml RIPA solution to each well and incubation of the dishes in the cold room (4 °C) for 30 minutes. After scraping and adding additional buffer to the dishes in order to detach most cells from the surface, the cells were transferred to labeled 15 ml tubes. Using a 21G syringe with needle, the contents of the tubes were drawn up and down several times until a foamy solution was formed and centrifuged at 13,500 rpm for 10 minutes at 4 °C. The supernatant was then collected into different labeled centrifuge tubes and stored at - 20 °C for protein determination using the Bradford assay and protein expression using western blotting.

2.6.2 Protein determination (Bradford assay)

The Bradford assay was first described by Bradford in 1976 and consists of a standard colorimetric assay used to determine total protein concentration. By using albumin at concentrations 0, 1, 2, 3, 4 and 5 μg/ml, a standard curve could be plotted.

After adding 200 μl of Bradford reagent to 5 μl of the standard solutions including a blank solution, the 96 well plate was left at room temperature for ten minutes and the standard curve could be plotted with each standard albumin against its corresponding concentration (Figure 2.3) (540 nm spectrophotometer).

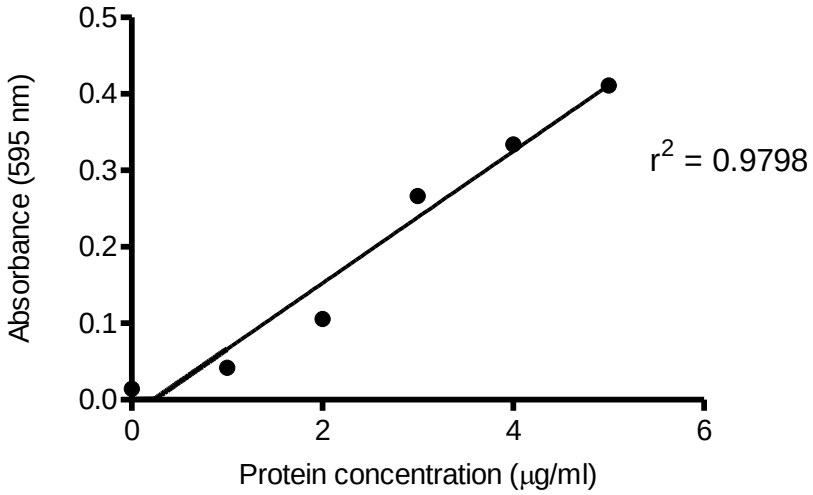

Figure 2.3: A representative protein standard curve

2.6.3 Protein expression assay – Western blotting

The western blotting technique was first described and developed by Burnette in 1981.

2.6.3.1 Preparation of the gel

The glasses were washed with 70 % ethanol and fixed into the support machine. After loading with water to ensure that there was no leaking, the running gel (Table 2.1) was loaded and allowed to set.

A stacking gel (Table 2.2) was then prepared and the gel added all the way to the top. The 10 well comb was then inserted in one movement and the water bath heated to 65 °C. A solution of 50 μl beta-mercaptoethanol and 950 μl Laemmli sample buffer (BioRad) was made up known as the loading buffer. An equal volume of sample and loading buffer was made up by adding PBS and the total sample volume was 50 μl. The resulting sample solution was heated at 65 °C for five minutes, refrigerated for ten minutes and kept on ice until the loading of the wells.

2.6.3.2 Running step

The running buffer (Table 2.3), which is ten times concentrated, was poured in the middle and around the glass on each side and the comb slowly pulled out. The samples (15 μl) were then loaded into the wells, including the marker, which is also known as the 'molecular ladder'. A first running was carried out at 100 volts for 15 minutes until the samples reached the lower gel. A second running at 120 volts was then performed until the end (approximately 1 hour 30 minutes). Before the end of the running, the pads, filter paper and membrane were immersed into the transfer buffer for ten minutes.

2.6.3.3 Transfer step

The gels were taken out and transferred onto the membrane after making it 'wet' with the transfer buffer. A 'sandwich' was made consisting of pad, filter paper, gel, membrane, filter paper and pad.

Any air bubbles were removed by applying gentle compression with a Pasteur pipette. This was then put in the transfer machine with the magnetic stirrer at the base and a block of ice at the back. The transfer buffer (Table 2.4) was added and the machine put on the top of the stirrer, followed by the actual 'transfer' for 1 hour 15 minutes at 100 volts in the cold room.

2.6.3.4 Blotting step

The membrane was blocked with T-TBS (0.1 %) and milk (5 %) for one hour in a taper and placed on a shaker at room temperature. The blocking mixture was then discarded, the primary antibody (Table 2.5) added and left overnight in the cold room. The following day the antibody solution was removed and stored in the freezer. After adding T-TBS (0.05 %), the membranes were washed three times at 10 minutes intervals. The secondary antibody (Table 2.5) was added and left on the shaker for 2 hours 30 minutes at room temperature. The secondary antibody mixture was discarded and the membranes washed three times at 10 minutes intervals. The membrane was then exposed to the film for variable times.

2.6.3.5 Development step

Further 4 washes were carried out at 10 minutes interval, immersed in an ECL plus detection solution (ECL Western Blotting Detection System, Amersham, Buckinghamshire, UK) for five minutes and drained of excess fluid. After wrapping in cling film, the membranes were exposed to a Kodak Biomax light film ECL hyperfilm in a cassette for 5 minutes followed by development in a Xograph Compact X4 automatic developer.

The expression of the protein could then be determined by comparing its size with the molecular ladder.

2.6.3.6 Preparation of solutions/reagents

Substance	Volume
Bis acrylamide 30 % (w/v)	3.3 ml
H_2O	4.3 ml
1.5 M Tris pH 8.8	2.5 ml
10 % SDS	100 µl
10 % APS	100 µl
TEMED	14 µl to be added prior to use only

Table 2.1: The constituents of the running gel

Substance	Volume
Bis acrylamide 30 %	830 µl
H_2O	2.8 ml
0.5 M Tris pH 6.8	1.26 ml
10 % APS	50 µl
10 % SDS	50 µl
TEMED	10 µl to be added prior to use only

Table 2.2: The constituents of the stacking gel

Substance	Volume
Glycine	144 g
Tris base	30.3 g
10 % SDS	10 ml

Table 2.3: The constituents of the running buffer

Substance	Volume
10 x Running buffer	100 ml
Methanol	200 ml
H_2O	700 ml

Table 2.4: The constituents of the transfer buffer

APS, ammonium persulfate; SDS, sodium dodecyl sulfate; Tris, hydroxymethyl)aminomethane; TEMED, tetramethylethylenediamine,

Primary Antibody	Blocking solution	Blotting solution	Primary antibody dilution	Secondary antibody solution	Secondary antibody dilution
Anti-CHOP	5 % milk in T-TBS	2.5 % milk in T-TBS	1: 500	2.5 % milk in T-TBS	1: 2,500
Anti-Actin	5 % milk in T-TBS	5 % milk in T-TBS	1: 10,000	5 % milk in T-TBS	1: 5,000

Table 2.5: The antibody solutions (Santa Cruz, Insight Biotechnology, Wembley, UK; Upstate Biotechnology, UK)

2.7 Ring experiments

The effect of the Atripla components on endothelial function was measured *ex vivo* using rat aortic rings connected to a transducer, providing an indication of the increased cardiovascular risk posed by antiretrovirals. For the experiments, thoracic aortae were isolated from male Wistar rats (University of Sussex) after the removal of periadvential fat. For each experiment, on average, 12 rings were isolated from each aorta and placed in a 12-well plate containing the different drug solutions as well as the control.

The rings were then incubated for 2, 4 and 6 hours and the transducer (IX-1188) was prepared in order to measure the isometric tension of the rings following the incubation period. After each incubation period, the rings were hung in a standard temperature and gas equilibrated Krebs' solution (Figure 2.4). The digital software used to visualise the tension curves was Chart version 5.2.2. A dose response curve to phenylephrine was first obtained by adding increasing concentrations of phenylephrine at 90 seconds intervals in order to pre-constrict the rings.

Then, increasing concentrations of Acetylcholine according to response were added to stimulate eNOS activity and induce vasorelaxation, thus determining the presence of any endothelial dysfunction following treatment with the different drugs. At least 6 rings per experimental treatment were combined and analysed for statistical significance.

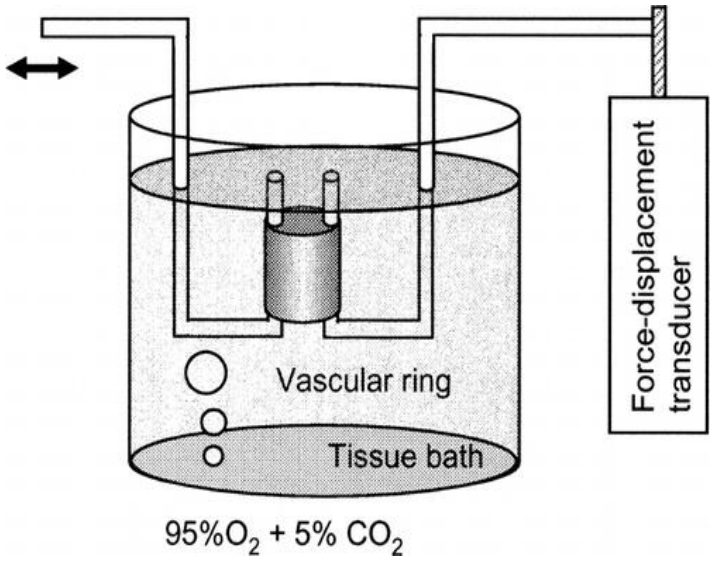

Figure 2.4: Illustration of the rat aortic ring organ bath

2.8 PARP assay

Measurement of PARP activity was conducted by the measurement of tritiated incorporation of NAD^+ as previously published (Mabley *et al.*, 2001). Briefly, ^{3}H-NAD was added to the buffer, giving a final concentration of 0.5 μCi/ml. After the incubation period, the culture medium was discarded and hot buffer (500 μl) was added to the wells and incubated for 15 minutes. The cells were then scraped from the wells and the solution transferred to Eppendorf tubes to which were added 200 μl of ice cold 50 % trichloroacetic acid (w/v TCA) and refrigerated for 4 hours.

Following this incubation period, the tubes were centrifuged at maximum speed for ten minutes followed by two subsequent washes with 500 μl ice-cold 5 % TCA. After aspirating off the second TCA wash, 2 % SDS:0.1 M NaOH (250 μl) was added and left overnight. The contents were transferred to 7 ml scintillation vials and 4 ml of Optiphase Scintillation fluid were added. Using a Beta Scintillation counter in Tritium spectrum, the samples were counted and the counts per minute used to express percentages of untreated control cells.

2.9 Barrier function measurement

In order to determine the effects of the various treatments on the transmembranal permeability, a barrier function assay was used. For this experiment, bEnd.3 cells were cultured on membrane inserts that were placed in 6 well plates. The plates were incubated at 37 °C and 5 % CO_2 and regularly visualised under the microscope until a tight cell monolayer was formed. Following drug treatment for 24 hours, the cells in the top portion were treated with 2 ml of a 200 μM albumin solution and 3 ml of non-albumin containing medium was placed in the bottom layer and left for 1 hour. Albumin levels were then determined in both top and lower solutions. The bromocresol green dye was made by mixing 25 ml of 1M NaOH with 600 ml of distilled water followed by the addition of 5.6 g succinic acid and 56 mg bromocresol powder. The volume was made up to 1000 ml with distilled water with pH 4.15.

2.10 Statistical analysis

All data described in the text and figures are expressed as mean ± SEM (standard error of mean) for n observations. The commercially available software GraphPad Prism version 5.0 (GraphPad Software, Inc., San Diego, CA, USA) was used to graph and analyse data. When only 2 means were compared, an unpaired, two-tailed Student's t-test was used. When more than 2 means were compared, a one-way analysis of variance (ANOVA) was performed, followed by a Dunnett's post-hoc test to compare each mean to the control. When only 2 means were compared post-hoc, an unpaired, two-tailed Student's t-test was used, whereas Bonferroni adjustment was used for making post-hoc comparisons for more than 2 means. Least square regression was used to calculate the line of best fit for the standard curves.

For the ring experiments, a two-way ANOVA was carried out, followed by Bonferroni's adjustment. The effective dose producing 50% maximal relaxation (EC_{50}) to ACh (log concentration) was calculated based on the curve fitting using log (inhibitor) vs. response variable slope (four parameters) with GraphPad Prism. A p-value of < 0.05 was accepted as statistically significant.

Chapter 3

Atripla - mediated cytotoxicity and potential protective strategies in the myocardial cell line H9c2

3.1 Introduction

The detrimental effects caused by HAART on cardiac cells have been well documented. Indeed, myocardial mitochondrial toxicity mediated by mitochondrial DNA depletion has been shown to alter myocardial function and structure (Dube *et al.*, 2008; Lewis *et al.*, 2006). The link between HAART and an increased risk of developing a myocardial infarction has been profoundly studied (Friis-Moller *et al.*, 2007).

H9c2 cardiomyocytes, an established cell line obtained from the embryonic rat ventricle is considered to be a good model to investigate the deleterious effects of pharmaceutical drugs on the heart. This immortalised cell line displays many of the myocardial cell characteristics, commonly used for cytotoxicity studies. The original BDIX clonal cell line was first described in 1976 by B. Kimes and B. Brandt and has since been used extensively in cardiovascular research, in particular because of the difficulty of isolated cardiac cells to replicate *ex vivo* (Kimes and Brandt, 1976). The H9c2 cells are a valid model to study various conditions such as ischaemia/reperfusion and diabetes.

Studies by L'Ecuyer et al. have shown that this cell line can be useful in elucidating free radical generation in cardiac injury (L'Ecuyer *et al.*, 2001; L'Ecuyer *et al.*, 2006). PPAR receptor activation in H9c2 cells has been shown to play a role in the protection against oxidative stress-induced apoptosis.

With anti-retroviral drugs demonstrating an increased risk of cardiovascular complications, the work presented in this chapter investigates the direct effects of the Atripla components, efavirenz, emtricitabine and tenofovir on H9c2 cells. In addition, as H9c2 cells have PPAR-γ receptors, the protective effect of PPAR-γ agonists was also studied.

3.2 Methods

3.2.1 Treatment protocols

In order to assess the effect of the different Atripla components on cellular functions, H9c2 cells were treated with increasing concentrations of the individual drugs efavirenz, emtricitabine and tenofovir. The concentrations chosen were 3, 10, 30 and 100 μM as they are clustered around the Cmax for each drug (efavirenz 12.9 μM, emtricitabine 7.28 μM and tenofovir 1.03 μM) (AIDSinfo, 2006). Depending on the experiment, cells were treated with the drug for between 2 and 48h. In some experiments, the H9c2 cells were treated with various pharmacological inhibitors of PARP (PJ-34 3 μM), NF-κB (QNZ 25, 50 and 100 nM and BAY 1, 3 and 10 μM) and cJun NH2-terminal kinase (JNK) (SP600125 10, 25 and 50 μM) to determine the role these play in any deleterious effects observed with the components of Atripla.

Rosiglitazone at 1, 3 or 10 μM was used to determine whether it was a potential therapeutic strategy to prevent cardiovascular side effects of any Atripla components. In the majority of experiments, rosiglitazone was added simultaneously with the Atripla components but in a series of addition experiments, H9c2 cells were either pre-treated or post-treated with rosiglitazone. The role of PPAR-γ and AMPK in the effects of rosiglitazone were investigated using specific inhibitors GW9662 (10μM) for PPAR-γ and Compound C (2 μM) for AMPK as well as activators GW1929 for PPAR-γ and AICAR for AMPK. After the appropriate treatment protocols, the following cellular parameters were then measured:

3.2.1.1 Cell viability

The cell viability following exposure to the different treatments was measured using the MTT assay, which is a colorimetric assay as fully described in Chapter 2.

3.2.1.2 Necrosis and apoptosis levels

Cell death measurement was performed by morphological analysis using the HPI staining method, by which the relative numbers of live, apoptotic and necrotic cells were counted under a fluorescence microscope as previously described in Chapter 2.

3.2.1.3 Oxidative stress

Levels of oxidative stress were measured using two assays. The MDA assay, a reliable method to evaluate the decomposition product of lipid peroxidation, specifically malondialdehyde (MDA) was performed as described in Chapter 2. The NBT assay is a reliable colorimetric assay used to detect the generation of superoxide anions as described in Chapter 2 and was used as an oxidative stress indicator.

3.2.1.4 PARP activation

PARP activation was measured by determining tritiated incorporation of NAD^+ into cellular proteins following exposure to the individual treatments as fully mentioned in Chapter 2.

3.2.1.5 Endoplasmic reticulum stress

ER stress was measured by determining the protein expression of specific cellular markers C/EBP homologous protein (CHOP) using western blotting as described in Chapter 2. Actin expression was used as a loading control.

3.2.2 Statistical analysis

Statistical analysis was performed using a one-way ANOVA and Student's t-test as fully described in Chapter 2.

3.3 Results

3.4 The effect of the Atripla components on H9c2 cells

Efavirenz was the only component of the Atripla pill to cause significant loss in cell viability with emtricitabine and tenofovir having no deleterious effect at the pharmacologically relevant concentrations. Efavirenz markedly reduced cell viability in a dose- and time dependent manner (Figure 3.1).

Tenofovir and emtricitabine were also seen to cause a significant time-dependent drop in cell viability but at a very unphysiological concentration (100 µM) (Figure 3.1).

When HPI staining was performed on the cells, efavirenz was the only drug seen to increase levels of apoptosis and necrosis after 24 hours in a dose dependent fashion. With regards to the mode of cell death, the cells seemed to be equally affected by apoptosis and necrosis, suggesting the presence of both pathways. Exposure to increasing concentrations of the other two Atripla components emtricitabine and tenofovir did not have a marked effect on the cells (Table 3.1).

Statistical analysis was performed using a one-way ANOVA, followed by Dunnett's post-hoc test (vs. Control). Time-dependent comparisons between 24- and 48-hour treatments were performed using a two-way ANOVA, followed by Bonferroni's adjustment.

A

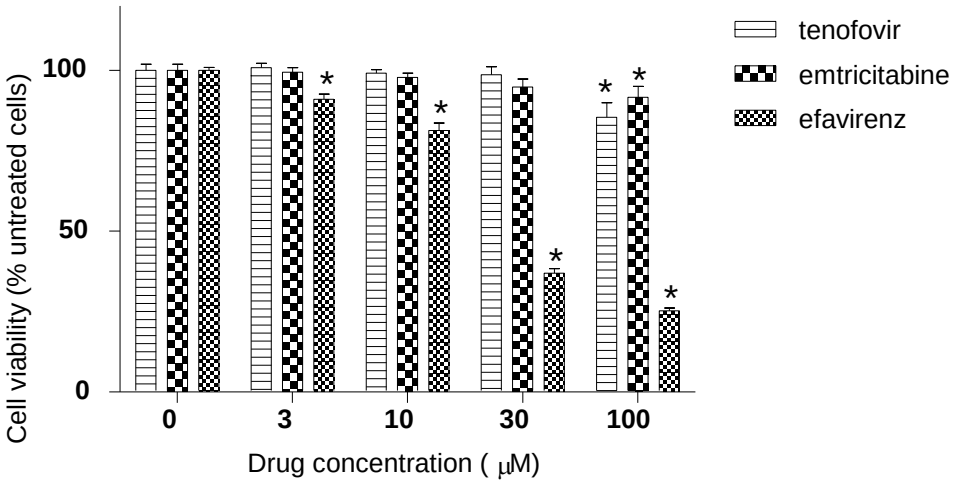

B

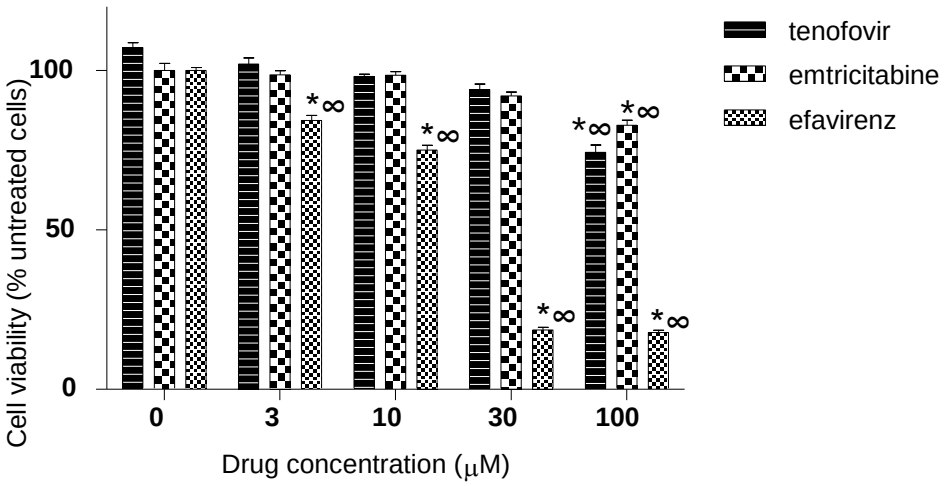

Figure 3.1: *Effect of the Atripla components on H9c2 cell viability (MTT) after 24 (A) and 48 (B) hours. Cells were treated with increasing concentrations (3, 10, 30 and 100 μM) of the individual components efavirenz, emtricitabine and tenofovir. Data are expressed as mean ± SEM of 4 experiments (6 replicas per experiment). * p < 0.01 when compared with control heart myoblasts (untreated cells) and ∞p < 0.01 when the 24-hour treatment was compared with the 48-hour treatment.*

A

	Live	Apoptotic	Necrotic
Control	98.50 ± 0.40	1.06 ± 0.15	0.80 ± 0.27
3 µM efavirenz	91.86 ± 3.93	3.33 ± 1.40*	4.99 ± 3.50
10 µM efavirenz	77.86 ± 5.79**	11.05 ± 4.39*	11.01 ± 4.96*
30 µM efavirenz	60.29 ± 12.35**	17.92 ± 11.09*	21.79 ± 4.85**

B

	Live	Apoptotic	Necrotic
Control	96.60 ± 0.22	1.86 ± 0.03	1.55 ± 0.19
3 µM emtricitabine	95.96 ± 0.61	2.16 ± 1.01	1.89 ± 0.40
10 µM emtricitabine	96.90 ± 0.06	1.64 ± 0.05	1.47 ± 0.11
30 µM emtricitabine	97.17 ± 0.00	1.47 ± 0.47	1.36 ± 0.48

C

	Live	Apoptotic	Necrotic
Control	96.85 ± 0.27	1.76 ± 0.61	1.40 ± 0.88
3 µM tenofovir	97.11 ± 0.11	1.84 ± 0.01	1.05 ± 0.11
10 µM tenofovir	97.06 ± 0.90	1.66 ± 0.04	1.30 ± 0.95
30 µM tenofovir	96.85 ± 0.37	1.68 ± 0.00	1.48 ± 0.36

Table 3.1: *Effect of Atripla components on H9c2 cell death (HPI) after 24 hours. Cells were treated with increasing concentrations (3, 10 and 30 µM) of the individual components efavirenz (A), emtricitabine (B) and tenofovir (C) for 24 hours. Data are expressed as mean ± SEM of 3 experiments (2 replicas per experiment). * $p < 0.05$ and ** $p < 0.01$ when compared with control heart myoblasts (untreated cells).*

3.5 The role of oxidative stress in the efavirenz-induced loss of cell viability

In order to detect oxidative stress generation by efavirenz, two assays were performed, namely NBT and MDA. Both assays were unable to fully confirm oxidative stress involvement in the cytotoxicity caused by efavirenz, despite a slight dose-dependent increase in MDA levels after 24 hours (Figure 3.2).

The NBT assay, despite showing a significant difference against untreated cells, was also inconclusive and further work will be needed to ascertain the involvement of oxidative stress in efavirenz-mediated cardiac cell dysfunction (Table 3.2).

Statistical analysis was performed using a one-way ANOVA, followed by Dunnett's post-hoc test (vs. Control).

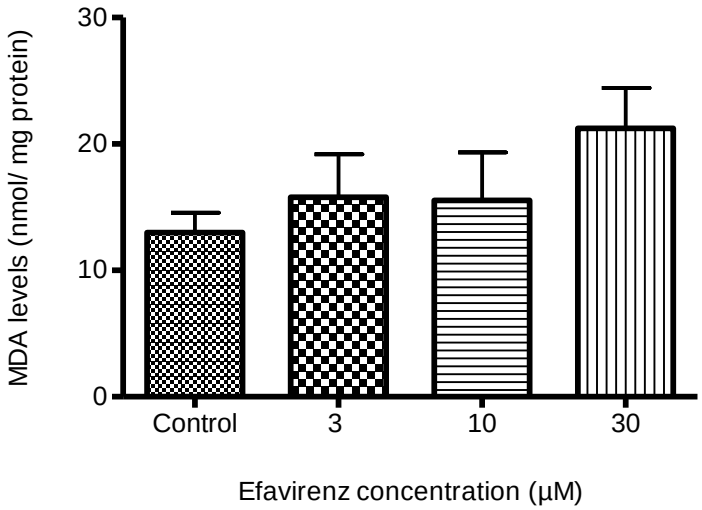

Figure 3.2: *MDA assay (oxidative stress) of efavirenz in H9c2 cells after 24 hours. Cells were treated with increasing concentrations (3, 10 and 30 µM) of efavirenz for 24 hours. Data are expressed as mean ± SEM of 2 experiments (2 replicas per experiment). * p < 0.05 when compared with control heart myoblasts (untreated cells).*

	2h	4h	6h
Control	100.00 ± 4.12	100.00 ± 1.83	100.00 ± 2.36
10 µM efavirenz	90.50 ± 2.57	84.24 ± 1.97*	90.02 ± 2.01*
20 µM efavirenz	94.22 ± 3.87	87.32 ± 2.36*	92.01 ± 3.68
30 µM efavirenz	106.89 ± 3.51	89.77 ± 2.98*	90.41 ± 1.23*

Table 3.2: *NBT assay (oxidative stress) of efavirenz in H9c2 cells. Cells were treated with increasing concentrations (10, 20 and 30 µM) of efavirenz at 2, 4 and 6 hours. Data are expressed as mean ± SEM of 4 experiments (3 replicas per experiment). * p < 0.01 when compared with control heart myoblasts (untreated cells).*

3.6 The role of PARP in the efavirenz-mediated loss of cell viability

In order to determine the role of PARP in the cytotoxicity induced by efavirenz, a PARP assay was performed. PARP activation was detected in all three components of the Atripla pill. After a 4-hour exposure to efavirenz, emtricitabine and tenofovir (3, 10 and 30 μM), only efavirenz was seen to cause a marked increase in PARP activation, suggesting an important role of PARP in the cytotoxicity seen in H9c2 cells. A 4-fold increase in PARP activity was seen with the highest concentration of efavirenz (30 μM) when compared with untreated control cells (Figure 3.3).

The addition of the pharmacological PARP inhibitor PJ-34 (3 μM) to 30 μM efavirenz for 24 hours partially reversed the loss of cell viability caused by efavirenz on its own with a 1.5-fold increase in cell viability (Figure 3.4). Using HPI staining on the cells, PJ-34 was seen to reduce the number of apoptotic and necrotic cells seen with efavirenz exposure after 24 hours (Table 3.3). As a control, exposure of the cells to 3 μM PJ-34 alone did not result in cytotoxicity. This was further confirmed by performing the PARP assay with 3 μM PJ-34 on efavirenz-treated cells (30 μM). The addition of PJ-34 markedly attenuated the 4-fold increase in PARP activity observed with efavirenz alone (Figure 3.5).

Statistical analysis was performed using a one-way ANOVA, followed by Dunnett's post-hoc test (vs. Control). In addition, an unpaired, two-tailed Student's t-test was used for comparisons between efavirenz-treated cells and efavirenz-treated cells exposed to PJ-34.

A

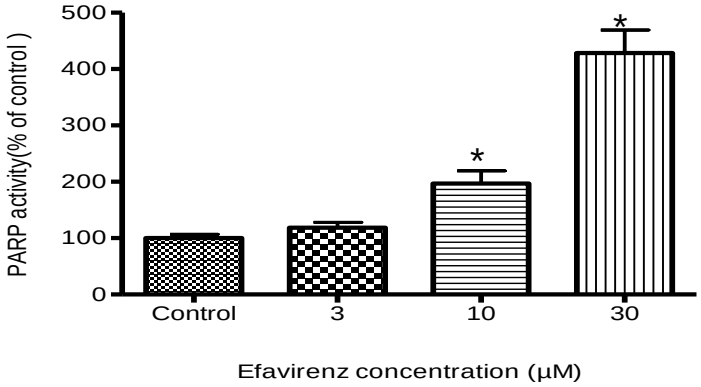

B

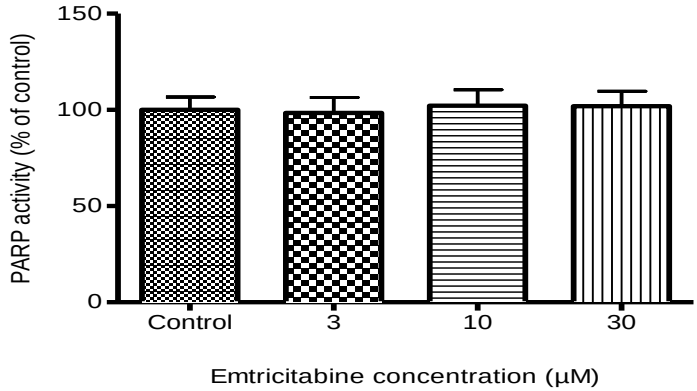

C

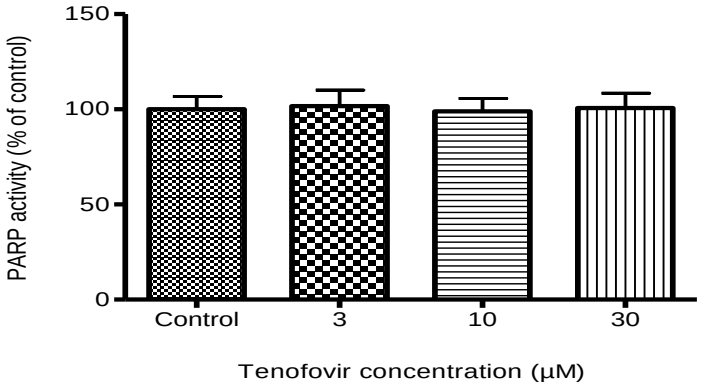

Figure 3.3: *Effect of the individual Atripla components on PARP activation (PARP assay). Cells were treated with increasing concentrations (3, 10 and 30 μM) of the individual Atripla components (A) efavirenz, (B) emtricitabine and (C) tenofovir for four hours. Only efavirenz caused a concentration dependent increase in PARP activation. Data are expressed as mean ± SEM of 3 experiments (3 replicas per experiment). * p < 0.01 when compared with control heart myoblasts (untreated cells).*

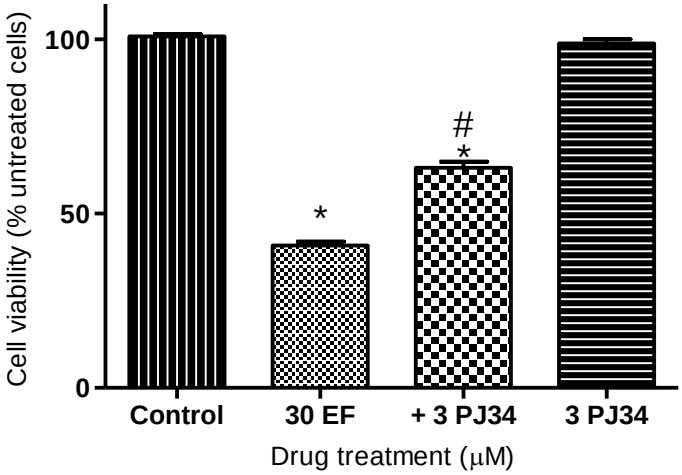

Figure 3.4: *Effect of PARP inhibitor PJ-34 on efavirenz-mediated loss of H9c2 cell viability after 24 hours. Cells were treated with 30 μM efavirenz, causing significant loss of cell viability which was partially reversed using 3 μM PJ-34. Data are expressed as mean ± SEM of 4 experiments (6 replicas per experiment). * p < 0.01 when compared with control heart myoblasts (untreated cells) and # p < 0.01 when compared with efavirenz-treated cells .*

	Live	Apoptotic	Necrotic
Control	98.15 ± 0.34	0.72 ± 0.23	1.13 ± 0.11
30 μM efavirenz	84.67 ± 4.17*	5.93 ± 1.95*	9.40 ± 0.92*
30 μM efavirenz +3 μM PJ-34	94.85 ± 1.45	2.13 ± 0.54*#	3.02 ± 0.92*#
3 μM PJ-34	97.99 ± 0.32	1.15 ± 0.16	0.86 ± 0.19

Table 3.3: *Effect of PARP inhibitor PJ-34 on efavirenz-mediated cell death after 24 hours. Cells were treated with 30 μM of efavirenz, causing significant cell death. The addition of 3 μM PJ-34 decreased the number of apoptotic and necrotic cells. Data are expressed as mean ± SEM of 3 experiments (2 replicas per experiment). * p < 0.05 when compared with control heart myoblasts (untreated cells) and # p < 0.05 when compared with efavirenz-treated cells .*

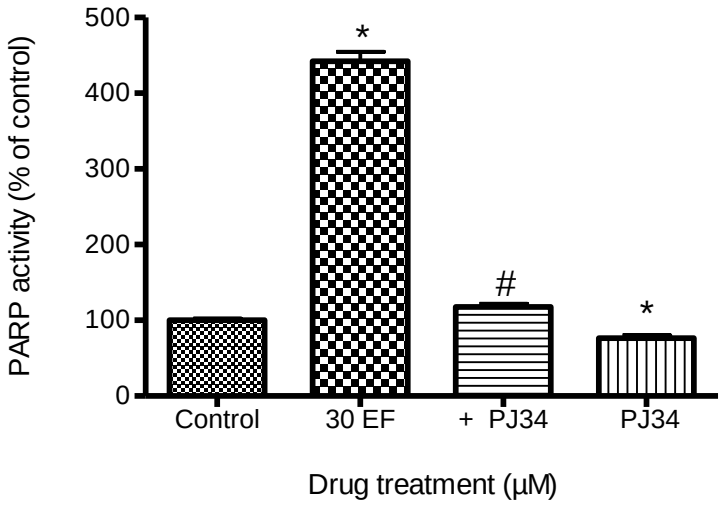

Figure 3.5: *Effect of PJ-34 on efavirenz-mediated PARP overactivation. Cells were treated with 30 μM efavirenz for 4 hours. The addition of 3 μM PJ-34 markedly attenuated the efavirenz-mediated increase in PARP activity. Data are expressed as mean ± SEM of 3 experiments (3 replicas per experiment). * p < 0.01 when compared with control heart myoblasts (untreated cells) and # p < 0.01 when compared with efavirenz-treated cells.*

3.7 The involvement of ER stress in the efavirenz-mediated loss of cell viability

In order to determine the role of ER stress in the efavirenz-mediated cytotoxicity, a series of western blots was carried out in H9c2 cell cultures treated with efavirenz and tunicamycin for 24 hours and the membranes blotted against the ER stress marker CHOP.

Exposure to increasing concentrations (3, 10 and 30 μM) of efavirenz for 24 hours was shown to dose-dependently increase CHOP expression, thus suggesting an additional mechanism of toxicity of efavirenz-mediated cytotoxicity. Compared to untreated control cells, 30 μM efavirenz was shown to markedly increase CHOP expression (Figure 3.6). The other two components of Atripla, emtricitabine and tenofovir showed no effect (Data not shown).

Exposure to the known ER stress inducer tunicamycin (positive control) at 10 μM produced a 3-fold increase in CHOP levels when compared to untreated control cells. The results obtained with efavirenz were similar with a nearly 3-fold increase in the ER stress marker (Figure 3.6 B). Actin was used as a positive control as the values were normalised based on the actin readings. This is important to correct for the total amount of protein on the membrane in case of errors.

Statistical analysis was performed using a one-way ANOVA followed by Dunnett's post-hoc test (vs. Control).

A

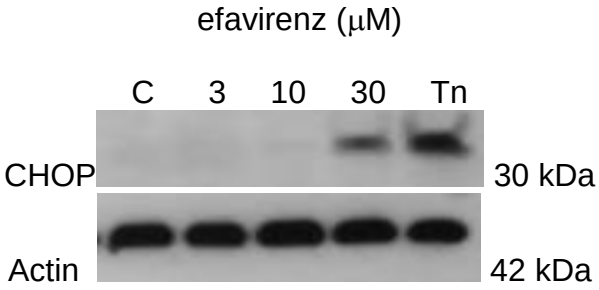

B

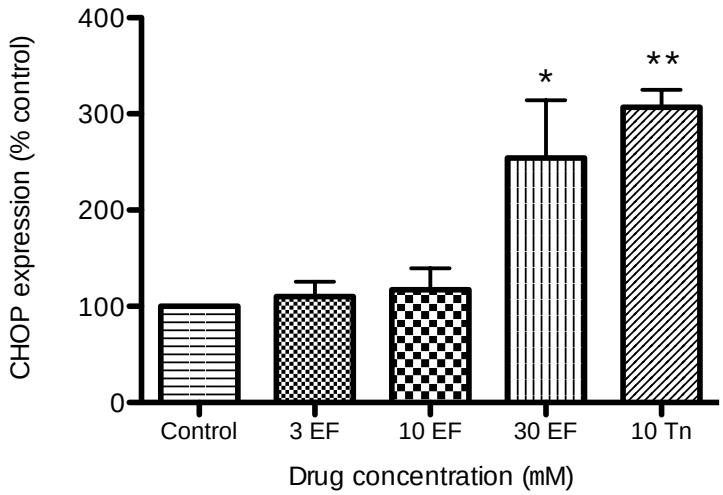

Figure 3.6: *CHOP expression in H9c2 cells treated with increasing concentrations (3, 10 and 30 μM) of efavirenz for 24 hours. (A) representative Western blot images and (B) densitometric analysis. Data are expressed as mean ± SEM of 5 experiments. * p < 0.05 and ** p < 0.01 when compared with control heart myoblasts (untreated cells).*

3.8 The activation of NF-κB and JNK by efavirenz

In order to investigate the role of NF-κB and c-Jun N-terminal kinase (JNK) in the cytotoxicity caused by efavirenz, potent inhibitors were used. QNZ (6-Amino-4-(4-phenoxyphenylethylamino)quinazoline), which displays a potent inhibitory effect on both NF-κB transcriptional activity and TNF-α production was shown to cause no effect when added to efavirenz in increasing concentrations (Table 3.4). Similarly, BAY ((2*E*)-3-[[4-(1,1-Dimethylethyl)phenyl]sulfonyl]-2-propenenitrile), which is a specific NF-κB inhibitor, has shown no significant effect when added to efavirenz (Table 3.5).

SP600125, which is a selective and reversible inhibitor of JNK, was shown to cause no significant effect when added to 30 µM efavirenz (Table 3.6).

Surprisingly, all the inhibitors were seen to cause significant toxicity on their own, which may be a confounding factor in the results observed and more direct measurements may be required.

Statistical analysis was performed using a one-way ANOVA followed by Dunnett's post-hoc test (vs. Control). In addition, Bonferroni's correction was used for comparisons between efavirenz-treated cells and efavirenz-treated cells exposed to the inhibitors.

QNZ	efavirenz	
	0 μM	30 μM
0	100 ± 1.78	30.30 ± 0.52*
25 nM	88.66 ± 0.80*	29.12 ± 0.50*
50 nM	88.73 ± 0.76*	29.54 ± 0.89*
100 nM	85.98 ± 0.51*	30.38 ± 0.56*

Table 3.4: *Effect of NF-KB inhibitor QNZ on efavirenz-mediated loss of H9c2 cell viability after 24 hours. Cells were treated with 30 μM of efavirenz, causing significant loss of cell viability. The addition of increasing concentrations (25, 50 and 100 nM) of QNZ did not show a significant difference compared to efavirenz alone. Data are expressed as mean ± SEM of 3 experiments (6 replicas per experiment). * p < 0.01 when compared with control heart myoblasts (untreated cells).*

BAY	efavirenz	
	0 μM	30 μM
0	100 ± 1.09	27.51 ± 0.47*
1 μM	88.05 ± 0.95*	28.29 ± 0.33*
3 μM	52.87 ± 1.04*	26.31 ± 0.54*
10 μM	26.52 ± 0.48*	24.48 ± 0.55*#

Table 3.5: *Effect of NF-KB inhibitor BAY on efavirenz-mediated loss of H9c2 cell viability after 24 hours. Cells were treated with 30 μM of efavirenz, causing significant loss of cell viability. The addition of increasing concentrations (1, 3 and 10 μM) of BAY did not show a significant difference compared to efavirenz alone. Data are expressed as mean ± SEM of 4 experiments (6 replicas per experiment). * p < 0.01 when compared with control heart myoblasts (untreated cells) and # < 0.01 when compared with efavirenz-treated cells.*

SP600125	efavirenz	
	0 μM	30 μM
0	100 ± 1.17	39.44 ± 1.34*
10 μM	92.79 ± 1.26*	37.86 ± 0.72*
25 μM	89.40 ± 1.27*	36.18 ± 0.97 *
50 μM	60.06 ± 1.14*	34.13 ± 1.02*

Table 3.6: *Effect of JNK-inhibitor SP600125 on efavirenz-mediated loss of H9c2 cell viability after 24 hours. Cells were treated with 30 μM of efavirenz, causing significant loss of cell viability. The addition of increasing concentrations (10, 25 and 50 μM) of SP600125 did not show a significant difference compared to efavirenz alone. Data are expressed as mean ± SEM of 3 experiments (6 replicas per experiment). * p < 0.01 when compared with control heart myoblasts (untreated cells).*

3.9 The protection of rosiglitazone against efavirenz-mediated cytotoxicity

The addition of rosiglitazone (1, 3 and 10 μM) to efavirenz (30 and 100 μM) for 24 hours was shown to dose-dependently protect against efavirenz-mediated loss of cell viability (Figure 3.7). As a control, rosiglitazone on its own at the highest concentration (10 μM) was not shown to cause any cytotoxicity after 24 hours. Similar experiments have been carried out with pioglitazone at the same concentrations used with rosiglitazone and resulted in protection against efavirenz, suggesting a drug class-specific protective effect and not a rosiglitazone - specific effect (data not shown). Using HPI staining, rosiglitazone was shown to decrease apoptosis and necrosis triggered by efavirenz after 24 hours (Table 3.7).

Cells were also pre-treated with rosiglitazone over a time period of 8 hours, followed by the removal of rosiglitazone and the addition of efavirenz at 30 μM (Figure 3.8). There was no protective effect when a 24-hour pre-treatment with rosiglitazone was performed (data not shown). Post-treatment consisted of treating the cells with rosiglitazone up to 10 hours after the start of efavirenz exposure, which still protected the cells against efavirenz-mediated loss of cell viability (Figure 3.8).

The effect of rosiglitazone on efavirenz-mediated PARP overactivation was also assessed. 30 μM efavirenz was shown to cause an over 4-fold increase in PARP activity after 4 hours, which was dose-dependently attenuated by the addition of rosiglitazone with its maximal concentration (10 μM) causing a 50 % drop in PARP activity compared to H9c2 cells exposed to efavirenz on its own. As a control, 10 μM rosiglitazone was shown to cause no increase in PARP activity, similar to untreated cells (Figure 3.9).

The western blotting was performed on H9c2 cells exposed to 30 μM efavirenz in the presence and absence of rosiglitazone (3 and 10 μM), showing a 50 % drop in the expression of the ER stress marker CHOP triggered by 30 μM efavirenz (Figure 3.10).

Statistical analysis was performed using a one-way ANOVA followed by Dunnett's post-hoc test (vs. Control) and Bonferroni's adjustment to compare efavirenz-treated cells with efavirenz-treated cells exposed to rosiglitazone.

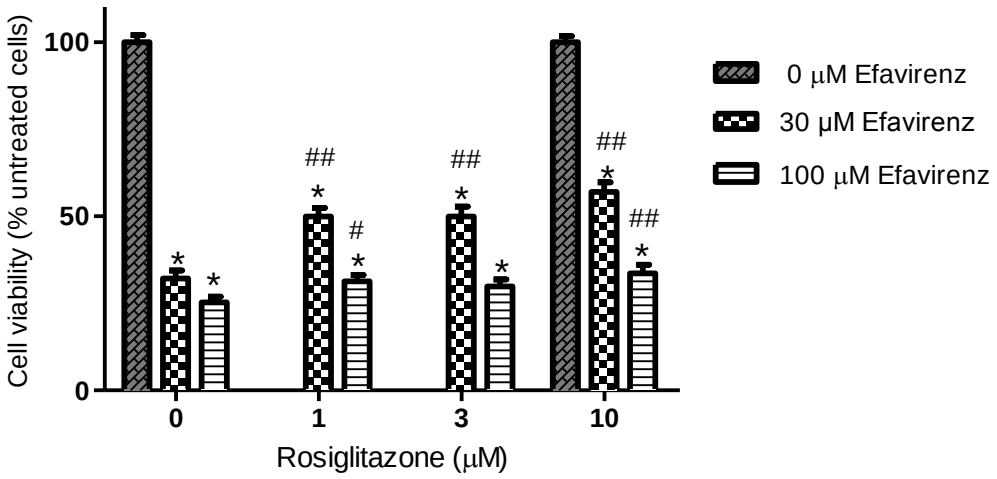

Figure 3.7: *Effect of rosiglitazone on efavirenz-mediated loss of H9c2 cell viability after 24 hours. Cells were treated with 30 and 100 μM of efavirenz with the addition of increasing concentrations (1,3 and 10 μM) of rosiglitazone for 24 hours. Data are expressed as mean ± SEM of 4 experiments (6 replicas per experiment). * p < 0.01 when compared with control heart myoblasts (untreated cells) and # p < 0.05 and ## p < 0.01 when compared with efavirenz-treated cells.*

	Live	Apoptotic	Necrotic
Control	96.42 ± 0.15	1.48 ± 0.56	2.10 ± 0.23
30 μM efavirenz	75.44 ± 0.12*	9.74 ± 1.25*	14.82 ± 0.52*
30 μM efavirenz + 3 μM rosiglitazone	94.02 ± 1.02 *#	2.30 ± 0.53*	3.68 ± 1.45*#
30 μM efavirenz + 10 μM rosiglitazone	95.45 ± 1.93*	1.44 ± 0.49	2.14 ± 0.76 #
10 μM rosiglitazone	95.45 ± 2.10	1.41 ± 0.23	3.14 ± 0.21

Table 3.7: *Effect of rosiglitazone on efavirenz mediated H9c2 cell death after 24 hours. Cells were treated with 30 μM of efavirenz in the presence and absence of rosiglitazone (3 or 10 μM). Data are expressed as mean ± SEM of 3 experiments (2 replicas per experiment). * $p < 0.01$ when compared with control heart myoblasts (untreated cells) and # $p < 0.05$ when compared with efavirenz-treated cells.*

A

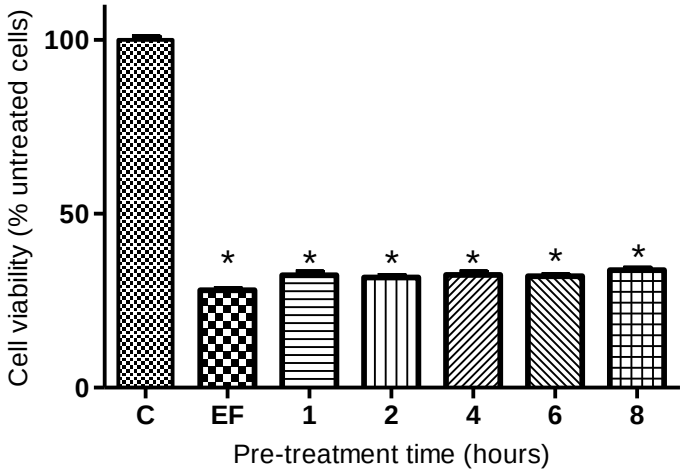

B

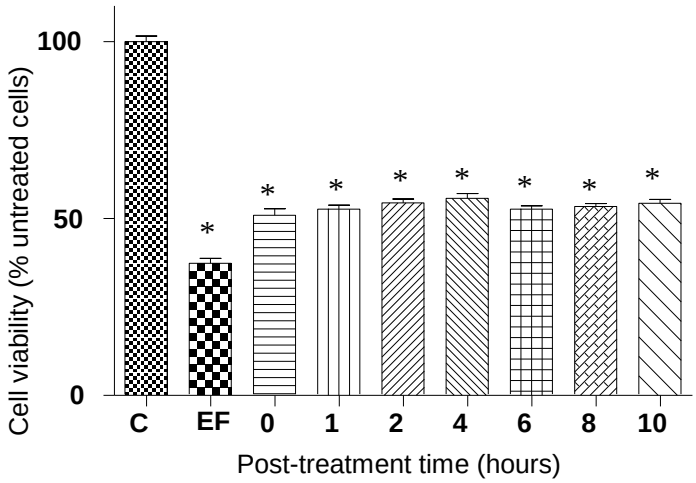

Figure 3.8: *Effect of (A) pre- and (B) post treatment with 3 μM rosiglitazone on efavirenz-mediated loss of H9c2 cell viability. (A) Cells were pre-treated with rosiglitazone over a time period of 8 hours, followed by the removal of rosiglitazone and the addition of 30 μM efavirenz. (B) Cells were treated with rosiglitazone up to 10 hours after the start of efavirenz exposure (30 μM), shown to still being able to provide protection against efavirenz-mediated loss of cell viability. Data are expressed as mean ± SEM of 3 experiments (6 replicas per experiment). * p < 0.01 when compared with control heart myoblasts (untreated cells).*

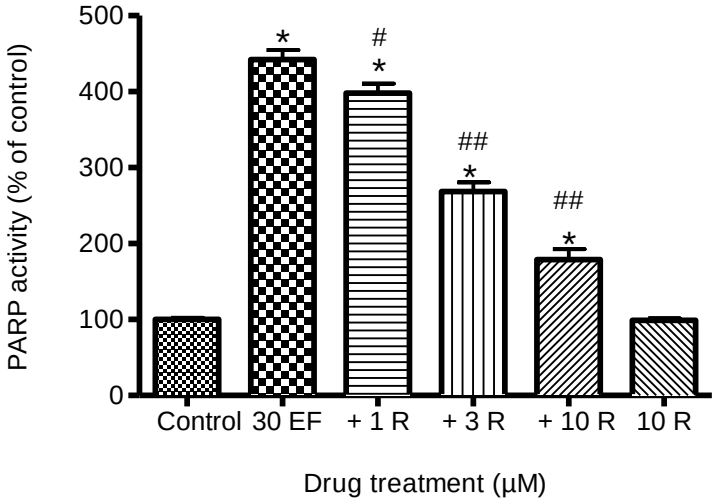

Figure 3.9: *Effect of rosiglitazone on efavirenz-mediated PARP overactivation. Cells were treated with 30 µM efavirenz for 4 hours. The addition of increasing concentrations (1, 3 and 10 µM) rosiglitazone markedly attenuated the efavirenz-mediated increase in PARP activity. Data are expressed as mean ± SEM of 3 experiments (3 replicas per experiment). * p < 0.01 when compared with control heart myoblasts (untreated cells) and # p < 0.05 and ## p < 0.01 when compared to efavirenz-treated cells.*

A

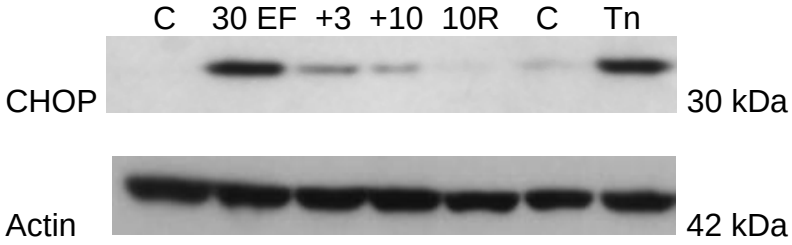

B

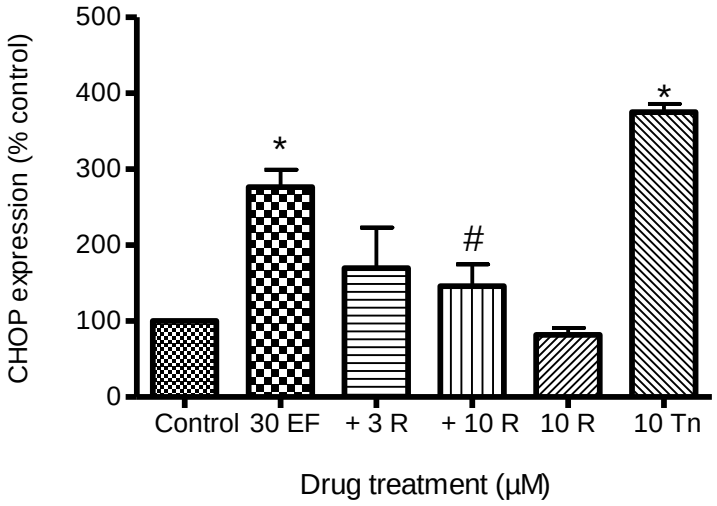

Figure 3.10: *CHOP expression in H9c2 cells treated with 30 µM of efavirenz in the presence and absence of 3 and 10 µM rosiglitazone for 24 hours. (A) representative Western blot images and (B) densitometric analysis. Data are expressed as mean ± SEM of 4 experiments. * p < 0.01 when compared with control heart myoblasts (untreated cells) and # p < 0.05 when compared with efavirenz-treated cells.*

3.10 The mechanism of protection of rosiglitazone against efavirenz-mediated loss of cell viability

Using a pharmacological inhibitor of PPAR-γ (GW9662) at 10 μM, the rosiglitazone-mediated protection (3 μM) against 30 μM efavirenz was seen to be blocked, suggesting a PPAR-γ-dependent mechanism of protection (Figure 3.11).

In order to confirm this, a pharmacological agonist of PPAR-γ was used (GW1929) at increasing concentrations (1, 3 and 10 μM) (Figure 3.12). At the concentrations used, GW1929 was not shown to confer protection against efavirenz-mediated cell damage. Neither the antagonist nor the agonist on their own showed any sign of toxicity in the H9c2 cells.

The addition of the pharmacological antagonist of AMPK (Compound C) at 2 μM to 30 μM efavirenz was not seen to block the rosiglitazone-mediated protection (3 μM), suggesting an AMPK independent mechanism of protection (Figure 3.13). Again, in order to confirm this, a pharmacological activator of AMPK was used (AICAR) at increasing concentrations (0.1, 0.25 and 0.5 mM), similar to the ones used on H9C2 cells previously (Stuck *et al.*, 2008), however no protection as seen with rosiglitazone was observed after 24 hours (Table 3.8).

Similarly, using HPI staining, the pharmacological inhibitors GW9662 (PPAR-γ) and Compound C (AMPK) failed to significantly block the protection seen with rosiglitazone against efavirenz-mediated increase in apoptotic and necrotic cells (Table 3.9 and 3.10).

Statistical analysis was performed using a one-way ANOVA followed by Dunnett's post-hoc test (vs. Control) and Bonferroni's adjustment to compare efavirenz-treated cells with efavirenz-treated cells exposed to rosiglitazone and GW9662/Compound C or with efavirenz-treated cells exposed to GW1929/AICAR.

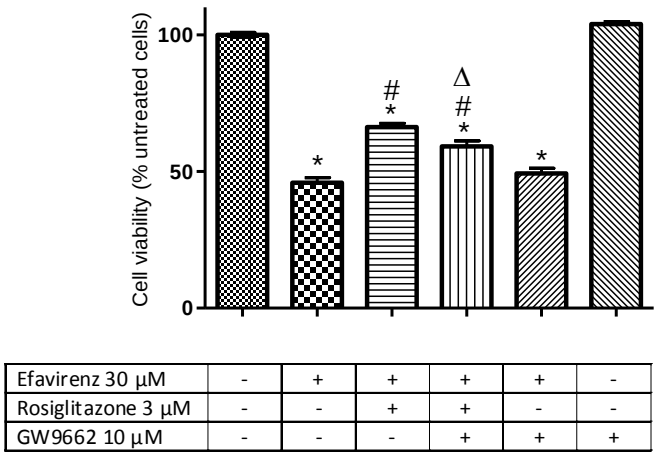

Efavirenz 30 µM	-	+	+	+	+	-
Rosiglitazone 3 µM	-	-	+	+	-	-
GW9662 10 µM	-	-	-	+	+	+

Figure 3.11: *Effect of PPAR-γ antagonist GW9662 on rosiglitazone-mediated protection against efavirenz-induced loss of H9c2 cell viability after 24 hours. Cells were treated with 30 µM of efavirenz, causing significant loss of cell viability, partly reversed by the addition of 3 µM rosiglitazone. The addition of 10 µM GW9662 was shown to block that protection. Data are expressed as mean $\pm$ SEM of 5 experiments (6 replicas per experiment). * $p < 0.01$ when compared with control heart myoblasts (untreated cells) and # $p < 0.01$ when compared with efavirenz-treated cells and Δ $p < 0.01$ when compared with efavirenz-treated cells exposed to rosiglitazone.*

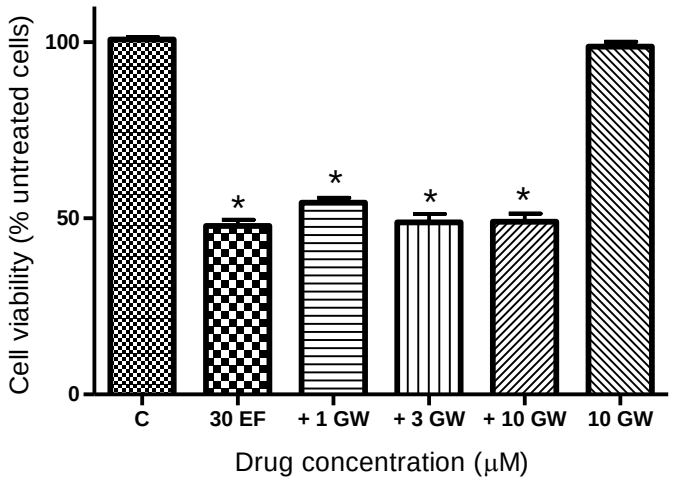

Figure 3.12: *Effect of PPAR-γ agonist GW1929 on efavirenz-mediated loss of H9c2 cell viability after 24 hours. Cells were treated with 30 μM of efavirenz, causing significant loss of cell viability. The addition of increasing concentrations (1, 3 and 10 μM) of GW1929 did not show to confer the protection seen with rosiglitazone after 24 hours. Data are expressed as mean $\pm$ SEM of 3 experiments (6 replicas per experiment). * $p < 0.01$ when compared with control heart myoblasts (untreated cells).*

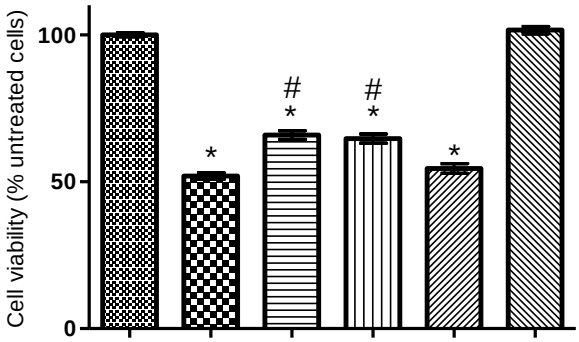

Efavirenz 30 µM	-	+	+	+	+	-
Rosiglitazone 3 µM	-	-	+	+	-	-
Compound C 2 µM	-	-	-	+	+	+

Figure 3.13: *Effect of AMPK-antagonist Compound C on rosiglitazone-mediated protection against efavirenz-induced loss of cell viability after 24 hours. Cells were treated with 30 µM efavirenz, causing significant loss of cell viability, partly reversed by the addition of 3 µM rosiglitazone. The addition of 2 µM Compound C was not shown to block that protection. Data are expressed as mean ± SEM of 4 experiments (6 replicas per experiment). * p < 0.01 when compared with control heart myoblasts (untreated cells) and # p < 0.01 when compared with efavirenz-treated cells.*

AICAR	efavirenz	
	0 µM	30 µM
0	100 ± 1.19	32.86 ± 0.62**
0.1 mM	78.04 ± 1.35**	35.76 ± 0.68**#
0.25 mM	75.97 ± 1.49**	34.90 ± 0.83**
0.5 mM	69.80 ± 1.74*	34.96 ± 0.90**

Table 3.8: *Effect of AMPK-agonist AICAR on efavirenz-mediated loss of H9c2 cell viability after 24 hours. Cells were treated with 30 µM of efavirenz, causing significant loss of cell viability. The addition of increasing concentrations (0.1, 0.25 and 0.5 mM) of AICAR was not shown to confer the protection seen with rosiglitazone. Data are expressed as mean ± SEM of 3 experiments (6 replicas per experiment). * p < 0.05 and ** p < 0.01 when compared with control heart myoblasts (untreated cells) and # < 0.01 when compared to efavirenz-treated cells.*

	Live	Apoptotic	Necrotic
Control	98.66 ± 0.25	0.73 ± 0.09	0.57 ± 1.45
30 μM efavirenz	80.75 ± 3.00**	6.94 ± 0.94**	12.3 ± 2.34**
30 μM efavirenz + 3 μM rosiglitazone	94.02 ± 1.02**#	2.30 ± 0.53**#	3.68 ± 1.54**#
30 μM efavirenz + 3 μM rosiglitazone + 10 μM GW9662	93.07 ± 1.13**#	1.04 ± 0.20##	5.89 ± 1.09**
30 μM efavirenz + 10 μM GW9662	89.70 ± 5.99**	2.64 ± 1.45*#	7.66 ± 4.53**
10 μM GW9662	96.76 ± 0.81*##	1.49 ± 0.53*##	1.40 ± 0.41*#

Table 3.9: *Effect of PPAR-γ antagonist GW9662 on rosiglitazone-mediated protection against efavirenz-induced H9c2 cell death after 24 hours. Cells were treated with 30 μM of efavirenz, significantly causing cell death, partly reversed by the addition of 3 μM rosiglitazone, protection not blocked by the addition of GW9662 after 24 hours. Data are expressed as mean ± SEM of 3 experiments (2 replicas per experiment). * p < 0.05 and ** p < 0.01 when compared with control heart myoblasts (untreated cells) and # p < 0.05 and ## p < 0.01 when compared with efavirenz-treated cells.*

	Live	Apoptotic	Necrotic
Control	98.66 ± 0.25	0.73 ± 0.09	0.57 ± 1.45
30 μM efavirenz	80.75 ± 3.00**	6.94 ± 0.94**	12.3 ± 2.34**
30 μM efavirenz + 3 μM rosiglitazone	94.02 ± 1.02**#	2.30 ± 0.53**#	3.68 ± 1.54**#
30 μM efavirenz + 3 μM rosiglitazone + 2 μM Compound C	87.49 ± 4.20**	4.03 ± 1.30**	8.49 ± 3.11**
30 μM efavirenz + 2 μM Compound C	88.31 ± 3.55**	3.90 ± 1.60**	7.79 ± 2.16**
2 μM Compound C	97.39 ± 0.52*##	1.16 ± 0.18*##	1.44 ± 0.38*#

Table 3.10: *Effect of AMPK antagonist Compound C on rosiglitazone-mediated protection against efavirenz-induced H9c2 cell death after 24 hours. Cells were treated with 30 μM efavirenz, significantly causing cell death, partly reversed by the addition of 3 μM rosiglitazone, protection not blocked by the addition of Compound C after 24 hours. Data are expressed as mean ± SEM of 3 experiments (2 replicas per experiment). * p < 0.05 and ** p < 0.01 when compared with control heart myoblasts (untreated cells) and # p < 0.05 and ## p < 0.01 when compared with efavirenz-treated cells.*

3.11 Discussion

We have found for the first time that only the efavirenz component of Atripla caused significant H9c2 cell injury, with emtricitabine and tenofovir showing no deleterious effect. The loss of cell viability mediated by efavirenz was dose- and time dependent. Efavirenz, dose-dependently increased levels of both apoptosis and necrosis in cardiomyocytes. The damaging effects of efavirenz were shown to trigger an increase of the DNA repair enzyme PARP as well as increased cellular ER stress, both of which can be induced by oxidative stress. This suggested that the efavirenz-mediated dysfunction might be triggered by oxidative/nitrosative stress. In addition, many reports have previously linked the cardiotoxicity caused by highly active antiretroviral agents to oxidative stress (Day and Lewis, 2004; Hulgan *et al.*, 2003). Similar mitochondrial toxicity has been seen in treatment naïve patients, suggesting that HIV *per se* could contribute to the toxicity observed (Fiala *et al.*, 2004). Previously, a link between HAART, specifically protease inhibitors and ER stress induction has been established in hepatocytes (Cao *et al.*, 2010).

In this study, however, the assays used to investigate whether efavirenz increases oxidative/nitrosative stress proved inconclusive on the H9c2 cell line and further work will be required to determine whether the activation of PARP and/or the induction of ER stress in cardiomyocytes by efavirenz are mediated by increased oxidative stress.

Efavirenz belongs to the NNRTI class of antiretroviral agents and works by directly binding to the HIV reverse transcriptase enzyme, causing termination of the DNA chain elongation (de Bethune, 2010). HIV-infected individuals display both loss of mitochondrial membrane potential and an increase in reactive oxygen species production (Kakuda, 2000). Unlike the NRTI's which competitively inhibit the viral reverse transcriptase and thereby also inhibit the mitochondrial DNA pol-γ, the NNRTI's have shown either no or very weak inhibitory activity against DNA pol-γ, suggesting that the efavirenz-mediated toxicity may be caused by an alternative mechanism (Lewis *et al.*, 2003), possibly by an increase in oxidative stress.

A recent study has shown that efavirenz directly affected the mitochondria, caused loss of mitochondrial membrane potential and an increase in superoxide levels in hepatic cells, as well as rejecting the mitochondrial DNA pol-γ hypothesis seen with NRTI's (Apostolova *et al.*, 2010).

It is known that HAART and/or HIV *per se* can cause other mitochondrial changes, such as alterations in oxidative phosphorylation enzyme activities including loss of cytochrome c oxidase, exhibiting enhanced anaerobic ATP synthesis, leading to lactic acid production or changes in expression of uncoupling proteins without mtDNA depletion (Badley *et al.*, 2003; Gerschenson *et al.*, 2001). Efavirenz was found to increase activation PARP in cardiac myocytes, an effect that has been observed with an older anti-retroviral drug AZT (Szabados *et al.*, 1999).

AZT has also been shown to increase PARP activation in heart cells (previous own data). However, emtricitabine and tenofovir had no effect on PARP activation in H9c2 cells.

PARP is a DNA repair enzyme, which can be over activated in response to DNA single strand breaks caused by significant cellular insults such as oxidative stress, triggering an energy consuming cycle, depleting NAD^+ and ATP and eventually resulting in cell death. PARP, when bound to damaged DNA, cleaves NAD^+ into nicotinamide and ADP-ribose, using the latter to form branched nucleic acid-like polymers poly (ADP-ribose) covalently attached to nuclear proteins (Virag, 2005).

Overactivation of PARP can lead to serious cell dysfunction, particularly in the cardiovascular system where it has been shown to play a critical role in myocardial and endothelial dysfunction in ageing, diabetes and septic shock (Pacher and Szabo, 2007). Indeed, hyperglycemia-induced mitochondrial formation of reactive oxygen intermediates and PARP overactivation have been shown to be key events in the pathogenesis of diabetic endothelial dysfunction (Mabley and Soriano, 2005). This dysfunction stems from cellular depletion of NAD^+ and ATP, which can influence the activity of essential enzymes such as nitric oxide synthase, and those of the electron transport chain. PARP activation can also affect cellular gene expression increasing activities of transcription factors such as NF-κB and AP-1 leading to a pro-inflammatory response of the cells (Aguilar-Quesada *et al.*, 2007; Oliver *et al.*, 1999).

In our study, however, the NF-κB inhibitors BAY and QNZ proved inconclusive in establishing involvement in the loss of cell viability caused by efavirenz. As these pharmacological inhibitors also proved to be fairly toxic in our system, more direct measurements of second messenger activation are needed to characterise the effect of efavirenz.

As well as the functional cellular effects, PARP overactivation can also result in increased cell death by both apoptosis and necrosis. Necrosis results from the energy depletion leading to activation of the necrotic pathway. Apoptosis results from mitochondrial release of cytochrome C and AIF, the latter mediated by the poly ADP-ribose polymers, resulting in caspase-3 activation and eventually leading to apoptotic cell death (Pieper *et al.*, 1999). This is in agreement with a recent study concluding that efavirenz induced apoptosis in hepatic cells via the mitochondrial pathway, with activation of caspase-3 and -9 but not caspase-8, as well as cytochrome c and AIF (Apostolova *et al.*, 2010). HIV-1 and glycoprotein 120 (gp120) have been shown to cause significant damage in the cardiovascular system by inducing apoptosis in cardiomyocytes and endothelial cells (Fiala *et al.*, 2004).

Several groups have reported that PARP inhibitors such as 3-aminobenzamide and PJ-34 could directly protect rat cardiomyoblasts *in vitro* against oxidative stress (Bowes *et al.*, 1999; Fiorillo *et al.*, 2006), concluding that oxidant-induced PARP overactivation is involved in the cytotoxicity observed in rat heart cells.

We also found that PJ-34 was able to reduce the PARP activation associated with efavirenz exposure and also reduce both the necrosis and apoptosis levels. This suggests that efavirenz-mediated damage to H9c2 cells is mediated at least in part by an increase in DNA single strand breaks leading to overactivation of PARP. The inability for both emtricitabine and tenofovir to activate PARP may explain why these anti-retroviral agents have no effect on H9c2 cell viability.

Previous work involving unsaturated fatty acids proposed that the damage caused by efavirenz might be triggered by oxidative stress with subsequent ER stress induction (previous own data). ER stress is a cytoprotective mechanism in response to cellular insults, resulting in misfolded or unfolded proteins, inhibiting protein synthesis to allow for cell recovery. If however, the stimulus such as oxidative stress is too significant, the UPR caused by the ER stress then ultimately triggers a pro-apoptotic response. This pro-apoptotic response has been linked to the activation of second messenger systems such as JNK and ultimately increased expression and activity of the pro-apoptotic protein CHOP (Oyadomari and Mori, 2004).

Treatment of the H9c2 cells with efavirenz increased CHOP expression, a marker for ER stress. This is the first time that this has been observed with highly active antiretroviral agents and may provide an explanation as to why these agents cause cardiovascular dysfunction as well as being a prospective screening tool for potential cardiotoxicity of new anti-retroviral agents being developed.

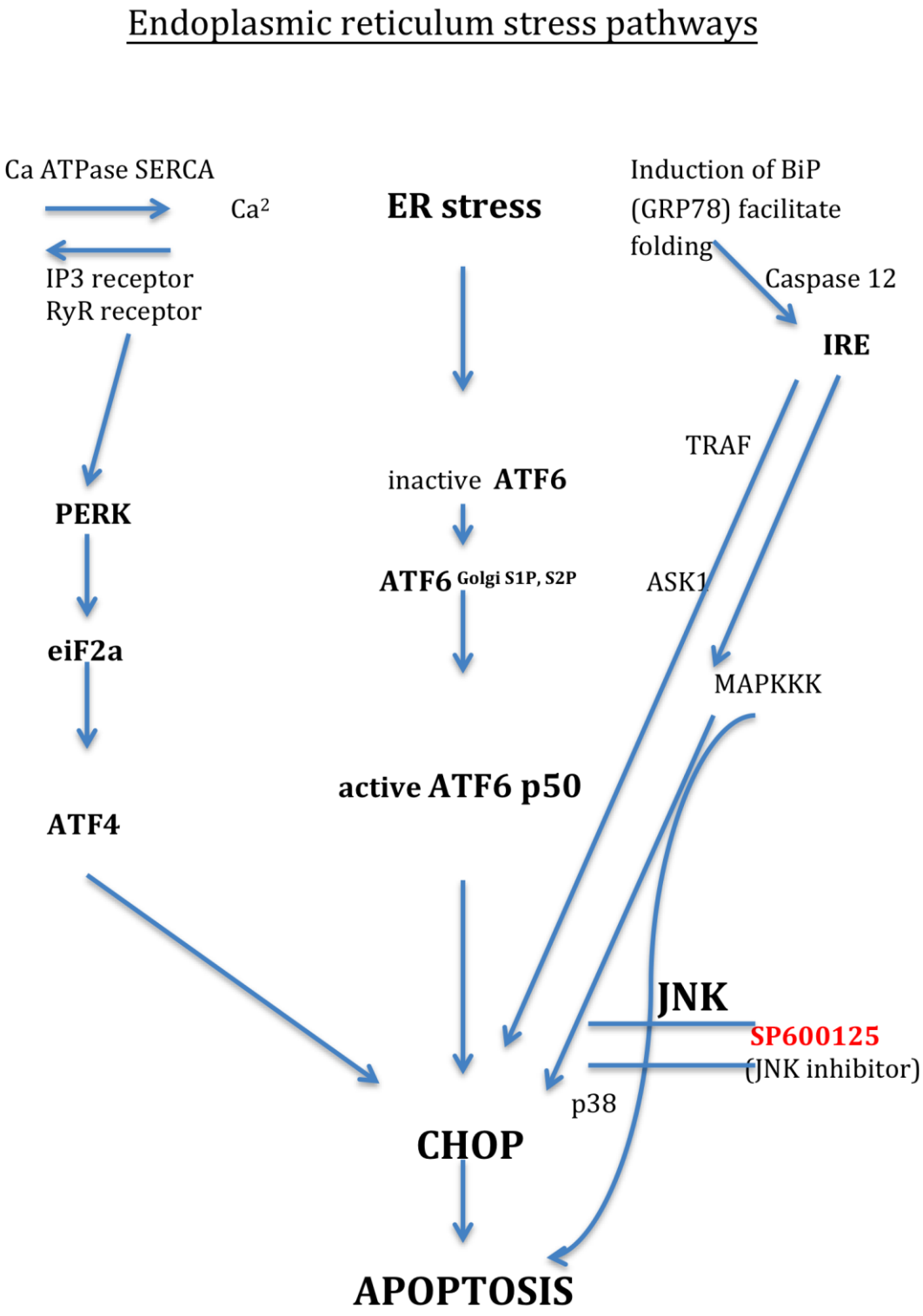

Figure 3.14: ER-stress induced apoptosis pathway

As there is a central role of second messenger systems in both PARP activation and ER stress mediated dysfunction we pharmacologically looked at the key pathways and their role in efavirenz mediated H9c2 cell dysfunction. JNK activation is thought to be involved in the apoptotic process following ER stress (Figure 3.14), however, no effect of the pharmacological JNK inhibitor SP600125 was observed on efavirenz-mediated loss of cell viability. Similarly, some groups have suggested a major role of PARP in the regulation of gene expression (Bakondi *et al.*, 2002; Virag and Szabo, 2002), a key transcription factor regulating the expression of inflammatory mediators such as chemokines

Rosiglitazone is an antidiabetic medication that belongs to the thiazolidinediones. It exerts its blood glucose regulating effect through the activation of PPAR-γ and AMPK cellular signaling pathways (Ceolotto *et al.*, 2007). A number of studies have shown rosiglitazone to be cardioprotective in pathologies mediated by oxidative stress such as ischaemia/reperfusion injury (Yue *et al.*, 2008). At the end of 2010, the drug was eventually withdrawn from the European market following reports of increased risk of MI in diabetic patients. In the U.S., it still remains available subject to restrictions (EMA assessment report, 2010). Another thiazolidinedione pioglitazone is still widely prescribed and was shown to be equally protective (data not shown).

The simultaneous addition of rosiglitazone (1, 3 or 10 μM) to H9c2 cells treated with efavirenz was able to protect against efavirenz-mediated loss of cell viability and reduce apoptosis and necrosis at pharmacological levels. In addition, pioglitazone has been studied in the same manner as rosiglitazone and has shown similar effects, suggesting a class- and not a drug specific protective effect (data not shown). Delaying the application of rosiglitazone by up to 10 hours after efavirenz exposure was still able to provide significant protection against loss of cell viability suggesting that its actions were on later components of the efavirenz-activated pathways.

Pre-treatment with rosiglitazone by up to 24 hours, however, was not shown to be protective against efavirenz-mediated loss of cell viability ruling out possible rosiglitazone effects on gene transcription or protein expression resulting in the H9c2 cells becoming more resistant to toxic insults such as efavirenz.

The protective effects of rosiglitazone have essentially been linked to the activation of PPAR-γ and AMPK. PPAR-γ is a nuclear ligand-activated transcription factor that regulates the target gene expression. It forms a heterodimer with a second receptor known as RXR, which upon binding with the ligand causes a conformational change, recruiting transcriptional co-activators such as AP-1 and NF-κB, leading to gene transcription (Ryan *et al.*, 2004).

Pharmacological activation of PPAR-γ by the agonist GW1929 showed no effect when added to efavirenz-treated cells. The PPAR-γ inhibitor GW9662, on the other hand, showed significant difference when compared with the H9c2 cells exposed to both efavirenz and rosiglitazone, which may indicate a PPAR-γ dependent mechanism of protection.

In the cell death assay, GW9662 seemed to confer protection when added to efavirenz, which may be a confounding factor. Due to this inconsistency in results, this specific PPAR-γ inhibitor may not be ideal for determining the involvement of PPAR-γ in the protection offered by rosiglitazone.

Pharmacological activation of AMPK by AICAR proved to be ineffective in mimicking the protection observed with rosiglitazone and very damaging on its own, which may also have been a confounding issue. The pharmacological inihibitor of AMPK (Compound C) did not have an effect on the protective effect mediated by rosiglitazone, concluding an AMPK-independent effect. However, rosiglitazone dose dependently inhibited efavirenz-mediated increase in PARP activity.

As inhibition of PARP proved at least partially effective in protecting cell viability and reducing both necrosis and apoptosis following efavirenz exposure this may be one possible protective mechanism by which rosiglitazone exerts its protective effect. Looking at the structure of rosiglitazone (Figure 3.15) and comparing it to known pharmacological inhibitors of PARP (Figure 3.16), there are similarities in the functional groups and as other drugs available on the market such as cilostazol have been recently shown to have direct PARP inhibitory activity so it is not inconceivable that rosiglitazone may also be a direct inhibitor of PARP.

Figure 3.15: The chemical structure of rosiglitazone

(www.rxlist.com/avandia-drug.htm, accessed 27th June 2011)

PJ-34

Figure 3.16: The chemical structure of the PARP inhibitor PJ-34

(www.chemicalbook.com, accessed 27th June 2011)

Interestingly, we also found that rosiglitazone reduced the efavirenz-mediated increase in ER stress. This is the first time that rosiglitazone has been shown to inhibit ER stress and it may explain some of its protective effects. As ER stress can lead to apoptosis, inhibition of this process by rosiglitazone may explain the observed protective effect.

ER stress is a relatively late event usually starting from 12h after the insult, supporting the results we observed with rosiglitazone still providing significant protection when added up to 10 hours after the start of the efavirenz exposure. Use of chemical ER chaperones or siRNA techniques to block CHOP activation would provide a fuller picture of the role of ER stress in efavirenz-mediated damage and whether this is the key process which rosiglitazone inhibits and provides protection.

In conclusion, efavirenz is the only component of Atripla that causes direct myocardial cell damage likely mediated by cellular PARP and ER stress activation. The protection we observed with rosiglitazone again appeared to be through prevention of the PARP and ER stress activation with the subsequent activation of apoptosis, though in a PPAR-γ-dependent and AMPK independent manner. It is unclear whether PARP activation and ER stress are linked in some way and whether PARP activation can lead to ER stress or vice versa, it may be that rosiglitazone inhibition of one of these processes affects the other and further characterisation of the protective effects of rosiglitazone is required to definitely identify its mechanism of action.

Chapter 4

Atripla - mediated cytotoxicity in rat aortic endothelial cells and in the human umbilical vein endothelial cell line EA.hy926

4.1 Introduction

Many studies have shown a prognostic link between endothelial cell dysfunction and the development of cardiovascular disease such as hypertension, atherosclerosis and heart failure. Direct effects caused by HAART on the vasculature have been reported (Dube *et al.*, 2008). It is well known that HAART has been linked with an increased risk in cardiovascular side effects but no direct cardiovascular studies of the effects of the Atripla components have been documented. The rat aortic rings used in the present project were thus a valid experimental model to study the effects of the different antiretroviral drugs on the endothelial cell function. In order to further confirm the findings, the human umbilical vein endothelial cell line EA.hy926 was used. Those cells are derived by the fusion of primary umbilical vein cells with a permanent human cell line (A549) and by exposure to polyethylene glycol. A study by Ahn et al. concluded that EA.hy926 cells preserved all the characteristics of endothelin converting enzyme (Ahn *et al.*, 1996). Endothelial function can be measured using *ex vivo* rat aortic rings as well as cultured endothelial cells. Female HIV patients are reported to exhibit fewer cardiovascular side effects from anti-HIV drugs than male patients.

The cells maintained morphological, phenotypic and functional features of human macro-vascular endothelial cells. EA.hy926 cells were therefore optimal to investigate the effects of the Atripla components efavirenz, emtricitabine and tenofovir on endothelial function.

4.2 Methods

4.2.1 Treatment protocols

In order to study the effect of the various Atripla components on the endothelial function, rat aortic rings were treated with increasing concentrations of the individual drugs efavirenz, emtricitabine and tenofovir. The initial experiments involved exposure of the rings for 2, 4 and 6 hours at concentrations 1, 3 and 10 μM of each individual drug. The involvement of PARP in the efavirenz-mediated endothelial dysfunction was assessed using the PARP inhibitor PJ-34 (3 μM) on efavirenz-treated rings (10 μM) after a 4-hour exposure.

As female patients seem to show less cardiovascular side effects compared to male patients, the involvement of oestrogen in rat aortic rings was also studied. Female aortic rings were exposed to increasing concentrations of efavirenz (1, 3 and 10 μM) for 4 and 6 hours. In order to confirm the results, the rings were exposed to efavirenz (10 μM) in the presence and absence of 17-beta oestradiol (10, 30 and 100 nM) for 4 hours.

The EA.hy926 cells were treated with 3, 10, 30 and 100 μM of the individual drugs for 24 and 48 hours. HPI staining was performed on EA.hy926 cells exposed to 3, 10 and 30 μM of the Atripla components for 24 hours. The cells were also treated with 30 μM efavirenz in the presence and absence of the PARP inhibitor PJ-34 (3 and 10 μM) for 24 hours as well as HPI staining using 30 μM and 3 μM PJ-34 for 24 hours.

PARP activity was assessed following the exposure of EA.hy926 cells to efavirenz (1, 3, 10 µM) for 2, 4 and 6 hours. The cells were also exposed to 10 µM efavirenz in the presence and absence of 3 µM PJ-34 and PARP activity measured after 4 hours. PARP deficient mouse endothelial cells (MEC -/-) were also exposed to 10 µM efavirenz and the involvement of PARP measured following a 4 hour exposure. After the appropriate treatment protocols the following cellular parameters were then measured:

4.2.1.1 Ring experiments

The effects of the Atripla components on endothelial function were assessed *ex vivo* using rat aortic rings connected to a transducer. The aortic rings were prepared and treated as fully described in Chapter 2.

4.2.1.2 Cell viability

The cell viability following exposure to the different drugs was assessed using the MTT assay, which is a colorimetric assay as fully described in Chapter 2.

4.2.1.3 Necrosis and apoptosis levels

Cell death measurement was carried out by morphological assessment using the HPI staining method, by which the relative numbers of live, apoptotic and necrotic cells were counted under a fluorescence microscope as previously described in Chapter 2.

4.2.1.4 Oxidative stress

Measurements of oxidative stress generation were assessed using two assays. The MDA assay, which is a reliable method to evaluate the decomposition product of lipid peroxidation, specifically malondialdehyde was carried out as fully described in Chapter 2. The NBT assay is a reliable colorimetric assay used to detect the generation of superoxide anions as shown in Chapter 2 and was used as an oxidative stress indicator.

4.2.1.5 PARP activation

The activation of PARP was measured by determining tritiated incorporation of NAD^+ into cellular proteins following exposure to the individual drugs as fully mentioned in Chapter 2.

4.2.2 Statistical analysis

Statistical analysis was performed using ANOVA and Student's t-test as fully described in Chapter 2.

4.3 Results

4.4 The effect of the Atripla components on endothelial dysfunction in rat aortic rings

Out of the three Atripla components, efavirenz was the only drug to cause significant decrease in endothelial function after rat aortic rings were exposed to increasing concentrations (1, 3 and 10 µM) of the different drugs for 2, 4 and 6 hours. Efavirenz caused endothelial damage in dose-dependent fashion (Figure 4.1). There was a significant increase in EC_{50} concentration of ACh following efavirenz exposure as compared to untreated control rings. Following a 6-hour exposure to 10 µM efavirenz, the EC_{50} of ACh increased from 52.13 ± 12.43 nM to 146.3 ± 26 nM ($p < 0.05$) (Table 4.1). The EC_{50} of ACh for rings exposed to efavirenz, emtricitabine or tenofovir did not show a statistically significant shift when time dependency was compared.

Neither emtricitabine nor tenofovir showed similar damaging effects over the same time range (Figure 4.2 and figure 4.3) and no change in EC_{50} was seen (Table 4.2 and table 4.3).

Statistical analysis was performed using a two-way ANOVA, followed by Bonferroni's adjustment. Time-dependent comparisons were performed using a two-way ANOVA, followed by Bonferroni's adjustment.

A (2h exposure):

Control	1 µM efavirenz	3 µM efavirenz	10 µM efavirenz
31.72 ± 7.91 nM	77.51 ± 15.93 nM *	116.5 ± 15.56 nM *	54.58 ± 11.93 nM

B (4h exposure):

Control	1 µM efavirenz	3 µM efavirenz	10 µM efavirenz
25.78 ± 3.42 nM	62.09 ± 7.12 nM	74.33 ± 11.69 nM	96.39 ± 26.92 nM *

C (6h exposure):

Control	1 µM efavirenz	3 µM efavirenz	10 µM efavirenz
52.13 ± 12.43 nM	79.61 ± 11.58 nM	133.1 ± 33.25 nM *	146.3 ± 26 nM *

Table 4.1: *Exposure to efavirenz for 2 (A), 4 (B) and 6 (C) hours increases the EC_{50} of ACh, * $p < 0.05$ when compared with untreated control rings.*

A (2h exposure):

Control	1 µM emtricitabine	3 µM emtricitabine	10 µM emtricitabine
28.39 ± 6.30 nM	28.64 ± 7.99 nM	28.91 ± 9.37 nM	27.96 ± 6.61 nM

B (4h exposure):

Control	1 µM emtricitabine	3 µM emtricitabine	10 µM emtricitabine
35.65 ± 5.21 nM	39.82 ± 6.94 nM	35.03 ± 9.79 nM	47.21 ± 6.15 nM

C (6h exposure):

Control	1 µM emtricitabine	3 µM emtricitabine	10 µM emtricitabine
36.15 ± 5.7 nM	51.62 ± 11.28 nM	81.18 ± 23.32 nM	35.13 ± 11.34 nM

Table 4.2: *Exposure to emtricitabine for 2 (A), 4 (B) and 6 (C) hours does not significantly increase the EC_{50} of ACh*.

A (2h exposure):

Control	1 µM tenofovir	3 µM tenofovir	10 µM tenofovir
33.98 ± 8.61 nM	62.87 ± 16.64 nM	73.97 ± 8.07 nM	50.43 ± 14.11 nM

B (4h exposure):

Control	1 µM tenofovir	3 µM tenofovir	10 µM tenofovir
24.65 ± 2.33 nM	47.40 ± 4.63 nM	40.73 ± 5.28 nM	23.73 ± 5.35 nM

C (6h exposure):

Control	1 µM tenofovir	3 µM tenofovir	10 µM tenofovir
43.89 ± 5.29 nM	44.42 ± 6.78 nM	85.32 ± 24.47 nM	54.30 ± 11.79 nM

Table 4.3: *Exposure to tenofovir for 2 (A), 4 (B) and 6 (C) hours does not significantly increase the EC_{50} of ACh.*

A

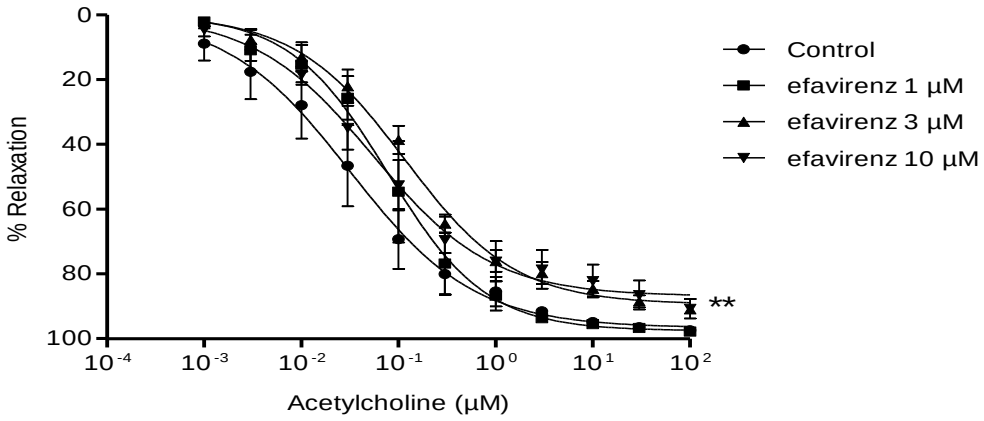

B

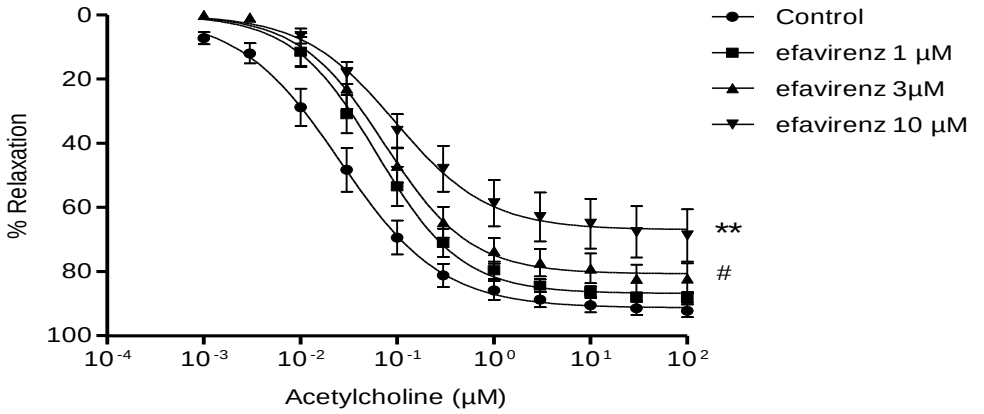

C

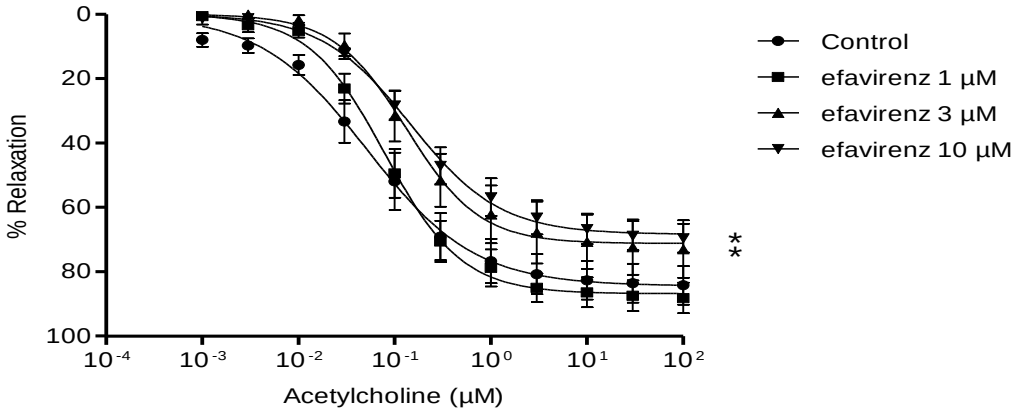

Figure 4.1: *Effect of efavirenz on the loss of endothelial function in rat aortic rings. The rings were exposed to increasing concentrations (1, 3 and 10 µM) of efavirenz for 2 (A), 4 (B) and 6 (C) hours. Data are expressed as mean ± SEM of 8 experiments * p < 0.05, ** p < 0.01 and # p < 0.001 when compared with control aortic rings (untreated cells).*

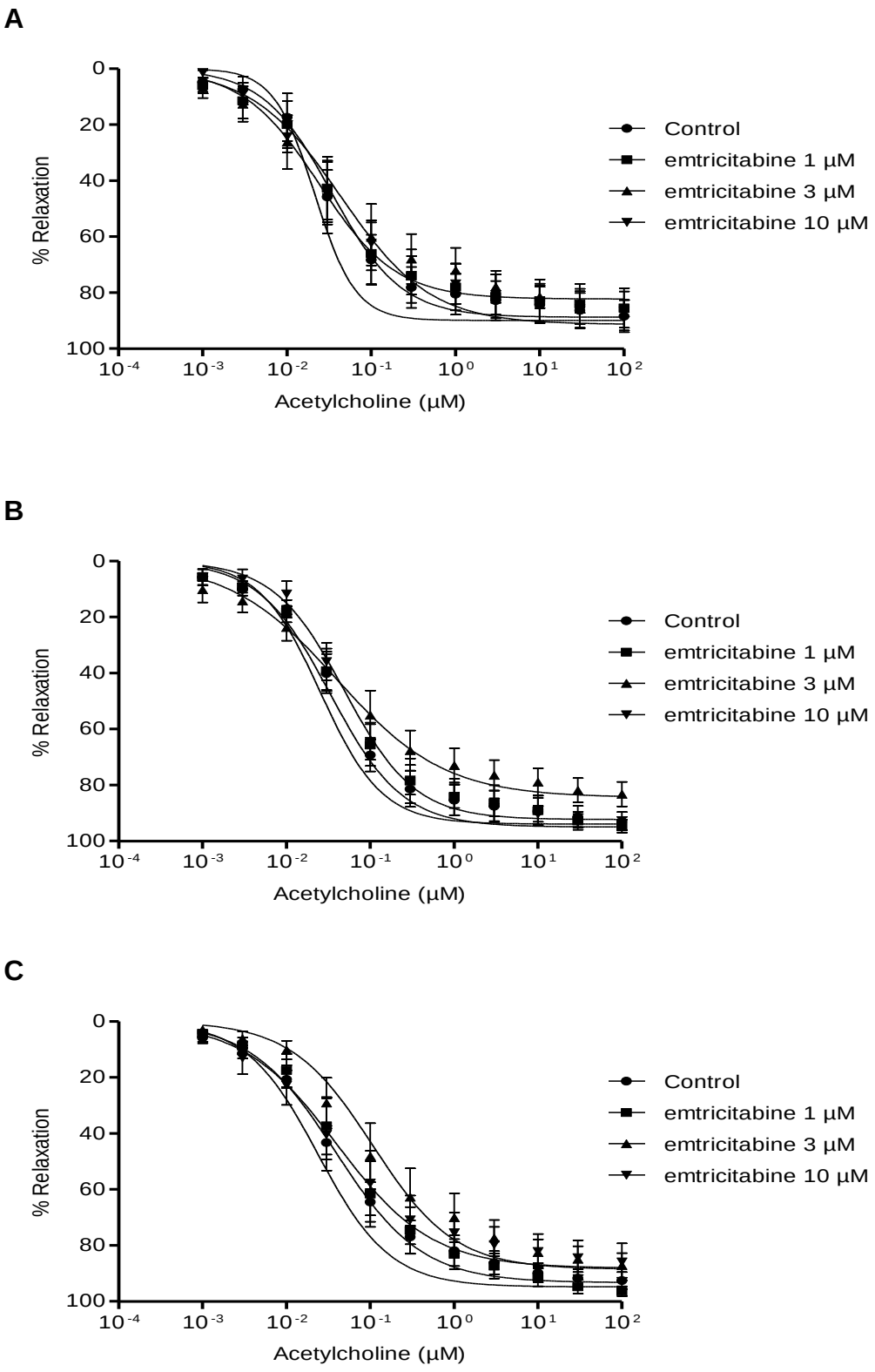

Figure 4.2: *Effect of emtricitabine on the loss of endothelial function in rat aortic rings. The rings were exposed to increasing concentrations (1, 3 and 10 µM) of emtricitabine for 2 (A), 4 (B) and 6 (C) hours. Data are expressed as mean ± SEM of 6 experiments * p < 0.05 when compared with control aortic rings (untreated cells).*

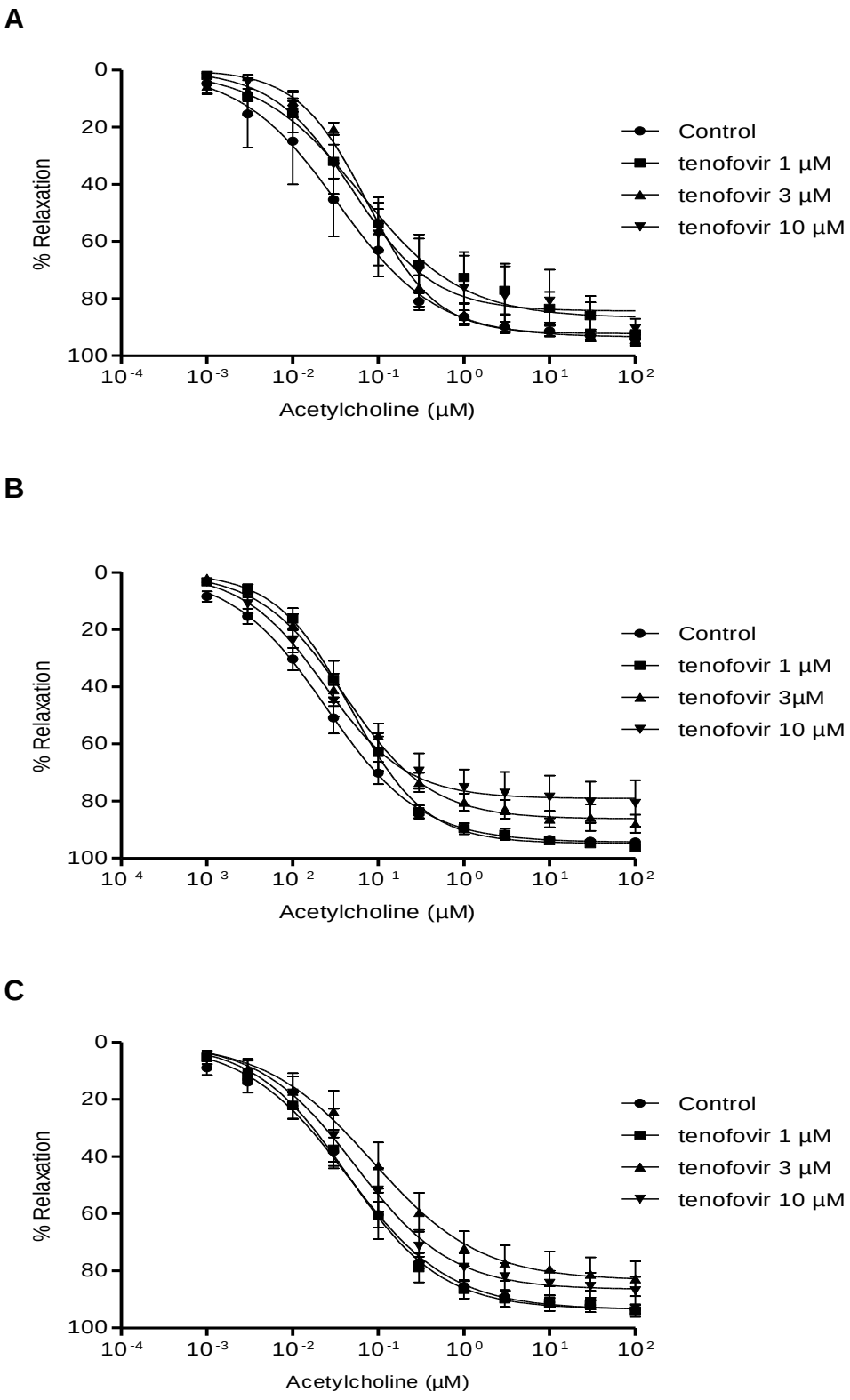

Figure 4.3: *Effect of tenofovir on the loss of endothelial function in rat aortic rings. The rings were exposed to increasing concentrations (1, 3 and 10 µM) of tenofovir for 2 (A), 4 (B) and 6 (C) hours. Data are expressed as mean ± SEM of 8 experiments * p < 0.05 when compared with control aortic rings (untreated cells).*

4.5 The effect of the Atripla components on EA.hy926 cells

Similarly, efavirenz was the only component of the Atripla pill to cause significant loss in endothelial cell viability after 24 and 48 hours. Emtricitabine and tenofovir had no deleterious effect on endothelial cell viability (Figure 4.4).

When HPI staining was performed on the endothelial cells, only efavirenz was seen to markedly cause cell death by apoptosis and necrosis after exposure to increasing drug concentrations (3-30 μM) for 24 hours. Emtricitabine and tenofovir did not show similar damaging effect on the endothelial cells after 24 hours (Table 4.1).

Statistical analysis was performed using a one-way ANOVA followed by Dunnett's post-hoc test (vs. Control). Time-dependent comparisons between 24- and 48-hour treatments were performed using a two-way ANOVA, followed by Bonferroni's adjustment.

A

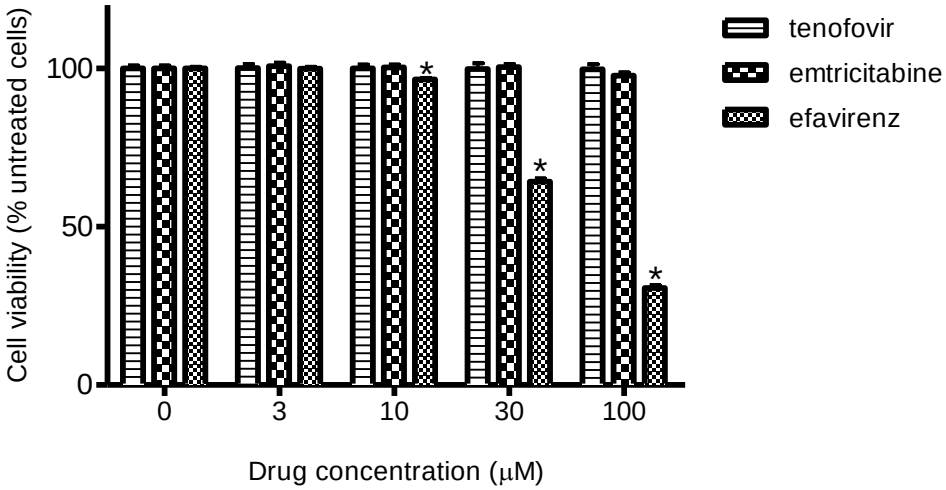

B

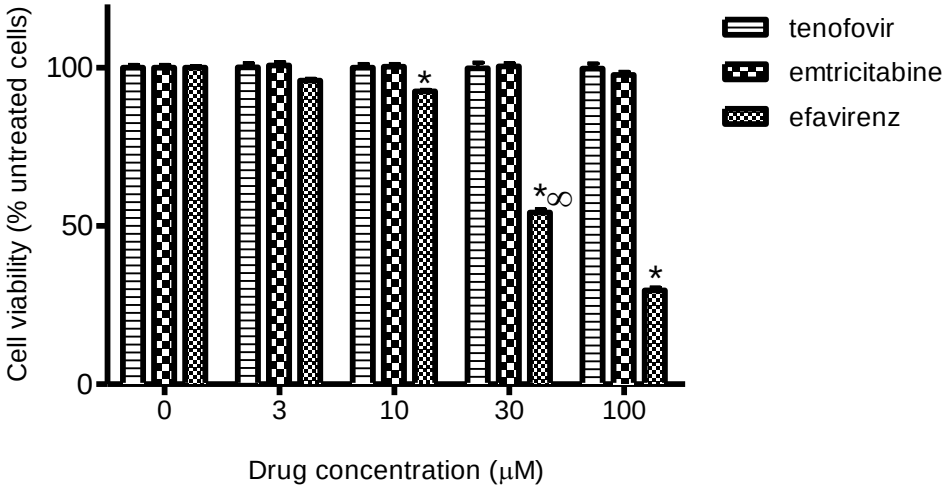

Figure 4.4: *Effect of the Atripla components on EA.hy926 cell viability (MTT) after 24 (A) and 48 (B) hours. Cells were treated with increasing concentrations (3, 10, 30 and 100 μM) of the individual components efavirenz, emtricitabine and tenofovir. Data are expressed as mean ± SEM of 4 experiments (6 replicas per experiment). * $p < 0.01$ when compared with control endothelial cells and ∞$p < 0.05$ when the 24-hour treatment was compared to the 48-hour treatment.*

A

	Live	Apoptotic	Necrotic
Control	96.92 ± 1.31	1.67 ± 0.80	1.42 ± 0.51
3 µM efavirenz	94.99 ± 1.66	3.06 ± 1.13	1.95 ± 0.61
10 µM efavirenz	91.59 ± 1.03*	4.86 ± 0.71*	3.55 ± 0.44*
30 µM efavirenz	75.14 ± 3.83**	17.34 ± 3.53*	7.52 ± 1.28*

B

	Live	Apoptotic	Necrotic
Control	97.02 ± 0.62	1.52 ± 0.20	1.47 ± 0.42
3 µM emtricitabine	96.83 ± 1.77	1.65 ± 1.01	1.53 ± 0.76
10 µM emtricitabine	96.29 ± 0.05	1.71 ± 0.04	2.01 ± 0.09
30 µM emtricitabine	95.54 ± 0.11	2.24 ± 0.21	2.23 ± 0.10

C

	Live	Apoptotic	Necrotic
Control	97.30 ± 1.20	1.36 ± 0.52	1.35 ± 0.68
3 µM tenofovir	97.27 ± 0.86	1.27 ± 0.47	1.47 ± 0.40
10 µM tenofovir	96.17 ± 2.03	1.75 ± 1.03	2.08 ± 1.00
30 µM tenofovir	97.22 ± 0.25	1.26 ± 0.08	1.53 ± 0.18

Table 4.4: *Effect of Atripla components on EA.hy926 cell death (HPI) after 24 hours. Cells were treated with increasing concentrations (3, 10 and 30 µM) of the individual components efavirenz (A), emtricitabine (B) and tenofovir (C) for 24 hours. Data are expressed as mean ± SEM of 3 experiments (2 replicas per experiment). * $p < 0.05$ and ** $p < 0.01$ when compared with control endothelial cells.*

4.6 The role of PARP in efavirenz-mediated loss of endothelial cell function in rat aortic rings

In order to determine the role of PARP in the deleterious effects induced by the Atripla pill, rat aortic rings were treated with the established concentration of efavirenz known to cause damage to the rat aortic endothelial cells. Exposure to 10 μM of efavirenz for 4 hours caused a marked increase in endothelial dysfunction in rat aortic rings as seen by a decrease in ACh-evoked relaxation compared to untreated control rings (Figure 4.5).

Control	10 μM efavirenz	10 μM efavirenz + 3 μM PJ-34	3 μM PJ-34
31.82 ± 4.21 nM	85.25 ± 25.67 nM	75.83 ± 10.61 nM	21.03 ± 112.8 nM *

Table 4.5: *The addition of PJ-34 to efavirenz-treated aortic rings did not cause a significant shift in the EC_{50} of ACh, *p < 0.05 when compared with untreated control rings.*

The addition of the PARP inhibitor PJ-34 (3 μM) to efavirenz (10 μM) markedly improved the relaxation of the rings compared to the treated rings, suggesting a role of PARP in the endothelial dysfunction caused by efavirenz after only 4 hours (Figure 4.5); however the EC_{50} of ACh did not reach statistical significance (Table 4.5). The addition of PJ-34 to the rings had no effect on its own (Data not shown).

Statistical analysis was performed using a two-way ANOVA followed by Bonferroni's adjustment.

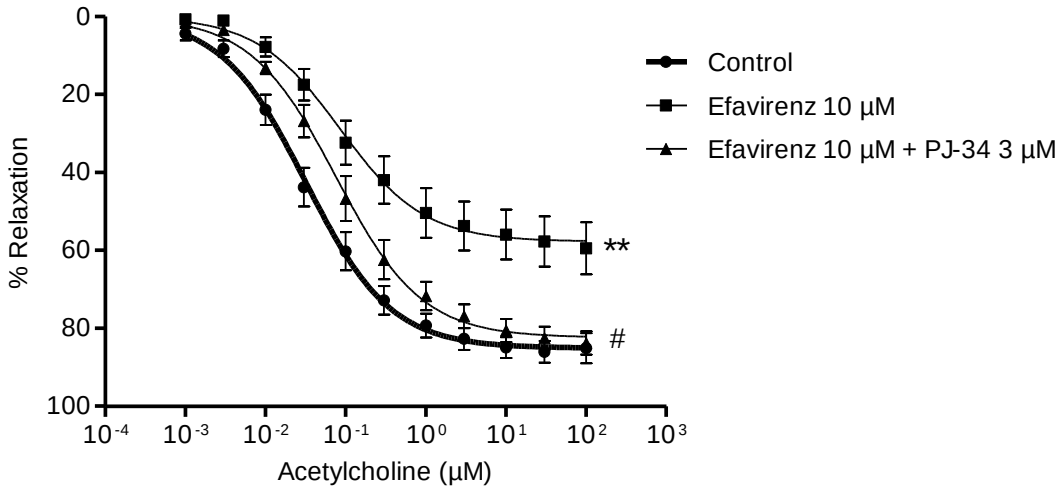

Figure 4.5: *Effect of PJ-34 on efavirenz-mediated loss of endothelial function in rat aortic rings. The rings were exposed to 10 µM of efavirenz for 4 hours. Data are expressed as mean ± SEM of 10 experiments ** p < 0.001 when compared with control aortic rings and # p < 0.05 when compared with efavirenz-treated aortic rings.*

4.7 The role of oxidative stress in efavirenz-mediated loss of cell viability in EA.hy926 cells

The oxidative stress assays NBT and MDA were performed on EA.hy926 cells and were unfortunately inconclusive in determining with certainty the generation of superoxide anions mediated by efavirenz in this cell line (data not shown).

4.8 The role of PARP in efavirenz-mediated loss of endothelial cell viability

In order to measure the activation of PARP after exposure to efavirenz in EA.hy926 cells, a PARP assay was performed. PARP activity was seen to increase in a dose- and time dependent manner (Figure 4.6). After 6 hours, using the highest concentration of efavirenz (10 μM), a 5-fold increase in PARP activity was measured compared to untreated control cells, suggesting an important role of PARP in the cytotoxicity caused by efavirenz (Figure 4.6). The addition of the PARP inhibitor PJ-34 to endothelial cells exposed to 30 μM of efavirenz attenuated the loss of cell viability observed when cells were treated with efavirenz alone after 24 hours (Figure 4.7). A similar outcome was also observed when performing a PARP assay. When cell death assessment was performed, PJ-34 was shown to significantly inhibit the levels of apoptosis and necrosis seen with efavirenz alone (Table 4.2). Exposure of EA.hy926 cells to 10 μM of efavirenz for 4 hours resulted in a 4-fold increase in PARP activity compared to untreated control cells. The addition of 3 μM of PJ-34 significantly reduced the activation of PARP down to levels seen in untreated cells (Figure 4.8). To further confirm the role of PARP in the efavirenz-mediated cytotoxicity, PARP deficient mouse endothelial cells were treated with 10 μM of efavirenz for 4 hours, showing no increase in PARP activation when compared to control cells, PARP containing mouse endothelial cells showed a 4-fold increase in PARP activation following exposure to 10 μM efavirenz for 4 hours (Figure 4.9).

Statistical analysis was performed using a one-way ANOVA followed by Dunnett's post-hoc test (vs. Control) and either Bonferroni's adjustment (MTT) or an unpaired, two-tailed Student's t-test (cell death and PARP assay) to compare efavirenz-treated cells with efavirenz-treated cells exposed to PJ-34. Time-dependent comparisons between 2-, 4- and 6-hour treatments (PARP assay) were performed using a two-way ANOVA, followed by Bonferroni's adjustment.

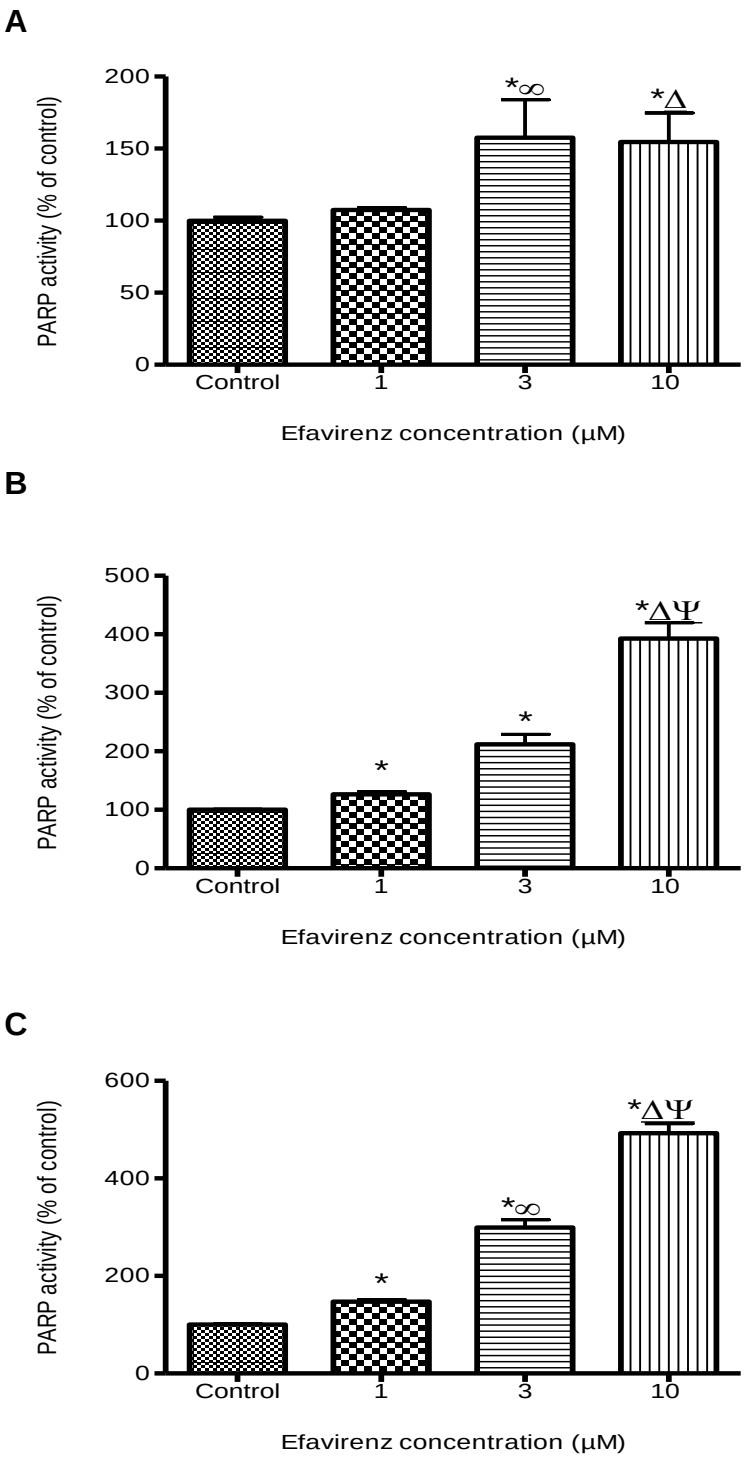

Figure 4.6: *Effect of efavirenz on PARP activation in EA.hy926 cells. Cells were treated with increasing concentrations (1, 3 and 10 μM) of efavirenz for 2 (A), 4 (B) and 6 (C) hours. Data are expressed as mean ± SEM of 3 experiments (3 replicas per experiment). * $p < 0.01$ when compared with control endothelial cells, ∞$p < 0.05$ when the 2-hour treatment was compared with the 6-hour treatment (3 μM), Δ$p < 0.05$ when the 2-hour treatment was compared with the 4- and 6-hour treatments and Ψ$p < 0.05$ when the 4-hour treatment was compared with the 6-hour treatment (10 μM).*

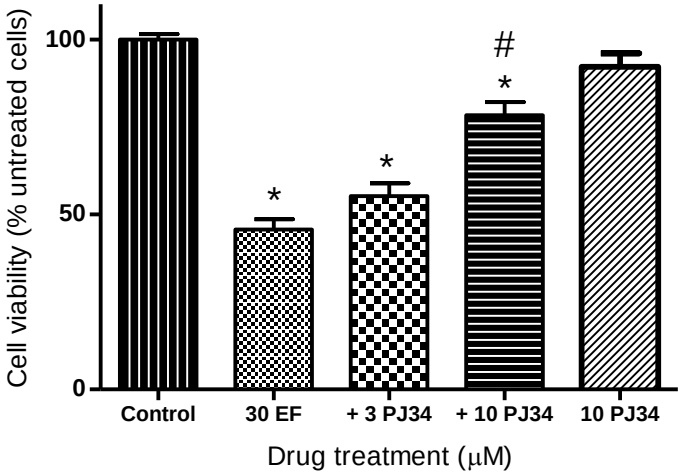

Figure 4.7: *Effect of PJ-34 on efavirenz-mediated loss of EA.hy926 cell viability (MTT) after 24 hours. The addition of 10 μM PJ-34 markedly attenuated the loss of cell viability seen with efavirenz alone. Data are expressed as mean ± SEM of 4 experiments (6 replicas per experiment). * p < 0.01 when compared with control endothelial cells and # p < 0.01 when compared with efavirenz-treated cells.*

	Live	Apoptotic	Necrotic
Control	98.08 ± 0.25	1.19 ± 0.21	0.74 ± 0.07
30 μM efavirenz	78.00 ± 0.91**	15.33 ± 0.21**	6.67 ± 0.97**
30 μM efavirenz + 3 μM PJ-34	98.10 ± 0.28#	0.77 ± 0.03#	1.13 ± 0.28#
3 μM PJ-34	98.92 ± 0.09*	0.71 ± 0.15	0.37 ± 0.12

Table 4.6: *Effect of PJ-34 on efavirenz mediated endothelial cell death after 24 hours. Cells were treated with 30 μM of efavirenz for 24 hours and the addition of PJ-34 significantly reduced levels of apoptotic and necrotic cells seen with efavirenz alone. Data are expressed as mean ± SEM of 3 experiments (2 replicas per experiment). * p < 0.05 and ** p < 0.01 when compared with control heart myoblasts (untreated cells) and # p < 0.01 when compared with efavirenz-treated cells.*

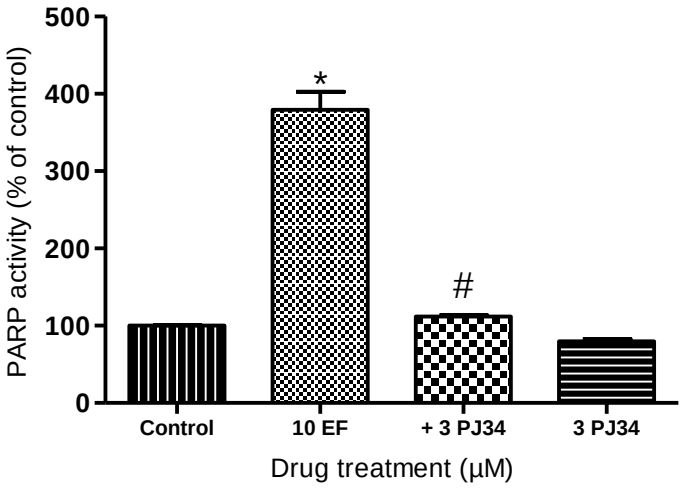

Figure 4.8: *Effect of PJ-34 on efavirenz-mediated PARP overactivation in EA.hy926 cells. Cells were treated with 10 μM of efavirenz 4 hours. The addition of 3 μM PJ-34 markedly attenuated the PARP activation induced by efavirenz on its own.. Data are expressed as mean ± SEM of 3 experiments (3 replica per experiment). * p < 0.01 when compared with control endothelial cells and # p < 0.01 when compared with efavirenz-treated cells.*

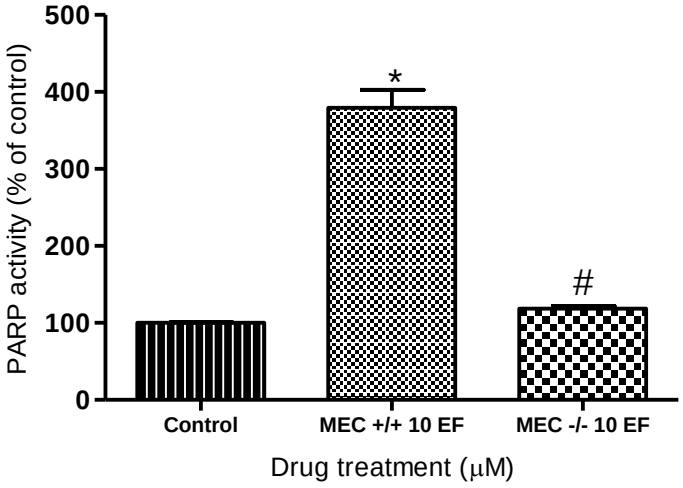

Figure 4.9: *Effect of efavirenz on PARP activation in PARP-deficient mouse endothelial cells (MEC-/-) after 4 hours. Both cell types were exposed to 10 μM efavirenz for 4 hours. Data are expressed as mean ± SEM of 3 experiments (3 replicas per experiment). * p < 0.01 when compared with control endothelial cells and # p < 0.01 when compared with efavirenz-treated cells.*

4.9 The gender difference in efavirenz-treated rat aortic rings

In order to determine whether there is a gender difference in efavirenz-treated endothelial cells, rat aortic rings were exposed to different drug treatments. The first part of the experiment consisted of treating female rat aortic rings with increasing concentrations of efavirenz (1-10 μM) for 4 and 6 hours. The reduced ability of the rings to relax after exposure to efavirenz seen in the standard male rat aortic rings was attenuated in female rat aortic rings, suggesting an oestrogen-mediated protective effect (Figure 4.9). Furthermore, following a 6-hour exposure to efavirenz, the EC_{50} is seen to increase as compared to untreated control rings (Table 4.7).

A (4h exposure):

Control	1 μM efavirenz	3 μM efavirenz	10 μM efavirenz
148.4 ± 18.87 nM #	87.37 ± 10.77 nM *	114 ± 13.25 nM	127.3 ± 19.38 nM

B (6h exposure):

Control	1 μM efavirenz	3 μM efavirenz	10 μM efavirenz
127.5 ± 11 nM	81.39 ± 12.99 nM *	91.63 ± 8.37 nM *	109.8 ± 7.68 nM

Table 4.7: *Exposure to efavirenz for 4 (A) and 6 (B) hours significantly increase the EC_{50} of ACh in female rat aortic rings, *p < 0.05 when compared with untreated control rings and # p < 0.01 when compared with untreated control male aortic rings (4h).*

The second part of the experiment consisted of exposing male rat aortic rings to 10 μM of efavirenz, which was shown to significantly compromise the ACh-mediated relaxation after 4 hours only. The addition of increasing concentrations of oestrogen (10-100 nM) to efavirenz-treated male aortic rings markedly improved the relaxation of the rings compared to male aortic rings exposed to efavirenz on its own (Figure 4.10). The addition of increasing concentrations of oestrogen to efavirenz-treated aortic rings was shown not to cause a significant shift in the EC_{50} of ACh after 4 hours (Table 4.8). There was a marked difference in EC_{50} of ACh when untreated female rat aortic rings were compared to untreated male rat aortic rings after 4 hours (Table 4.7 and Table 4.8).

Control	10 μM efavirenz	10 μM efavirenz + 10 nM oestrogen	10 μM efavirenz + 30 nM oestrogen	10 μM efavirenz + 100 nM oestrogen
31.82 ± 4.21 nM #	85.25 ± 25.67 nM	47.20 ± 15.30 nM	37.61 ± 9.8 nM	54.39 ± 6.27 nM

Table 4.8: *The addition of increasing concentrations of oestrogen to efavirenz-treated rings does not increase the EC_{50} of ACh in male rat aortic rings after 4 hours, #p < 0.01 when compared with untreated control female aortic rings (4h).*

Statistical analysis was performed using a two-way ANOVA followed by Bonferroni's adjustment.

A

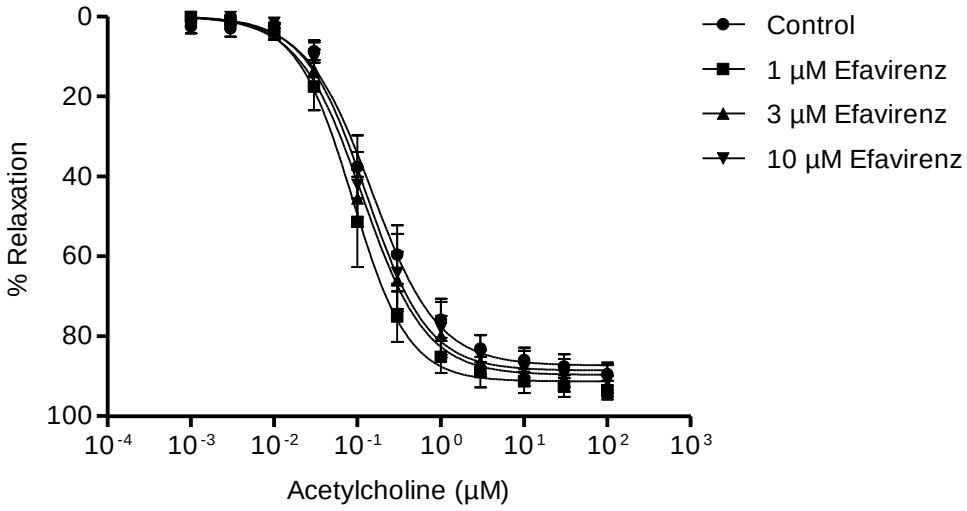

B

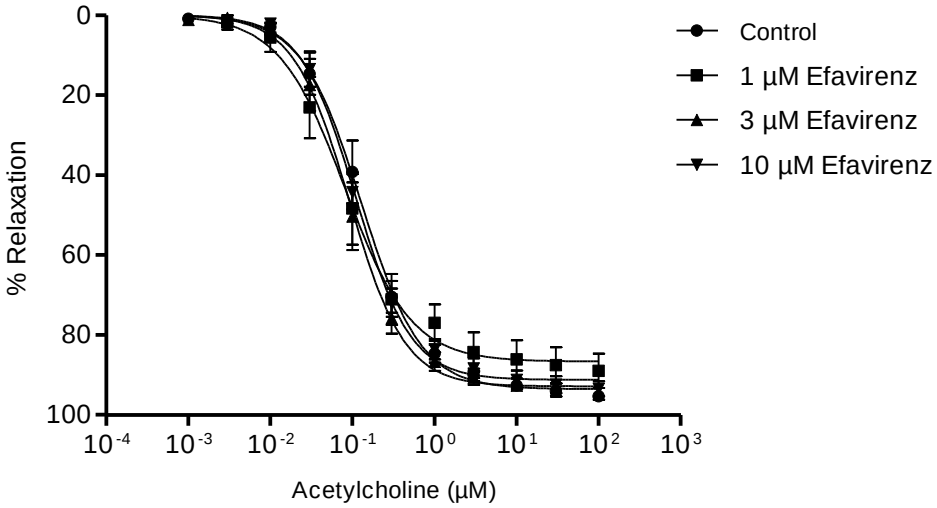

Figure 4.10: *Effect of efavirenz on female rat aortic rings. The rings were exposed to increasing concentrations (1, 3 and 10 µM) of efavirenz for 4 (A) and (6) hours. Data are expressed as mean ± SEM of 6 experiments ** p < 0.05 when compared with control aortic rings.*

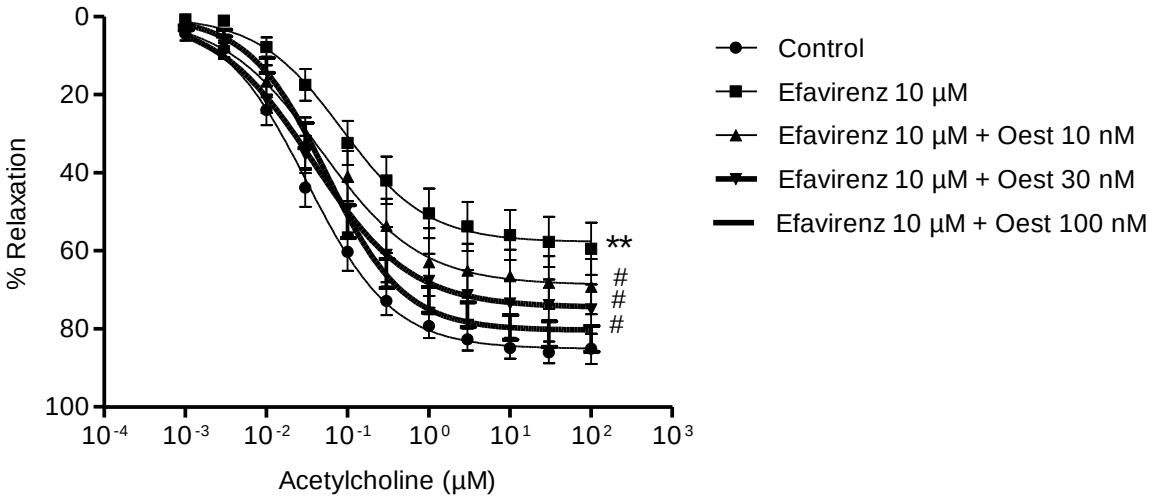

Figure 4.11: *Effect of oestrogen on efavirenz-mediated loss of endothelial function in male rat aortic rings. The rings were exposed to 10 µM of efavirenz for 4 hours. The addition of increasing concentrations (10, 30 and 100 nM) of oestrogen markedly attenuated the loss of endothelial function seen with efavirenz alone. Data are expressed as mean ± SEM of 6 experiments ** p < 0.001 when compared with control aortic rings and # p < 0.001 when compared with efavirenz-treated aortic rings.*

4.10 The role of PARP in efavirenz-treated mouse endothelial cells exposed to oestrogen

Mouse endothelial cells were exposed to 10 µM of efavirenz for four hours, causing a 4-fold increase in PARP activity, compared to untreated cells. The addition of 100 nM oestrogen attenuated the PARP overactivation by 50 %. As a control, 100 nM oestrogen on its own did not cause a significant increase in PARP activity, similar to control levels.

Statistical analysis was performed using a one-way ANOVA followed by Dunnett's post-hoc test (vs. Control) and an unpaired, two-tailed Student's t-test for comparison between efavirenz-treated cells and efavirenz-treated cells exposed to oestrogen.

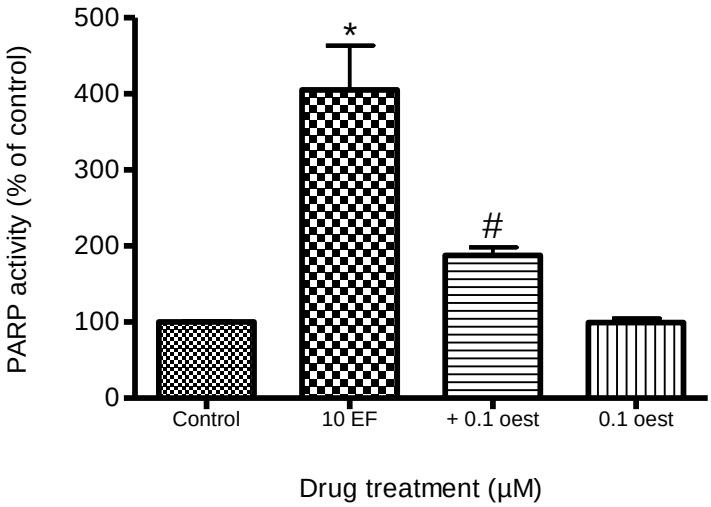

Figure 4.12: *Effect of oestrogen on efavirenz-mediated PARP overactivation in mouse endothelial cells. Cells were treated with 10 µM of efavirenz 4 hours. The addition of 0.1 µM oestrogen markedly attenuated the PARP activation induced by efavirenz on its own.. Data are expressed as mean ± SEM of 3 experiments (3 replica per experiment). * $p < 0.01$ when compared with control endothelial cells and # $p < 0.01$ when compared with efavirenz-treated cells.*

4.11 Discussion

The results obtained suggest that out of the Atripla components, i) only efavirenz causes endothelial dysfunction in rat aortic rings and EA.hy926 cells, ii) neither emtricitabine nor tenofovir caused a toxic effect on the rings and cells iii) both apoptosis and necrosis pathways seem to be involved in the cytotoxicity mediated by efavirenz, iv) PARP appears to play an important role in the efavirenz-induced loss of cell viability, v) female aortic rings seem to display a protective effect against efavirenz-mediated endothelial cell dysfunction.

The activation of PARP seems to be the major mechanism by which efavirenz causes endothelial cell damage. Indeed, the depletion of cellular energy following PARP activation appears to be the main mechanism of dysfunction. Pharmacological inhibition of PARP conferred protection against efavirenz-mediated vascular function impairment.

Efavirenz was shown to cause a time- and dose- dependent loss of endothelial function and cell viability in rat aortic rings and EA.hy926 cells respectively. It was previously shown to have a similar concentration dependent effect on hepatic cell viability, while in this same study , human umbilical vein endothelial cells (HUVEC's) were also used to see whether the effect was cell specific and found the loss of cell viability following a 24 hour exposure with 25 µM efavirenz to be even more significant (Apostolova *et al.*, 2010).

It is known that long term exposure to efavirenz-containing HAART seems to worsen endothelial function (Gupta *et al.*, 2012), however our data suggests that short term treatment with efavirenz already appears to cause significant endothelial damage, predisposing HIV patients to hypertension and cardiovascular disease.

While the steady state plasma concentration of efavirenz following a daily 600 mg regime is reported to be 12.4 ± 3.7 µM (AIDSinfo, 2006), numerous clinical studies have shown that as many as 20 % of patients reach Cmax of up to 50 µM (Burger *et al.*, 2006; Marzolini *et al.*, 2001). Interindividual pharmacokinetic variability such as genetic polymorphism among patients receiving efavirenz can significantly influence the clinical outcome of efavirenz treatment (Elens *et al.*, 2010).

The exposure of rat aortic rings to increasing concentrations of efavirenz clearly showed a marked reduction in maximal vascular relaxation to acetylcholine after only 4 hours. Similar experiments have previously been carried out with different classes of anti HIV drugs (PI's and NRTI's) and for longer treatment periods, also concluding impaired endothelial function in aortic rings (Conklin *et al.*, 2004; Jiang *et al.*, 2006).

A very recent report by Gupta et al. confirmed our results in that the use of efavirenz-based HAART, especially those with an emtricitabine/tenofovir backbone may worsen endothelial function compared to PI-based regimen over 12 months (Gupta *et al.*, 2012).

Likewise, a follow up of patients on long term efavirenz-based regimens concluded that the efavirenz group showed a higher risk of developing cardiovascular disease (Maggi *et al.*, 2011). In contrast, the large observational D:A:D study reported no link between NNRTI's including efavirenz and an increased cardiovascular risk (Friis-Moller *et al.*, 2007)

The other Atripla components emtricitabine and tenofovir on their own did not cause endothelial damage. This is in contrast to certain studies showing that this class of antiretrovirals NRTI's such as AZT and stavudine (d4T) induce significant endothelial damage (Jiang *et al.*, 2006; Sutliff *et al.*, 2002). A recent study, however, has associated tenofovir exposure to an increased significant cardiovascular risk, especially of heart failure (Choi *et al.*, 2011). Similarly, a clinical study concluded that tenofovir based treatment was linked to a higher likelihood of subclinical atherosclerosis progression (Aragones *et al.*, 2012).

Efavirenz at 30 μM was seen to induce both apoptosis and necrosis, with apoptotic levels being more than double that of necrosis. This confirms the results of various reports in which efavirenz was shown to cause cell death via the apoptosis pathway in Jurkat T cells (measured by flow cytometry and Propidium iodide) (Pilon *et al.*, 2002), hepatocytes (colorimetric caspase-3 activity assay) (Bumpus, 2011) and hepatocytes (annexin V/ bivariate PI analysis) (Apostolova *et al.*, 2011).

The ‘mitochondrial dysfunction hypothesis’, by which inhibition of DNA pol-γ activity causes mtDNA depletion and reduced energy production (Lewis *et al.*, 2001) can’t account for the detrimental effects seen with efavirenz, since NNRTI’s are known not to inhibit DNA pol-γ or reduce mtDNA levels, in fact, they are even reported to increase mtDNA in murine adipocytes (Rodriguez de la Concepcion *et al.*, 2005).

Efavirenz-induced toxicity has been linked to oxidative stress in the past, particularly in human arterial endothelial cells which may constitute a precipitating factor in the cardiovascular side effects seen in HIV patients on HAART (Mondal *et al.*, 2004). Efavirenz was also reported to cause oxidative stress in human hepatic cells (Apostolova *et al.*, 2010; Gomez-Sucerquia *et al.*, 2012).

Previously, several studies have shown a strong causative link between oxidative stress and PARP activation (Soriano *et al.*, 2001; Szabo, 1997). DNA single strand breaks caused by oxygen- and nitrogen-derived free radicals bring about the activation of PARP, triggering an energy consuming cycle, depleting NAD^+ and ATP, eventually resulting in cell death (Szabo, 2005; Ungvari *et al.*, 2005). PARP, when bound to damaged DNA, cleaves NAD^+ into nicotinamide and ADP-ribose, using the latter to form branched nucleic acid-like polymers poly (ADP-ribose) covalently attached to nuclear proteins (Virag, 2005). NAD^+ is indispensable in a number of cellular processes in that it acts as a cofactor in glycolysis and tricarboxylic acid cycle, hence providing ATP for most cellular processes.

It is also a precursor for NADP, which serves as a cofactor for the pentose shunt, for bioreductive synthetic pathways and plays a role in the maintenance of reduced glutathione pools (Virag and Szabo, 2002). Pharmacological inhibition or genetic ablation of PARP has been shown to provide beneficial effects in many pathologies and has been linked to reduced expression of inflammatory cytokines, as well as iNOS. The negative feedback regulation of PARP, mediated by NO at the iNOS promoter is thought to be an endogenous mechanism to limit excessive NO production in pathological conditions (Yu *et al.*, 2006).

In our study, efavirenz was shown to increase PARP activity in endothelial cells and the subsequent deleterious effects on both the metabolic and antioxidant pathways are most likely the main mechanism by which this NNRTI causes endothelial cell dysfunction. Besides increasing apoptotic levels, efavirenz also caused a reduction of intracellular glutathione content in hepatic cells after a 4 hour exposure with 25 and 50 µM (Apostolova *et al.*, 2010), a further effect that PARP activation may be responsible for.

In order to investigate whether PARP activation by efavirenz is mediated by oxidative stress, two assays were carried out. The results of our experiments were inconclusive in that neither the NBT nor the MDA assay could confirm the generation of oxidative stress by efavirenz in EA.hy926 cells. On the other hand, PARP activation has been suggested to be the preceding event and cause oxidative stress (Obrosova *et al.*, 2005).

Further work using assays like the dichlorofluorescein (DCF) assay or the more costly commercially available kits such as MitoSOX^{TM} (Red mitochondrial superoxide indicator) will be essential in order to confidently determine an association of efavirenz with oxidative stress.

An increase in oxidative stress is known to alter the nitric oxide bioavailability in endothelial cells, thus contributing to vascular cell dysfunction (Ogita and Liao, 2004).

Interestingly, using HIV transgenic mice, HIV proteins *per se* were shown to cause a marked increase in oxidative stress themselves, alter the NO bioavailabilty and consequently cause endothelial dysfunction (Kline and Sutliff, 2008).

The role of PARP in endothelial dysfunction has previously been reported in the context of diabetes (Soriano *et al.*, 2001) and angiotensin II (Szabo *et al.*, 2004). Our findings confirm that PARP may play an important role in the endothelial dysfunction observed with efavirenz after only 4 hours. The PARP inhibitor PJ-34 at 3 μM was successful at reversing the reduction in vascular relaxation caused by efavirenz (10 μM) back to almost control levels. In addition, PJ-34 attenuated the loss of endothelial cell viability and cell death mediated by efavirenz. Furthermore, the addition of PJ-34 to efavirenz-treated endothelial cells significantly lowered the PARP overactivation caused by efavirenz on its own.

Hyperglycemia-induced oxidative stress and PARP overactivation in HUVEC's was shown to be markedly attenuated by the addition of 1 µM PJ34 (Soriano *et al.*, 2001). This is in accord with previous reports demonstrating the restoration of the aortic endothelial impairment by PJ-34 (Pacher *et al.*, 2002a; Soriano *et al.*, 2001).

Exposure to increasing concentrations of efavirenz (1- 10 µM) in EA.hy926 cells, the maximal dose showed a 5-fold increase in PARP activity compared to control levels after 6 hours. For comparison's sake, in a recent study, the oxidant H_2O_2 (0.35 mM) was shown to cause more than a 1.5-fold increase in PARP activation after 30 minutes exposure in HUVEC's compared to control cells (Kwok *et al.*, 2010). In another study, mouse endothelial cells were treated with the environmental pollutant PCB 104 (10 µM) which is thought to predispose to cardiovascular disease and resulted in a 5-fold increase in PARP activity compared to control levels after 4 hours (Helyar *et al.*, 2009).

PARP overactivation results in the depletion of cellular ATP, NAD^+ and NADPH in endothelial cells which subsequently may reduce NADPH-dependent nitric oxide production leading to endothelial dysfunction and predisposing individual to cardiovascular side effects (Soriano *et al.*, 2001) (Tasatargil *et al.*, 2005). Depletion of cellular NADPH levels in endothelial cells treated with efavirenz may therefore cause a reduction in nitric oxide synthesis in endothelial cells, thus reducing vasorelaxation and likely predispose to hypertension and subsequently lead to cardiovascular disease.

There have been conflicting reports with regards to the effects of HAART on blood pressure. Several studies have concluded that HAART and in particular protease inhibitors are strongly linked to the development of high blood pressure (Cattelan *et al.*, 2001; Chow *et al.*, 2003). One large cohort study following HIV patients over 10 years reported a significantly higher prevalence in hypertension associated with long term HAART exposure (Seaberg *et al.*, 2005). On the other hand, other groups have reported no direct link between HIV treatment *per se* and the development of hypertension (Friis-Moller *et al.*, 2003).

Crane and colleagues reported that individuals receiving lopinavir/ritonavir-based treatment were more than twice likely to develop hypertension compared with patients on efavirenz-based regimens (Crane *et al.*, 2006).

Previous studies have shown efavirenz to have pro-inflammatory and thus pro-atherosclerotic effects on endothelial cells (Mondal *et al.*, 2004). Recently, efavirenz was reported to increase the monolayer permeability in human coronary artery endothelial cells and thus cause endothelial dysfunction (Jamaluddin *et al.*, 2010). This increase in vascular permeability is linked to the development of atherosclerosis (Bonetti *et al.*, 2003).

Others have reported decreased levels of fibrinogen, an inflammatory factor contributing to atherosclerosis in patients treated with efavirenz compared to PI's (Madden *et al.*, 2008).

The underlying molecular mechanism of the pro-atherosclerotic effects of efavirenz may include increased activation of NF-κB (Jamaluddin *et al.*, 2010) and MAPK JNK (Bumpus, 2011), increased induction of pro-inflammatory cytokines such as Chemokine (C-C motif) ligand 2 (CCL-2), IL-6 and interleukin-8 (IL-8) as well as plasminogen activator inhibitor-1(PAI-1) and hepatocyte growth factor (HGF) (Diaz-Delfin *et al.*, 2011), downregulation of tight junction proteins (ZO-1, occludin, claudin-1 and JAM-1) disrupting the endothelial cell barrier function (Jamaluddin *et al.*, 2010), increased levels of cell adhesion molecules such as vascular cell adhesion molecule (VCAM) and ICAM (Mondal *et al.*, 2004) and activation of AMPK (Blas-Garcia *et al.*, 2010), which are all effects that may result from efavirenz-induced PARP activation.

PARP inhibition has been shown to be very favorable in reducing plaque formation (Xie *et al.*, 2009), reducing plaque size (Oumouna-Benachour *et al.*, 2007), increasing their stability and promoting their regression (Hans *et al.*, 2009) in an animal model of atherosclerosis.

PARP is known to regulate transcription factors such as NF-κB (Csiszar *et al.*, 2008; Tsou *et al.*, 2003) in endothelial cells, activation of which is increased by efavirenz (Jamaluddin *et al.*, 2010). In addition, inflammatory cytokine expression such as IL-6 and IL-8, which can be upregulated by efavirenz in endothelial cells (Diaz-Delfin *et al.*, 2011) can also be blocked by PARP inhibition (Piconi *et al.*, 2004). Recently, efavirenz was shown to increase the activation of MAPK JNK in endothelial cells (Jamaluddin *et al.*, 2010).

The increase in JNK phosphorylation can be induced by ROS formation via an activation of upstream kinases such as apoptosis signal-regulating kinase 1 (ASK-1) (Czaja *et al.*, 2003), and thus may be following efavirenz-induced oxidative stress. ROS-mediated hepatotoxicity has been linked to overactivation of the JNK/AP-1 pathway following efavirenz exposure (Bumpus, 2011).

Likewise, the disruption of the endothelial barrier function has previously been shown to be protected by PARP inhibition (Lenzser *et al.*, 2007; Tsou *et al.*, 2003), the tight junction proteins of which can be downregulated in endothelial cells following treatment with efavirenz (Jamaluddin *et al.*, 2010).

PARP inhibition has been successful in blocking the overexpression of cell adhesion molecules such as ICAM and VCAM, the increased activation of which has been linked to the development of atherosclerosis (Giddings, 2005; Piconi *et al.*, 2004) and which can be upregulated following the exposure to efavirenz in endothelial cells (Mondal *et al.*, 2004). For that reason, there seems to be a strong suggestion that PARP activation in endothelial cells may be responsible for the pro-atherosclerotic effects of Atripla. When the cellular insult is too severe for the cell to recover, PARP overactivation can ultimately lead to cell death, either by apoptosis or necrosis (van Wijk and Hageman, 2005).

In our study, PJ-34 (3 µM) appeared to significantly reduce the apoptotic and necrotic levels seen with efavirenz (30 µM) on its own, suggesting a possible pathway by which efavirenz causes endothelial cell death by either apoptosis or necrosis depending on the severity of the cellular injury (Koh *et al.*, 2005).

In our *ex vivo* experiments involving rat aortic rings, exposure to efavirenz caused a dose- dependent decrease in maximal relaxation to acetylcholine. PJ-34 (3 µM) significantly attenuated the endothelial damage seen with efavirenz (10 µM) on its own. Pretreatment of endothelium-intact aortic rings with PJ-34 was shown to protect against lipopolysaccharide-induced endothelial dysfunction in a model of systemic endotoxemia (Tasatargil *et al.*, 2005).

Similarly, acetylcholine-induced endothelium-dependent relaxation in rat aortic rings was seen to be greatly improved after PJ-34 exposure in an experimental model of CHF (Pacher *et al.*, 2002a) and particularly in established streptozotocin-induced diabetic animals after a 1-hour incubation with 3 µM PJ-34 (Soriano *et al.*, 2001).

In order to further confirm these results, using PARP deficient mouse endothelial cells, exposure to efavirenz did not increase PARP activation as seen with the intact cells, thus implying a strong role of PARP in the cytotoxicity caused by efavirenz. PARP-deficient mouse endothelial cells have previously been used extensively in order to demonstrate the role of PARP in various pathologies ranging from diabetes to rheumatoid arthritis (Andreone *et al.*, 2012; Garcia *et al.*, 2006).

Endothelial dysfunction is an important precursor of HIV-associated atherosclerosis and cardiovascular disease (Widlansky *et al.*, 2003). HIV *per se* has been reported to be pro-apoptotic in endothelial cells and have a significant deleterious effect on the cardiovascular system (Fiala *et al.*, 2004).

In addition, HIV can directly affect endothelial cells by changing their phenotype from anti to prothrombotic (Francisci *et al.*, 2009). Moreover, the HIV gp120 has been reported to directly activate arterial smooth muscle with subsequent release of pro-coagulant tissue factor (Schecter *et al.*, 2001).

There seems to be a gender difference with regards to the incidence of cardiovascular side effects suffered by HIV patients on HAART, with women being less affected than men, (Neumann *et al.*, 2004). Interestingly, several studies concluded that post-menopausal female subjects on HAART displayed an increased cardiovascular risk than their male counterparts due to the loss of their natural oestrogen protection (Pernerstorfer-Schoen *et al.*, 2001; Triant *et al.*, 2007).

In the non-infected population, the male gender is considered to be a risk factor for cardiovascular events, which already offers female HIV patients an additional benefit regardless of HAART. Therefore, the findings from our experiments need to be taken with caution since there are a number of factors that play a role in female HIV patients appearing to show less cardiovascular side effects than male patients such as symptom perception and reporting.

In order to investigate whether oestrogen offered a protective effect against efavirenz-induced endothelial cell dysfunction, female rat aortic rings were exposed to increasing concentrations of efavirenz for four hours and the impairment of vascular relaxation seen with efavirenz on male rings was fully reversed, suggesting a protective effect by oestrogen. In addition, efavirenz (10 µM)-treated rat aortic rings were incubated with increasing concentrations of oestrogen (10-100 nM) for 4 hours and the maximal relaxation to acetylcholine measured. Oestrogen, in a dose-dependent fashion reversed the impairment of vascular relaxation seen with rings treated with 10 µM efavirenz only.

Raloxifene, a selective oestrogen receptor modulator at 1 µM, protected against H_2O_2-induced impairment of ACh-dependent relaxation of rat aortic rings after a 30 minute exposure (Wong *et al.*, 2008). Similarly, long term treatment with oestrogen was shown to improve endothelial function as well as reduce blood pressure in a model of hypertension (Yen and Lau, 2004). Contradicting reports also exist with oestrogen contributing to an increased cardiovascular risk.

Several studies concluded that hormone replacement therapy (HRT) may be beneficial in improving vascular function and protecting women against cardiovascular disease (Kernohan *et al.*, 2004; Schneider *et al.*, 2009; Stevenson *et al.*, 2009), while others claimed HRT to be contributing to an increased risk of cardiovascular disease (Aubuchon and Santoro, 2004; Samsioe, 2003). In line with our conclusions, a study showed that basal NO release from endothelium-intact rings from female rabbits is increased compared to male rings (Hayashi *et al.*, 1992). Oestrogen has previously been reported to have a PARP inhibitory effect (Zaremba *et al.*, 2011).

Based on the results presented in this part of the study, we conclude that exposure to efavirenz may lead to oxidative stress and an increased activation of PARP in vascular endothelial cells, causing impairment of vasorelaxation and predisposing HIV patients on efavirenz-based regimens to the development of hypertension and consequently cardiovascular disease.

Chapter 5

Protective role of rosiglitazone against Atripla-mediated endothelial cell dysfunction

5.1 Introduction

Previous studies have shown rosiglitazone to confer protection against endothelial dysfunction (Cuzzocrea *et al.*, 2004; Hetzel *et al.*, 2005; Pistrosch *et al.*, 2004). The mechanism by which rosiglitazone exerts its protective effects is however unclear and further research will be required to elucidate the underlying mode of protection. The activation of PPAR-γ and/or AMPK may be one way by which rosiglitazone offers protection in the vascular cells against oxidative stress-induced hyperglycemia (Ceolotto *et al.*, 2007).

Since rosiglitazone has been shown to inhibit PARP activation in H9c2 cells and that PARP activity is increased by efavirenz in EA.hy926, the possible protective role of rosiglitazone against efavirenz-mediated endothelial dysfunction was investigated and its effect on efavirenz-induced PARP activation studied. The results of this part of the study may provide useful insights into novel protection strategies against HAART-mediated cardiovascular side effects and open way for further research into the thiazolidinediones as an effective therapy against cardiovascular dysfunction in general.

5.2 Methods

5.2.1 Treatment protocols

In order to study the effect of rosiglitazone on efavirenz-mediated endothelial dysfunction, the rat aortic rings were treated with 10 µM efavirenz for 4 hours and increasing concentrations (3 and 10 µM) of rosiglitazone and the relaxation (following pre-constriction to phenylephrine) to increasing concentrations of ACh measured. Similarly, rat aortic rings were exposed to 10 µM efavirenz in the presence and absence of the PPAR-γ agonist GW1929 for 4 hours and the effect on vascular relaxation to ACh measured.

For the cell viability experiments, EA.hy926 cells were exposed to 30 µM efavirenz for 24 hours. The effect of adding increasing concentrations (1, 3 and 10 µM) of rosiglitazone was also assessed using the MTT assay. In order to elucidate the mechanism of protection of rosiglitazone against efavirenz-mediated endothelial damage, the PPAR-γ antagonist GW9662 was used with the aim to study whether the protection is PPAR-γ-mediated. The cells were exposed to 30 µM efavirenz for 24 hours in the presence and absence of rosiglitazone (3 µM) and GW9662 (10 µM). In addition, a selective PPAR-γ agonist GW1929 was used in increasing concentrations (1, 3 and 10 µM) for 24 hours and the effect assessed using the MTT assay.

Finally, in order to study the role of AMPK in the protection conferred by rosiglitazone, the selective AMPK activator AICAR was used in increasing concentrations (0.1, 0.25 and 0.5 mM) in the presence and absence of 30 µM efavirenz for 24 hours using the MTT assay.

For the cell death assay, the cells were exposed to 30 µM efavirenz for 24 hours and the addition of 10 µM rosiglitazone assessed using HPI staining.

The involvement of PARP in the possible protection offered by rosiglitazone against efavirenz-mediated endothelial dysfunction was studied using the PARP assay and the EA.hy926 cells were exposed to 10 µM efavirenz for 4 hours and PARP activity measured. The cells were also exposed to efavirenz with the addition of 3 and 10 µM rosiglitazone for 4 hours and the effect on efavirenz-mediated PARP activation assessed. After the appropriate treatment protocols, the following cellular parameters were then measured:

5.2.1.1 Ring experiments

The effect of rosiglitazone on efavirenz-mediated endothelial dysfunction was assessed *ex vivo* using rat aortic rings connected to a transducer. The aortic rings were prepared and treated as fully described in Chapter 2.

5.2.1.2 Cell viability

The cell viability following exposure to the different drugs was assessed using the MTT assay, which is a colorimetric assay as fully described in Chapter 2.

5.2.1.3 Necrosis and apoptosis levels

Cell death measurement was carried out by morphological assessment using the HPI staining method, by which the relative numbers of live, apoptotic and necrotic cells were counted under a fluorescence microscope as previously described in Chapter 2.

5.2.1.4 PARP activation

The activation of PARP was measured by determining tritiated incorporation of NAD^+ into cellular proteins following exposure to the individual drugs as fully mentioned in Chapter 2.

5.2.2 Statistical analysis

Statistical analysis was performed using ANOVA and Student's t-test as fully described in Chapter 2.

5.3 Results

5.4 The protection by rosiglitazone against efavirenz-mediated endothelial cell dysfunction in rat aortic rings

Rat aortic rings were treated with efavirenz (10 μM) for 4 hours and significantly reduced the rings' ability to relax in response to ACh compared to untreated control rings. The addition of increasing concentrations of rosiglitazone (3-10 μM) improved relaxation, thus conferring a protective effect on the efavirenz-treated rings (Figure 5.1), the EC_{50} of ACh, however, did not reach statistical significance (Table 5.1).

Control	10 μM efavirenz	10 μM efavirenz + 3 μM rosiglitazone	10 μM efavirenz + 10 μM rosiglitazone
31.82 ± 4.21 nM	70.91 ± 12.70 nM	41.76 ± 4.26 nM	39.21 ± 8.17 nM

Table 5.1: *The addition of rosiglitazone to efavirenz-treated aortic rings does not significantly increase the EC_{50} of ACh after 4 hours.*

Statistical analysis was performed using a two-way ANOVA followed by Bonferroni's adjustment to compare efavirenz-treated cells with efavirenz-treated cells exposed to rosiglitazone.

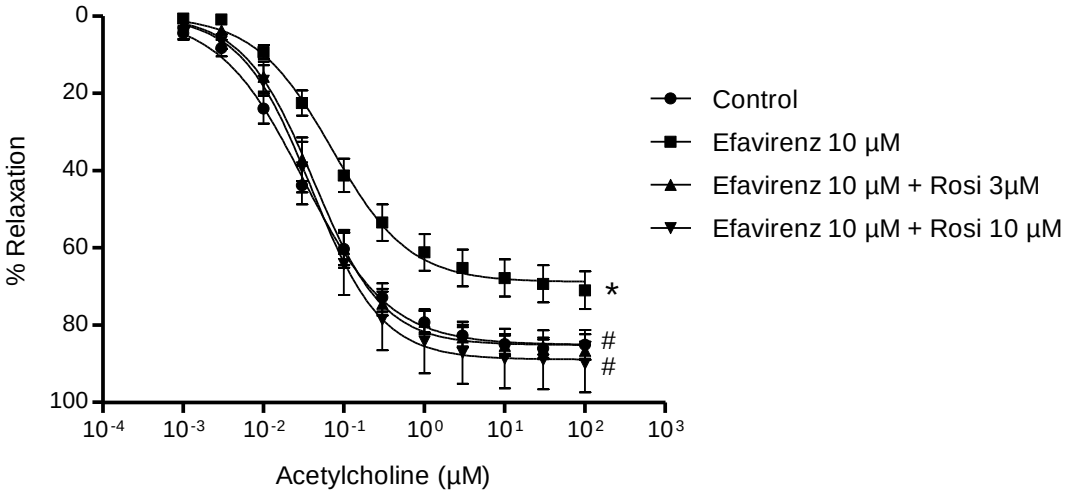

Figure 5.1: *Effect of rosiglitazone on efavirenz-mediated loss of endothelial function. The rings were exposed to 10 µM of efavirenz for 4 hours. The addition of increasing concentrations (3 and 10 µM) of rosiglitazone significantly reduced the efavirenz-mediated endothelial dysfunction. Data are expressed as mean ± SEM of 6 experiments * p < 0.01 when compared with control aortic rings and # p < 0.001 when compared with efavirenz-treated rings.*

5.5 The protection by rosiglitazone against efavirenz-mediated loss of cell viability in EA.hy926 cells

The addition of increasing concentrations of rosiglitazone (1-10 μM) to efavirenz-treated (30 μM) cells for 24 hours was shown to improve the loss of cell viability induced by efavirenz (Figure 5.2). Efavirenz on its own was shown to cause a 73 % drop in cell viability, while the addition of the maximal concentration (10 μM) of rosiglitazone attenuated the loss of cell viability to 34 % after 24 hours.

Using HPI staining, the addition of rosiglitazone to efavirenz-treated cells was shown to markedly reduce the number of apoptotic and necrotic cells that are seen (Table 5.1).

Statistical analysis was performed using a one-way ANOVA followed by Dunnett's post-hoc test (vs. Control) and either Bonferroni's adjustment (MTT) or an unpaired, two-tailed Student's t-test (Cell death) to compare efavirenz-treated cells with efavirenz-treated cells exposed to rosiglitazone.

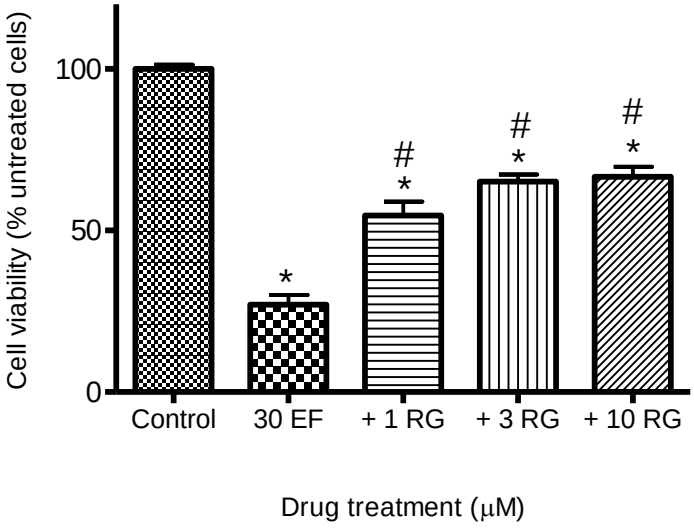

Figure 5.2: *Effect of the rosiglitazone on efavirenz-mediated loss of cell viability in EA.hy926 cells. Cells were treated with 30 μM of efavirenz for 24 hours. The addition of increasing concentrations (1, 3 and 10 μM) of rosiglitazone markedly decreased the loss of cell viability seen with efavirenz alone. Data are expressed as mean ± SEM of 3 experiments (6 replicas per experiment). * p < 0.01 when compared with control endothelial cells and # p < 0.01 when compared with efavirenz-treated cells.*

	Live	Apoptotic	Necrotic
Control	96.51 ± 0.91	1.69 ± 0.17	1.80 ± 0.78
30 μM efavirenz	84.15 ± 0.58**	7.95 ± 0.39**	7.90 ± 0.55**
30 μM efavirenz + 10 μM rosiglitazone	95.43 ± 0.80#	2.34 ± 0.04*#	2.23 ± 0.78#
10 μM rosiglitazone	96.75 ± 0.27	1.66 ± 0.30	1.59 ± 0.30

Table 5.2: *Effect of rosiglitazone on efavirenz-mediated endothelial cell death after 24 hours. Cells were treated with 30 μM of efavirenz for 24 hours and the addition of rosiglitazone significantly reduced levels of apoptotic and necrotic cells seen with efavirenz alone. Data are expressed as mean ± SEM of 3 experiments (2 replica per experiment). * p < 0.05 and ** p < 0.01 when compared with control endothelial cells (untreated cells) and # p < 0.01 when compared with efavirenz-treated cells.*

5.6 The effect of rosiglitazone on efavirenz-mediated PARP activation

The endothelial cells were exposed to 10 µM efavirenz for 4 hours and PARP activity measured. Efavirenz evoked a 4-fold increase in PARP activity when compared to untreated endothelial cells. The addition of increasing concentrations (3 and 10 µM) of rosiglitazone significantly attenuated the efavirenz-mediated PARP overactivation after 4 hours. As a control, cells were also treated with 10 µM rosiglitazone on its own, showing no increase in PARP activity (Figure 5.3).

Statistical analysis was performed using a one-way ANOVA followed by Dunnett's post-hoc test (vs. Control) and Bonferroni's adjustment to compare efavirenz-treated cells with efavirenz-treated cells exposed to rosiglitazone.

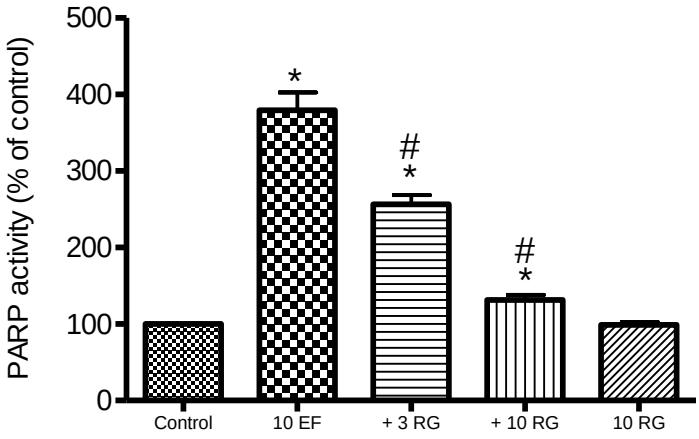

Figure 5.3: *Effect of rosiglitazone on efavirenz-mediated PARP overactivation in EA.hy926 cells. Cells were treated with 10 μM of efavirenz for 4 hours. The addition of increasing concentrations (3 and 10 μM) of rosiglitazone markedly attenuated the PARP activation induced by efavirenz on its own. Data are expressed as mean ± SEM of 3 experiments (3 replicas per experiment. * p < 0.01 when compared with control endothelial cells and # p < 0.01 when compared with efavirenz-treated cells.*

5.7 Investigation into the mechanism of protection of rosiglitazone against efavirenz-mediated loss of cell viability

In order to elucidate the mechanism by which rosiglitazone confers protection against efavirenz-induced loss of endothelial cell viability, the pharmacological inhibitor of PPAR-γ GW9662 was used. The addition of 10 μM of GW9662 to efavirenz (10 μM) treated cells showed a trend of blocking the protection by rosiglitazone (3 μM) after 24 hours, suggesting a PPAR-γ dependent mechanism of protection. This PPAR-γ inhibitor has previously been shown to not be ideal in providing conclusive results (previous own data).As a control, the addition of GW9662 (10 μM) to 30 μM of efavirenz was also shown not to have an effect on its own on the cell damage mediated by efavirenz. Similarly, cells exposed to 10 μM of GW9662 on its own did not show any signs of cytotoxicity (Figure 5.4).

In order to confirm that the mechanism of protection may be PPAR-γ mediated, the agonist of PPAR-γ (GW1929) was used at increasing concentrations (1-10 μM) for 24 hours. The addition of GW1929 to efavirenz-treated cells (30 μM) was seen to attenuate the loss of cell viability caused by efavirenz alone. 10 μM GW1929 on its own did not cause cell damage (Figure 5.5).

Exposure of the rat aortic rings to 10 μM of efavirenz for 4 hours impaired the relaxation of the rings compared to untreated control rings and increased the EC_{50} of ACh from 26.08 ± 4.39 nM to 94.05 ± 24.91 nM (Table 5.3).

Interestingly, the addition of 10 μM of GW1929 conferred protection to the endothelial cells, thus further suggesting an involvement of PPAR-γ in the rosiglitazone-mediated mechanism of protection (Figure 5.6).

Control	10 μM efavirenz	10 μM efavirenz + 10 μM GW1929	10 μM GW1929
26.08 ± 4.39 nM	94.05 ± 24.91 nM *	32.30 ± 6.03 nM #	24.67 ± 4.77 nM

Table 5.3: *The EC_{50} of ACh following the addition of GW1929 to efavirenz-treated aortic rings after 4 hours, *p < 0.05 when compared with untreated rings and #p < 0.05 when compared with efavirenz-treated rings.*

Using the pharmacological activator AICAR at increasing concentrations (0.1, 0.25 and 0.5 mM), an AMPK-dependent mechanism of protection by rosiglitazone was identifed. AICAR was shown to confer a similar protection as seen with rosiglitazone after 24 hours at the highest concentration used (10 μM) (Table 5.2),

Statistical analysis was performed using a one-way ANOVA followed by Dunnett's post-hoc test (vs. Control) and Bonferroni's adjustment to compare efavirenz-treated cells with efavirenz-treated cells exposed to rosiglitazone and GW9662 or efavirenz-treated cells exposed to GW1929/AICAR. For the ring experiments, a two-way ANOVA, followed by Bonferroni's adjustment was carried out.

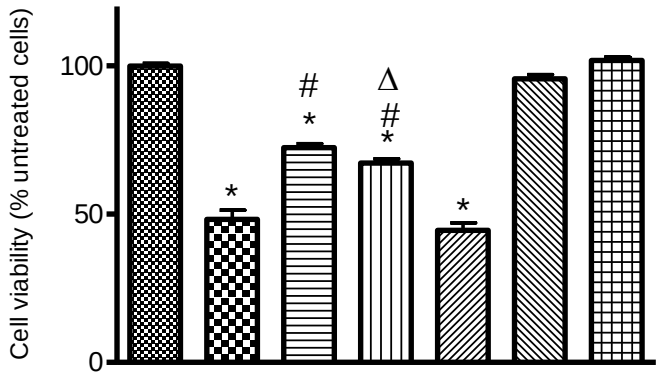

Efavirenz 30 µM	-	+	+	+	+	-	-
Rosiglitazone 3 µM	-	-	+	+	-	+	-
GW9662 10 µM	-	-	-	+	+	-	+

Figure 5.4: *Effect of PPAR-γ antagonist GW9662 on rosiglitazone-mediated protection against efavirenz-induced loss of EA.hy926 cell viability after 24 hours. Cells were treated with 30 µM of efavirenz, causing significant loss of cell viability, partly attenuated by the addition of 3 µM rosiglitazone. The addition of 10 µM GW9662 was shown to partly block that protection. Data are expressed as mean $\pm$ SEM of 3 experiments (6 replicas per experiment). * $p < 0.01$ when compared with control endothelial cells and # $p < 0.01$ when compared with efavirenz-treated cells and Δ $p < 0.05$ when compared with efavirenz-treated cells exposed to rosiglitazone.*

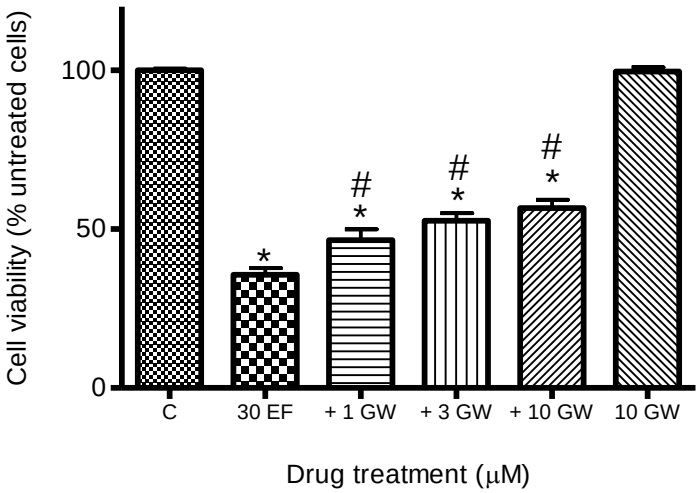

Figure 5.5: *Effect of PPAR-γ agonist GW1929 on efavirenz-mediated loss of EA.hy926 cell viability after 24 hours. Cells were treated with 30 μM of efavirenz, causing significant loss of cell viability. The addition of increasing concentrations (1, 3 and 10 μM) of GW1929 was shown to partly confer protection after 24 hours. Data are expressed as mean ± SEM of 3 experiments (6 replicas per experiment). * $p < 0.01$ when compared with control endothelial cells and # $p < 0.01$ when compared with efavirenz-treated cells.*

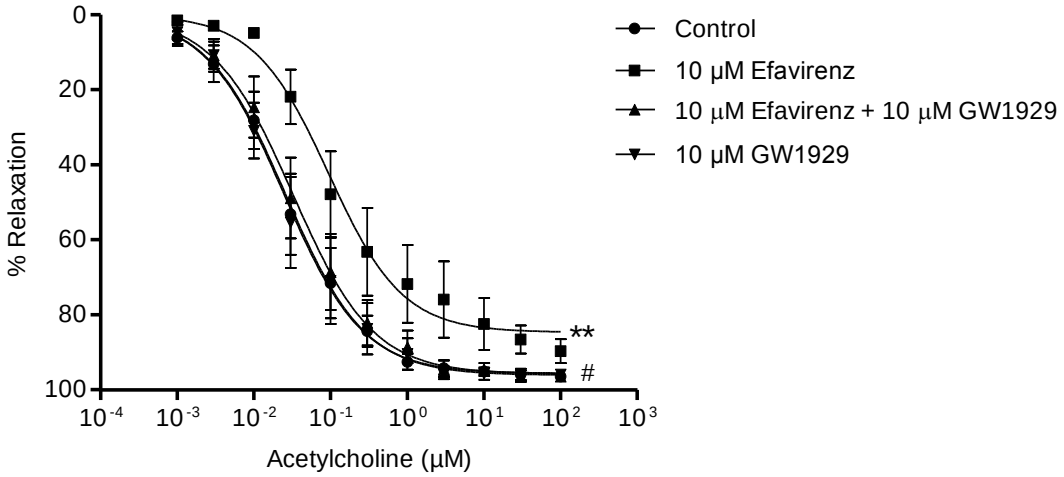

Figure 5.6: *Effect of PPAR-γ agonist GW1929 on efavirenz-mediated loss of endothelial function. The rings were exposed to 10 µM of efavirenz for 4 hours. The addition of 10 µM of GW1929 significantly reduced the efavirenz-mediated endothelial dysfunction. Data are expressed as mean ± SEM of 6 experiments ** p < 0.05 when compared with control aortic rings and # p < 0.05 when compared with efavirenz-treated rings.*

AICAR	efavirenz	
	0 μM	30 μM
0	100 ± 3	34.41 ± 0.82*
0.1 mM	93.59 ± 2.44	43.90 ± 1.26**#
0.25 mM	92.28 ± 2.82	51.85 ± 2.31**#
0.5 mM	88.99 ± 3.07*	50.99 ± 1.32**#

Table 5.4: *Effect of AMPK agonist AICAR on efavirenz-mediated loss of EA.hy926 cell viability after 24 hours. Cells were treated with 30 μM of efavirenz, causing significant loss of cell viability. The addition of increasing concentrations (0.1, 0.25 and 0.5 mM) of AICAR showed a significant difference compared to efavirenz alone. Data are expressed as mean ± SEM of 3 experiments (6 replicas per experiment). * $p < 0.05$ and ** $p < 0.01$ when compared with control endothelial cells and # $p < 0.01$ when compared with efavirenz-treated cells.*

5.8 Discussion

The present chapter establishes the protective role of rosiglitazone against efavirenz-induced PARP activation and endothelial cell toxicity in rat aortic rings and EA.hy926 cells. Rosiglitazone, a PPAR-γ agonist has been used in the treatment of type 2 diabetes for over a decade; however, its beneficial effects have been shown to go beyond its insulin sensitising actions. The protective effects of rosiglitazone are reported in a number of pathologies such as renal ischemia/reperfusion (Betz *et al.*, 2012), cisplatin-induced nephrotoxicity (Kim *et al.*, 2010), neurodegeneration (Martin *et al.*, 2012; Toledo and Inestrosa, 2010), steatohepatitis (Wu *et al.*, 2010), cancer (Farrow and Evers, 2003), inflammatory bowel disease (Adachi *et al.*, 2006) and ischemia-induced retinopathy (Higuchi *et al.*, 2010). The cardiovascular protection of rosiglitazone is widely disputed.

The current study demonstrates for the first time that rosiglitazone was indeed able to offer protection against efavirenz-mediated endothelial cell toxicity which seems to be partially mediated through PPAR-γ and AMPK activation. Our results show that rosiglitazone improved the loss of cell viability and cell death mediated by efavirenz, reversed the impairment of vascular relaxation of rat aortic rings and significantly reduced the PARP overactivation induced by efavirenz.

The main mechanism of protection of rosiglitazone is essentially suggested to arise from a reduction of efavirenz-induced PARP overactivation possibly induced by oxidative stress (Ceolotto *et al.*, 2007) via PPAR-γ and AMPK activation in endothelial cells. Rosiglitazone has been the subject of great controversy with regards to its cardiovascular effects. A number of reports suggested rosiglitazone to be cardiotoxic while others claimed it to be cardioprotective.

Endothelial cells highly express PPAR-γ receptors in the nucleus and to a lesser degree in the cytosol (Satoh *et al.*, 1999; Xin *et al.*, 1999), which suggests that the beneficial vascular effects of rosiglitazone may be through PPAR-γ activation. However, a growing body of evidence suggests that the vasculoprotective effect of rosiglitazone may not be mediated by a PPAR-γ-dependent mechanism. Previous studies have shown that PPAR-γ activation can modulate transcription factors such as NF-κB and subsequently inhibit the expression of pro-atherosclerotic gene products such as cytokines, chemokines, matrix metalloproteinases and cell adhesion molecules (Duez *et al.*, 2001).

Rosiglitazone was shown to cause dose - dependent improvement of efavirenz-mediated loss of endothelial function and cell viability in rat aortic rings and EA.hy926 cells respectively. The dose range over which rosiglitazone exerted its protective effects was similar to the one used in previous studies (Boyle *et al.*, 2008; Polikandriotis *et al.*, 2005).

Treating rat aortic rings with efavirenz clearly showed significant impairment of vascular relaxation to acetylcholine. The addition of rosiglitazone markedly improved the endothelial dysfunction seen with efavirenz alone. In accord with our findings, rosiglitazone was shown to reverse the impaired vascular relaxation to ACh in diabetic rat aortic rings as well as the impaired ACh-stimulated NO production (El-Bassossy *et al.*, 2012). On the other hand, one study using aortic rings from spontaneous hypertensive rats shows vascular improvement mediated by PPAR-alpha receptor activation and not by the PPAR-gamma receptor agonist rosiglitazone (Qu *et al.*, 2012).

In order to gain an understanding of the underlying mechanism of action by which rosiglitazone exerts its protective effects against the toxicity induced by efavirenz, the specific pharmacological inhibitor of PPAR-γ GW9662 was used and shown to partially block the protection of rosiglitazone, suggesting a PPAR-γ dependent mechanism. In c-reactive protein-stimulated vascular smooth muscle, rosiglitazone was shown to have an anti-inflammatory effect by activating glucocorticoid receptor and subsequently blocking p38/MAPK- toll like receptor 4 (TLR4) signalling pathway as GW9662 was not able to inhibit this protection (Liu *et al.*, 2011).

Another study, however, reported the increase in endothelial NO synthesis by rosiglitazone to be PPAR-γ dependent as the effect was blocked by the treatment with either GW9662 or siRNA directed against PPAR-γ RNA (Polikandriotis *et al.*, 2005). GW9662 was not able to block the ability of rosiglitazone to inhibit the IL-1β or TNF-α induced - release of pro-inflammatory mediators from human airway smooth muscle cells, suggesting a PPAR-γ and AMPK-independent mechanism of protection (Zhu *et al.*, 2011).

The protection seen with rosiglitazone in endothelial cells may be a class effect as similar results were obtained using pioglitazone, another thiazolidione which activates PPAR-γ receptor (data not shown).

To further confirm the partial involvement of PPAR-γ in the protection seen with rosiglitazone, the PPAR-γ agonist GW1929 was used, the addition of which to efavirenz-treated cells was seen to partially reverse the loss of cell viability induced by efavirenz alone. Pretreatment of HUVEC's with GW1929 for 24 hours inhibited the VEGF-stimulated cyclooxygenase-2 (COX-2) expression, mimicking the anti-inflammatory effect seen with rosiglitazone and concluding an essential role of PPAR-γ in their mechanism (Scoditti *et al.*, 2010).

Treating rat aortic rings with efavirenz and following the addition of GW1929 a similar protective effect as in EA.hy926 cells was observed, further suggesting an involvement of PPAR-γ in the rosiglitazone-mediated mechanism of protection.

Following the addition of rosiglitazone to efavirenz-treated EA.hy926 cells, the apoptotic and necrotic levels induced by efavirenz alone were seen to be dramatically reduced after 24 hours. An interesting study using endothelial progenitor cells (EPC's) has shown that rosiglitazone significantly attenuated TNF-α-mediated apoptosis of EPC's dose dependently by reducing the expression of caspase-3 and caspase-7 as well as inhibiting the release of cytochrome c mediated by the inhibition of extracellular signal-regulated kinase (ERK) /MAPK and NF-κB pathways (Xu *et al.*, 2011).

PPAR agonists have been reported to show anti-inflammatory effects (Duan *et al.*, 2008; Nakajima *et al.*, 2001) by downregulating NF-κB (Lee *et al.*, 2006) and subsequently inhibiting the expression of pro-inflammatory mediators such as TNF-α, IL-1 and LPS (Mako *et al.*, 2010). In addition, PPAR-γ activation has been reported to reduce TNF-α-induced overexpression of ICAM and VCAM (Bruemmer *et al.*, 2005). HIV *per se* may cause endothelial dysfunction. Indeed exposure of human brain endothelial cells (Khan *et al.*, 2003) and human breast cancer cells (Lee *et al.*, 2005) to Tat which is an essential regulatory protein for HIV transcription has been shown to have inflammatory effects which could successfully be reversed by rosiglitazone and blocked by GW9662, protection partly mediated by inhibition of NF-κB transcription (Huang *et al.*, 2008).

TNF-α has been shown to be crucial in the early development of atherosclerosis (Kleemann *et al.*, 2008; Kleinbongard *et al.*, 2010) and as a mediator of vascular inflammation (Libby *et al.*, 1995). In TNF-α-activated endothelial cells, the overexpression of PPAR-γ receptors was reported to attenuate NF-κB activity (Mun *et al.*, 2011).

In diabetic patients, treatment with rosiglitazone was shown to decrease TNF-α levels (Marx *et al.*, 2003), whereas treatment with rosiglitazone in healthy nondiabetic subjects did not alter TNF-α levels despite being vasculoprotective (Hetzel *et al.*, 2005). Therefore, since NF-κB activation has strongly been associated with atherosclerotic development and progression (Gareus *et al.*, 2008; Monaco and Paleolog, 2004), rosiglitazone may be exerting its beneficial vascular effects via PPAR-γ activation and subsequent NF-κB inhibition.

AMPK plays an important role in maintaining cellular energy homeostasis and responds to reduced intracellular ATP and increased AMP/ATP ratio, by switching on ATP-generating pathways and turning off ATP-consuming pathways (Hardie, 2008). Previous studies have shown that rosiglitazone and other thiazolidinediones can activate AMPK (Boyle *et al.*, 2008; Fryer *et al.*, 2002), which has also been associated with cardioprotection (Russell *et al.*, 2004). Using the pharmacological AMPK activator AICAR at increasing concentrations, our results conclude that rosiglitazone exerts its effect via an AMPK-dependent mechanism.

Exposure of HUVEC to high glucose was seen to increase ROS generation, which rosiglitazone subsequently attenuated via protein kinase C (PKC) inhibition and with a PPAR-γ independent and AMPK-dependent mechanism. The inhibition of the diacylglycerol (DAG)-PKC pathway by rosiglitazone is dependent on the activation of AMPK and an essential target for the antioxidant effect of rosiglitazone (Ceolotto *et al.*, 2007).

Rosiglitazone was reported to confer rapid protection in human aortic endothelial cells via an AMPK-dependent and PPAR-γ-independent mechanism, increasing NO bioavailability and remaining unaffected by the exposure to GW9662 (Boyle *et al.*, 2008).

The underlying mechanism of protection of rosiglitazone against efavirenz-induced cytotoxicity may involve a number of systems such as modulation of the NO pathway involving iNOS and eNOS, affecting NO bioavailability (Betz *et al.*, 2012), inhibition of transcription factors such as NF-κB (Lee *et al.*, 2006), attenuation of MAPK JNK and p38 (Han *et al.*, 2012), downregulation of pro-inflammatory cytokines such as IL-1 and TNF-α (Mako *et al.*, 2010), modulation of endothelial cell barrier proteins (Huang *et al.*, 2009) and decrease in the expression of cell adhesion molecules such as ICAM and VCAM (Bruemmer *et al.*, 2005) in endothelial cells, which are all effects that can also be achieved by the inhibition of PARP.

However, not all the effects of NF-κB are detrimental to the vascular system as Davis et al. reported that with acute shear stress, NF-κB-dependently increases eNOS generation with subsequent NO synthesis required for vascular regulation (Davis *et al.*, 2004). Furthermore, NF-κB has been shown to inhibit apoptosis by upregulating the expression of several antiapoptotic genes. Interestingly, NF-κB has also been reported to downregulate prolonged TNF-α-induced JNK activation (De Smaele *et al.*, 2001). Since efavirenz has been shown to increase the activation of NF-κB (Jamaluddin *et al.*, 2010) in endothelial cells, which can be downregulated by PARP inhibition (Csiszar *et al.*, 2008), it is conceivable that the mechanism of protection of rosiglitazone involves modulation of the transcription factor NF-κB.

Several reports have shown a link between rosiglitazone and oxidative stress in endothelial cells. Rosiglitazone was reported to reduce hyperglycaemia-induced oxidative stress (Ceolotto *et al.*, 2007) and induce NO production in endothelial cells (Boyle *et al.*, 2008) via the AMPK pathway. PPAR-γ activation was shown to decrease the production of superoxide and NADPH expression in vascular endothelial cells (Hwang *et al.*, 2005) and increase NO bioavailability via a PPAR-γ dependent mechanism (Polikandriotis *et al.*, 2005).

Hwang and colleagues reported that short-term treatment with rosiglitazone attenuated vascular superoxide generation by inhibiting the expression of NADPH oxidase subunits, independent of its metabolic effects (Hwang *et al.*, 2007). An interesting study has shown that oxidative stress, possibly through activation of inhibitory redox-regulated transcription factors, reduces PPAR-γ expression and activity in HUVEC's via suppression of PPAR-γ transcription (Blanquicett *et al.*, 2010).

Rosiglitazone has convincingly been shown to reduce glucose-induced oxidative stress by activating AMPK, followed by the inhibition of the DAG-PKC pathway, which subsequently prevents NADPH oxidase-mediated ROS generation (Ceolotto *et al.*, 2007). Since efavirenz was shown to increase the production of superoxide anion in endothelial cells (Jamaluddin *et al.*, 2010), rosiglitazone may be inhibiting either the initial ROS generation or the subsequent PARP overactivation that results from efavirenz-induced oxidative stress.

By inhibiting PARP activation, rosiglitazone is thus able to inhibit the subsequent cellular depletion of ATP and NAD^+ and ultimately prevent or attenuate endothelial dysfunction mediated by efavirenz. As mentioned before, rosiglitazone may exhibit direct PARP inhibitory effects due to the similarity of its structure to known pharmacological PARP inhibitors and recently drugs such as cilostazol have been shown to be direct inhibitors.

Rosiglitazone was shown to significantly reduce the PARP activation mediated by efavirenz. In line with our results, rosiglitazone was reported to reduce PARP activation in an animal model of inflammation (Cuzzocrea *et al.*, 2004). Sivarajah and colleagues suggested that rosiglitazone may be exerting its protective effect by reducing oxidative stress and subsequently PARP activation via inhibition of ICAM expression and a reduction of polymorphonuclear cell infiltration in an animal model of renal ischemia/reperfusion injury (Sivarajah *et al.*, 2003). MAPK pathways which include JNK, ERK1/2 and p38 have been reported to play a crucial role in the generation of various pro-inflammatory cytokines (Dong *et al.*, 2002). Inhibition of the ERK signalling cascade by rosiglitazone was shown to prevent TNF-α and IFN-γ – mediated inflammatory response (Lombardi *et al.*, 2008).

There is still much debate over PPAR-γ and AMPK crosstalk. Some groups argue that AMPK activation is PPAR-γ dependent, while others report that the two events occur independently of each other. Fryer et al. suggest that acute rosiglitazone treatment rapidly activates AMPK in a PPAR-γ independent manner (Fryer *et al.*, 2002). In contrast, PPAR-γ-dependent transcriptional activity has been shown to increase the formation of adiponectin, which in turn confers AMPK-dependent cardioprotection (Ding *et al.*, 2007).

In conclusion, the results presented in the present chapter suggest that whilst the underlying mechanism of vasculoprotection by rosiglitazone still remains elusive, the general pathway of protection based on our study suggest to arise from a PPAR-γ- and AMPK- mediated effect, reducing the efavirenz-induced PARP overactivation, presumably following ROS generation and the subsequent cellular energy depletion, hence preventing or attenuating endothelial dysfunction (Figure 5.7). Future work is needed in order to fully elucidate the exact pathway involved in the vasculoprotection conferred by rosiglitazone in the endothelial dysfunction mediated by efavirenz. Direct measurements, rather than pharmacological inhibitors will be essential in order to precisely pinpoint the mechanism of action of rosiglitazone.

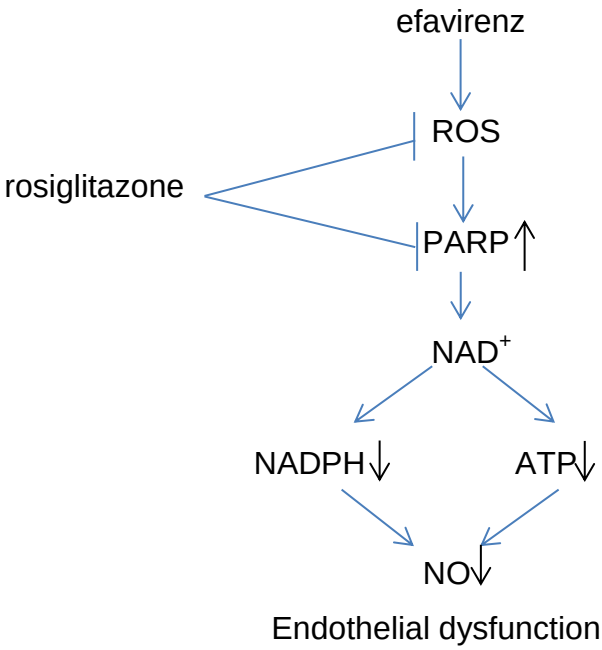

Figure 5.7: Proposed general pathway of the protection of rosiglitazone against efavirenz-induced endothelial dysfunction

efavirenz induces oxidative stress which subsequently increases PARP activation followed by celluar energy depletion and eventually leading to endothelial dysfunction. rosiglitazone either inhibits the generation of oxidative stress in efavirenz-treated endothelial cells or stops the PARP overactivation and therefore prevents the significant decrease in NAD^+ and ATP levels and thus preventing or attenuating efavirenz-mediated endothelial dysfunction.

Chapter 6

Atripla - mediated cytotoxicity and potential protective strategies in the brain endothelial cell line bEnd.3

6.1 Introduction

The breakdown of the blood brain barrier is thought to contribute to the development of HIV-associated dementia as well as neurological pathologies that are not usually associated with HIV infection such as stroke, brain tumors and multiple sclerosis (Wang *et al.*, 2008). HAART has been associated with an increase in the incidence of neurological side effects (Letendre *et al.*, 2010).

HIV-infected patients receiving Atripla may be showing neurological side effects after long-term use, since exposure to efavirenz has been shown to cause neuropsychological toxicity (Clifford *et al.*, 2005). In addition, efavirenz was reported to decrease the expression of tight junction molecules such as ZO-1, occludin, claudin-1 and JAM-1, compromising the integrity of the barrier function of endothelial cells (Jamaluddin *et al.*, 2010).

The results of this part of the study may provide insights on efavirenz-mediated neurological toxicity, its underlying mechanism of damage and whether any cell damage observed may be attenuated by the use of thiazolidinediones.

6.2 Methods

6.2.1 Treatment protocols

In order to assess the effect of the different Atripla components on cellular functions, bEnd.3 cells were treated with increasing concentrations of the individual drugs efavirenz, emtricitabine and tenofovir for 24 and 48 hours. The concentrations chosen were 3, 10, 30 and 100 μM. Using HPI staining, the effect of the different components were evaluated for apoptosis and necrosis after 24 hours, using 3, 10 and 30 μM of each drug. The effect of efavirenz on barrier function was assayed using 3 and 10 μM for 24 hours and albumin translocation measured as described in Chapter 2.

Rosiglitazone at 1, 3 or 10 μM was used to determine whether it had a protective role in the possible efavirenz-mediated loss of cell viability. The role of PPAR-γ was investigated using a specific inhibitor GW9662 (10μM). The role of oxidative stress was then assayed using the NBT assay and following exposure to 3, 10 and 30 μM efavirenz for 2, 4 and 6 hours. After the appropriate treatment protocols, the following cellular parameters were then measured:

6.2.1.1 Cell viability

The cell viability following exposure to the different treatments was measured using the MTT assay, which is a colorimetric assay as fully described in Chapter 2.

6.2.1.2 Necrosis and apoptosis levels

Cell death measurement was performed by morphological analysis using the HPI staining method, by which the relative numbers of live, apoptotic and necrotic cells were counted under a fluorescence microscope as previously described in Chapter 2.

6.2.1.3 Oxidative stress

Levels of oxidative stress were measured using the NBT assay. The NBT assay is a colorimetric assay used to detect the generation of superoxide anions as described in Chapter 2 and was used as an oxidative stress indicator

6.2.1.4 Barrier function

In order to measure the effect of the various Atripla components on transmembrane permeability, a barrier function assay was used as descriped in Chapter 2.

6.2.2 Statistical analysis

Statistical analysis was performed using ANOVA as fully described in Chapter 2.

6.3 Results

6.4 The effect of the Atripla components on the loss of cell viability and cell death in bEnd.3 cells

The bEnd.3 cells were exposed to increasing concentrations (3-100 µM) of the Atripla components efavirenz, emtricitabine and tenofovir for 24 and 48 hours. Efavirenz was seen to cause a dose- and time-dependent loss of cell viability (Figure 6.1).

When HPI staining was performed on the cells exposed to increasing concentrations (3-10 µM) of each component, efavirenz was shown to cause increased levels of cell death, with the apoptotic cells being double that of the necrotic cells following exposure to 30 µM efavirenz for 24 hours (Table 6.1).

Statistical analysis was performed using a one-way ANOVA followed by Dunnett's post-hoc test (vs. Control). Time-dependent comparisons between 24- and 48-hour treatments were performed using a two-way ANOVA, followed by Bonferroni's adjustment.

A

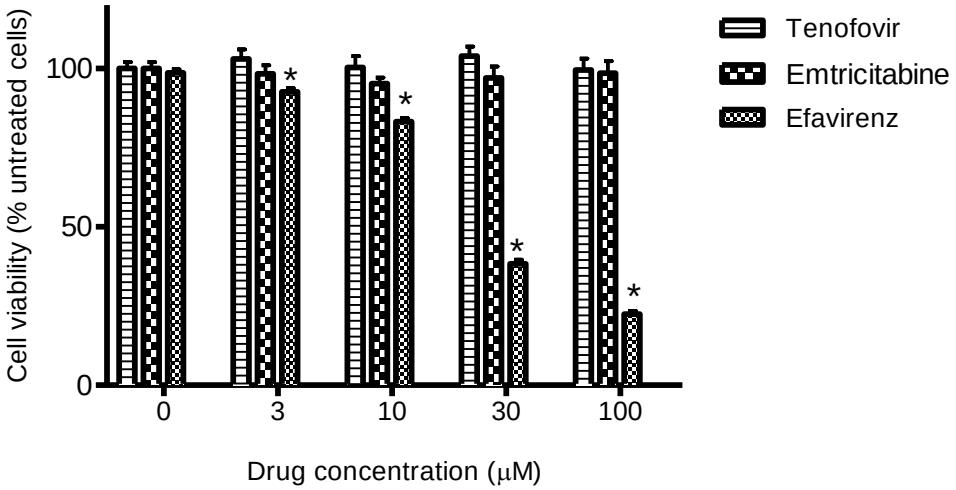

B

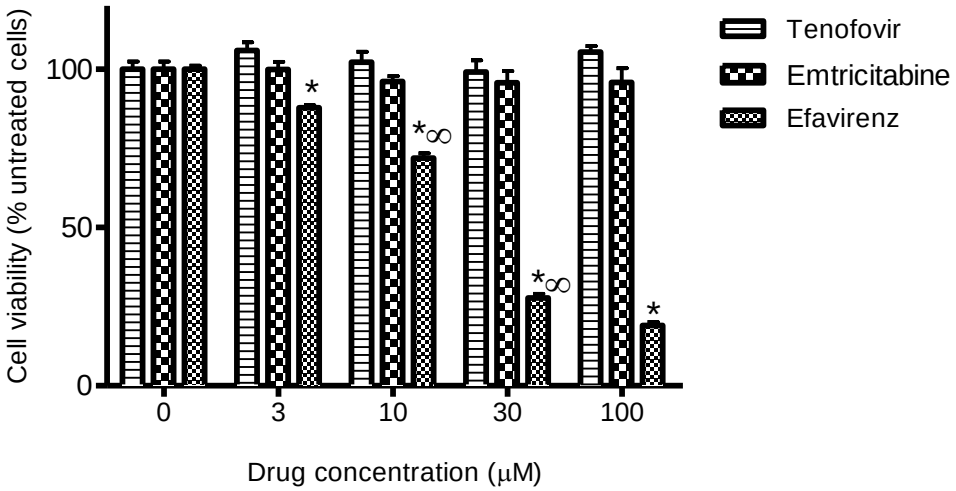

Figure 6.1: *Effect of the Atripla components on bEnd.3 cell viability (MTT) after 24 (A) and 48 (B) hours. Cells were treated with increasing concentrations (3, 10, 30 and 100 μM) of the individual components efavirenz, emtricitabine and tenofovir. Data are expressed as mean ± SEM of 4 experiments (6 replicas per experiment). * p < 0.01 when compared with control bEnd.3 cells and ∞p < 0.05 when the 24-hour treatment was compared with the 48-hour treatment.*

A

	Live	Apoptotic	Necrotic
Control	95.96 ± 0.81	2.18 ± 0.78	1.86 ± 0.57
3 µM efavirenz	91.81 ± 3.43	4.85 ± 2.70	3.34 ± 0.97
10 µM efavirenz	82.73 ± 4.79	10.21 ± 3.67	7.07 ± 1.25*
30 µM efavirenz	74.83 ± 5.69*	16.28 ± 4.04*	8.90 ± 2.28*

B

	Live	Apoptotic	Necrotic
Control	97.46 ± 0.18	1.63 ± 0.01	0.92 ± 0.17
3 µM emtricitabine	97.53 ± 1.15	1.42 ± 0.68	1.06 ± 0.47
10 µM emtricitabine	96.40 ± 0.83	2.09 ± 0.21	1.51 ± 0.63
30 µM emtricitabine	96.69 ± 0.20	2.33 ± 0.12*	1.00 ± 0.07

C

	Live	Apoptotic	Necrotic
Control	97.19 ± 0.07	1.42 ± 0.11	1.40 ± 0.18
3 µM tenofovir	96.77 ± 0.39	1.91 ± 0.12	1.34 ± 0.29
10 µM tenofovir	96.73 ± 0.96	2.04 ± 0.74	1.24 ± 0.23
30 µM tenofovir	96.40 ± 0.30	1.86 ± 0.02	1.75 ± 0.27

Table 6.1: *Effect of Atripla components on bEnd.3 cell death (HPI) after 24 hours. Cells were treated with increasing concentrations (3,10 and 30 µM) of the individual components efavirenz (A), emtricitabine (B) and tenofovir (C) for 24 hours. Data are expressed as mean ± SEM of 3 experiments (2 replicas per experiment). * $p < 0.05$ when compared with control bEnd3 cells.*

6.5 The effect of efavirenz on brain endothelial barrier function

The bEnd.3 cells were exposed to 3 and 10 µM efavirenz for 24 hours and brain barrier function measured by albumin translocation (data not shown). Unfortunately the data obtained is inconclusive and further work will be required to ascertain the role of efavirenz on brain endothelial permeability.

6.6 The protection by rosiglitazone against efavirenz-mediated loss of cell viability in bEnd.3 cells

Following the exposure of the bEnd.3 cells to 30 µM efavirenz for 48 hours, there was a 72 % drop in cell viability, which was attenuated to a 50 % drop in cell viability following the addition of 10 µM rosiglitazone. As a control, the addition of 10 µM rosiglitazone to the cells did not cause cell damage (Figure 6.2).

Statistical analysis was performed using a one-way ANOVA followed by Dunnett's post-hoc test (vs. Control) and Bonferroni's adjustment to compare efavirenz-treated cells with efavirenz-treated cells exposed to rosiglitazone.

A

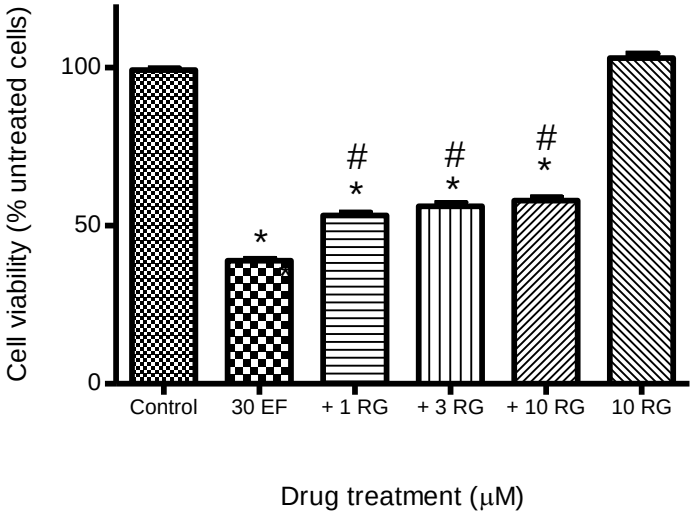

B

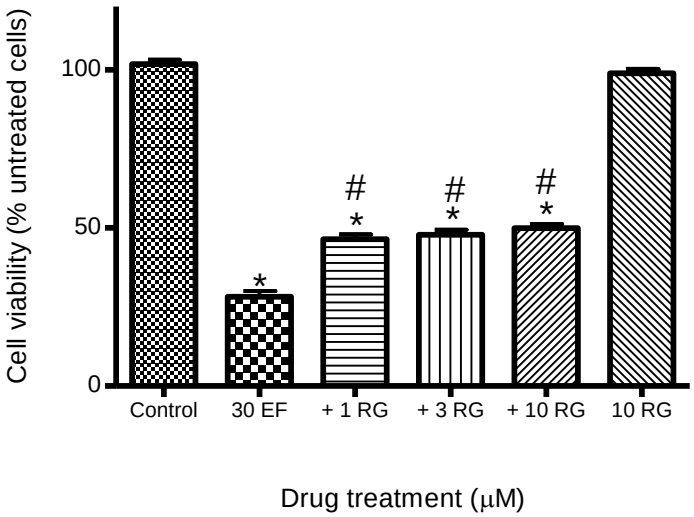

Figure 6.2: *Effect of the rosiglitazone on efavirenz-mediated loss of cell viability in bEnd.3 cells. Cells were treated with 30 μM of efavirenz for 24 (A) and 48 (B) hours. The addition of increasing concentrations (1, 3 and 10 μM) of rosiglitazone markedly decreased the loss of cell viability seen with efavirenz alone. Data are expressed as mean ± SEM of 3 experiments (6 replicas per experiment). * p < 0.01 when compared with control bEnd.3 cells and # p < 0.01 when compared with efavirenz-treated cells.*

6.7 The mechanism of protection of rosiglitazone against efavirenz-mediated loss of cell viability

In order to elucidate the mechanism by which rosiglitazone confers protection against efavirenz-induced loss of endothelial cell viability, the pharmacological inhibitor of PPAR-γ GW9662 was used. The addition of 10 μM of GW9662 to efavirenz (10 μM) treated cells did not block the protection against efavirenz-mediated cell damage, suggesting a PPAR-γ independent mechanism of protection in bEnd.3 cells.

As a control, the addition of GW9662 (10 μM) to 30 μM of efavirenz was shown not to have an effect on its own on the cell damage mediated by efavirenz. Similarly, cells exposed to 10 μM of GW9662 on its own did not show any signs of cytotoxicity (Figure 6.3).

Statistical analysis was performed using a one-way ANOVA followed by Dunnett's post-hoc test (vs. Control) and Bonferroni's adjustment to compare efavirenz-treated cells with efavirenz-treated cells exposed to rosiglitazone and GW9662.

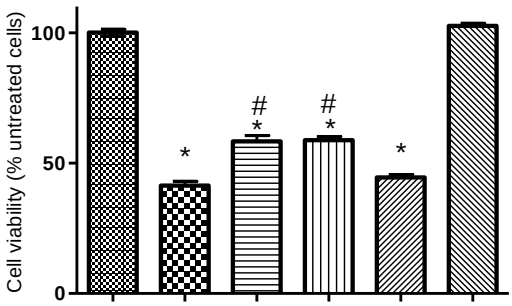

Efavirenz 30 µM	-	+	+	+	+	-
Rosiglitazone 3 µM	-	-	+	+	-	-
GW9662 10 µM	-	-	-	+	+	+

Figure 6.3: *Effect of PPAR-γ antagonist GW9662 on rosiglitazone-mediated protection against efavirenz-induced loss of bEnd.3 cell viability after 24 hours. Cells were treated with 30 µM of efavirenz, causing significant loss of cell viability, partly attenuated by the addition of 3 µM rosiglitazone. Data are expressed as mean $\pm$ SEM of 3 experiments (6 replicas per experiment). * $p < 0.01$ when compared with control bEnd.3 cells and # $p < 0.01$ when compared with efavirenz-treated cells.*

6.8 The role of oxidative stress in efavirenz-mediated loss of cell viability in bEnd.3 cells

In order to assess the role of oxidative stress generation in efavirenz-mediated loss of cell viability, the NBT assay was performed. The cells were exposed to increasing concentrations (3, 10 and 30 µM) of efavirenz for 2, 4 and 6 hours. With the maximal concentration used (30 µM) of efavirenz, the levels of superoxide anions generated were seen to increase significantly (Table 6.2).

Statistical analysis was performed using a one-way ANOVA followed by Dunnett's post-hoc test (vs. Control).

	2h	4h	6h
Control	100 ± 2.52	100.44 ± 2.17	99.67 ± 2.13
3 μM efavirenz	93.88 ± 1.37*	97.50 ± 2.40	97.83 ± 2.36
10 μM efavirenz	103.57 ± 3.95	102.58 ± 5.63	103.06 ± 5.59
30 μM efavirenz	134.03 ± 7.69**	146.50 ± 10.06**	147.39 ± 9.83**

Table 6.2: *NBT assay (oxidative stress) of efavirenz in bEnd.3 cells. Cells were treated with increasing concentrations (3, 10 and 30 μM) of efavirenz at 2, 4 and 6 hours. Data are expressed as mean ± SEM of 4 experiments (3 replicas per experiment). * $p < 0.05$ and ** $p < 0.01$ when compared with control untreated cells.*

6.9 Discussion

This part of the study focused on the effects of the Atripla components on brain endothelial cell viability and concluded that i) out of the three drugs; efavirenz caused a dose- and time- dependent loss of cell viability, ii) efavirenz showed an increase in apoptotic and necrotic cells after 24 hours, iii) rosiglitazone was able to partially protect against the efavirenz-mediated loss of cell viability after 24 and 48 hours, iv) the PPAR-γ antagonist GW9662 was not able to block that protection, implying a PPAR-γ independent mechanism, v) efavirenz seems to be causing oxidative stress generation in brain endothelial cells.

The use of HAART has significantly improved the prognosis of HIV-infected individuals and decreased the incidence of HIV-associated dementia (HAD), however the incidence of HIV-associated neurocognitive disorders (HAND) seems to be on the increase despite antiretroviral treatment (Heaton *et al.*, 2010; Letendre *et al.*, 2010). A recent study has looked at the effect of efavirenz and its metabolite (8-OH-EFV) on neuronal function and found that the metabolite caused a nearly 10-fold increase in neurotoxicity compared to the parent drug (Tovar-y-Romo *et al.*, 2012). Efavirenz was shown to increase apoptotic and necrotic cells in bEnd.3 cells after 24 hours, with apoptotic levels being double that of necrosis. This is in agreement with the previous study showing that 8-OH-EFV also elicited neuronal apoptosis at low doses (Tovar-y-Romo *et al.*, 2012). Rosiglitazone was shown to protect against efavirenz-mediated loss of cell viability in a dose-dependent manner.

Recently, Araujo and colleagues have demonstrated the protective role of rosiglitazone against brain microvascular dysfunction in a model of sepsis (Araujo *et al.*, 2012). Using the PPAR-γ antagonist GW9662, a PPAR-γ dependent mechanism of protection was not conclusive in this study and further investigation is warranted in order to fully ascertain the role of PPAR-γ in the protection seen.

Interestingly, in this cell line bEnd.3, the NBT assay resulted in a significant induction of superoxide anions and may provide insight into the mechanism of damage of efavirenz. Oxidative stress has previously been linked to efavirenz in brain endothelial cells and may account for the loss of cell viability observed in this cell line (Igbigbi, 2012). In contrast, another study concluded that efavirenz did not alter antioxidant levels in cultured brain astrocytes (Brandmann *et al.*, 2012). The barrier function assay was inconclusive in this study; however, an important study has shown efavirenz to significantly reduce the levels of tight junction proteins claudin-1, occludin and zonula occluden-1 (Jamaluddin *et al.*, 2010), a paper which prompted us to look at the effects of Atripla on cultured brain endothelial cells.

In conclusion, this part of the study emphasises the damaging effect of efavirenz in a different cell line and confirms its role in the endothelial dysfunction observed in HIV-infected patients and further research will be required to fully elucidate the effect of efavirenz on the brain endothelial dysfunction seen in patients receiving Atripla.

Chapter 7

General Discussion

Highly active antiretroviral therapy has proved very successful in prolonging the lifespan and improving the quality of life of HIV patients. Unfortunately, HAART-related cardiovascular side effects have come to light following long term use of these anti-HIV agents. Cardiovascular side effects reported include atherosclerosis, hypertension, myocarditis, congestive heart failure and dilated cardiomyopathy (Barbaro *et al.*, 2001). Endothelial dysfunction is an important early precursor for the development of cardiovascular disease and perhaps the most plausible link between HAART and atherosclerosis in the HIV population in the absence of general cardiovascular risk factors. HIV patients on HAART have been reported to have a 26 % relative risk increase in the rate of myocardial infarction per year of HAART exposure (Friis-Moller *et al.*, 2003).

Current treatment strategies aimed at reducing HAART-related cardiovascular toxicity include cardiovascular risk stratification of patients receiving HAART, especially those with underlying cardiovascular risk factors such as hypertension or diabetes (Barbaro, 2003). The introduction of the once daily fixed dose pill Atripla on the global market was hoped to improve compliance and adherence associated with HAART. The Atripla components efavirenz, emtricitabine and tenofovir were considered to be significantly safer than conventional antiretroviral agents; however, no detailed research had been carried out on the cardiovascular toxicity of these components.

The results presented in this study clearly show that out of the three Atripla constituents, efavirenz significantly causes cardiovascular dysfunction, which in the long run may contribute to the development of cardiovascular disease in HIV patients receiving Atripla.

7.1 Main findings

The main work described in this thesis focuses on the detrimental effects caused by the Atripla components, in particular efavirenz, which was shown to induce cell dysfunction and cell death in cardiac, vascular and brain endothelial cells. As we shall see, the mechanism by which efavirenz causes cell toxicity comprises a number of possible pathways. The general mechanism of action of efavirenz is thought to include oxidative stress generation with subsequent PARP activation and possibly ER stress, eventually leading to cell dysfunction and cell death. The antidiabetic agent rosiglitazone clearly improved the efavirenz-mediated cardiovascular side effects, possibly by inhibition of ROS and/or the following PARP activation involving PPAR-γ and AMPK activation and thus preventing or attenuating the damage caused by efavirenz alone. The underlying precise mechanism is yet to be elucidated but the probable pathways by which efavirenz and rosiglitazone exert their effect will be summarised in the following sections and the relevance of our findings put into a clinical context.

7.1.1 Oxidative stress

The experiments used in this study to investigate whether efavirenz induces oxidative stress were inconclusive in H9c2 and EA.hy926 cells, however, in bEnd.3, efavirenz was shown to significantly induce superoxide generation. Further research with more direct methods is warranted for definite conclusions. Efavirenz-mediated ROS generation is however the most plausible mechanism by which it causes the cardiovascular toxicity. Previous work has linked oxidative stress to HAART in all cell types used in this study, cardiac (Hulgan *et al.*, 2003) and endothelial cells (Mondal *et al.*, 2004) and brain endothelial cells (Igbigbi, 2012).

Using EUK-134, a synthetic superoxide dismutase/catalase mimetic, the oxidant-scavenging effect on efavirenz-mediated cardiovascular dysfunction (data not shown) was explored and also proved to be inconclusive, calling for further investigation into the oxidative ability of efavirenz. In addition, regardless of HAART, HIV positive patients seem to display higher levels of oxidative stress as evidenced for instance by a study using transgenic HIV rat model which expressed increased superoxide and 3-nitrotyrosine levels as well as reduced superoxide dismutase and glutathione and reduced NO production leading to endothelial dysfunction and in the HIV population to increased risk of cardiovascular disease (Kline and Sutliff, 2008).

7.1.2 Endoplasmic reticulum stress

The ER stress marker CHOP was seen to be significantly increased following the exposure of efavirenz and this is the first time that this has been observed with HAART and may provide an explanation as to why these agents cause cardiovascular dysfunction as well as being a prospective screening tool for potential cardiotoxicity of new antiretroviral agents in development.

The crosstalk between oxidative and ER stress is now well documented and both events are thought to be able to precede one another. Sustained ER stress has been shown to induce oxidative stress in HIP-deficient cells that can't eliminate misfolded proteins from the ER (Haynes *et al.*, 2004). The activation of NFE2-related factor 2 (Nrf2) and activating transcription factor 4 (ATF4) transcription factors is thought to induce PKR-like Endoplasmic Reticulum Kinase (PERK) signalling and may be the main link between ER and the subsequent oxidative stress generation (Cullinan and Diehl, 2006).

The production of ROS can be stimulated by many physiological and pathological conditions, which subsequently target ER-based calcium channels and chaperones, causing the release of calcium from the ER to the cytosol. This may further stimulate mitochondria-derived ROS generation, which in turn can increase calcium release from the ER and may lead to ROS accumulation and the perturbation of ER calcium homeostasis can upset the protein folding process, leading to ER stress and the UPR activation.

The UPR can then induce certain effects such as the inflammatory response, anti-oxidative stress response and apoptosis (Zhang, 2010). As seen in renal epithelial cells, cadmium, thapsigargin and tunicamycin contribute to ER stress by inducing an increase in calcium in the cytosol, followed by ROS generation and the cells in order to attenuate ER stress and cell death, upregulate Bestrophin-3 by activating ERK 1/2, which inhibits the expression of CHOP, apoptosis and promotes cell survival. Interestingly, Bestrophin-3 knockdown caused PARP activation and cell death (Lee *et al.*, 2012).

7.1.3 PARP activation

Efavirenz was shown to cause a significant increase in PARP activity after a short term exposure in both types of cells, H9c2 and EA.hy926. Furthermore, the pharmacological inhibition of PARP was shown to attenuate the deleterious effects seen with efavirenz alone, suggesting a crucial role of PARP in the toxicity observed.

Previously, oxidative stress and PARP activation have been convincingly shown to be closely interrelated and many studies have sought to establish a causal link between the two events, indeed the most plausible one seems to be that if the levels of ROS are high enough, PARP becomes activated in the nucleus, followed by cellular energy depletion in the form of reduced ATP and NAD^+ levels and eventually leading to cellular death by apoptosis or necrosis.

The results of a study by Racz et al. concluded that ROS-mediated PARP activation regulated the activation of JNK and p38 MAPK via its effects on Mitogen-activated protein (MAP) kinase phosphatase 1 (MKP-1), which dephosphorylates JNK and p38 MAPK under oxidative stress and the expression of which is increased by PARP inhibition (Racz *et al.*, 2010). This is the first time that the importance of PARP has been shown in HAART-related cardiovascular adverse effects and opens the way for future research focusing on modulation of PARP in order to counteract HAART-related cardiovascular toxicity.

7.1.4 Protective role of rosiglitazone

In the present study, rosiglitazone was observed to be partially protective against the injurious effects mediated by efavirenz in all cell types by either inhibiting efavirenz-induced ROS generation and/or PARP activation and this is the first time that this drug was seen to protect against HAART-mediated cardiovascular toxicity and gives way for further research into this drug class as pioglitazone was seen to exert similar protection (data not shown). Since the drug is readily available, although with certain restrictions, PPAR agonists in general including fibrates may be useful as an additional therapy to Atripla in order to prevent the long term cardiovascular side effects. Interestingly, a very recent study looked at the protective role of the thiazolidinediones against the detrimental effects against PI-mediated endothelial dysfunction in human aortic endothelial cells.

This same study concluded that nelfinavir decreased tyrosine phosphorylation of insulin receptor beta (IR-β), insulin receptor substrate-1 (IRS-1) and phosphatidylinositol 3'-kinase (PI3K) and that simultaneous exposure to troglitazone improved the suppressive effects of nelfinavir on insulin signaling and NO production, as well as lead to increased eNOS expression in treated human aortic endothelial cells (Mondal *et al.*, 2013). Future research may be focused on PPAR agonists in general as the beneficial effects of these agents can easily be extrapolated into the clinical setting.

7.2 Main limitations

Although every effort has been employed to elucidate the underlying mechanisms of the different drugs, factors including time and cost have made it challenging to expand on the experiments. There still remain a number of unanswered questions in this thesis. These include whether efavirenz causes oxidative stress in H9c2 and EA.hy926 cell lines and if yes, which oxidants are being generated? Does efavirenz cause increased activation of NF-κB and MAPK JNK? Does it affect other transcription factors such as AP-1 or is it NF-κB specific? Can it cause increased induction of pro-inflammatory cytokines such as IL-6 and IL-8 in the cell lines used? How does it downregulate tight junction proteins such as ZO-1 and occludin? Does it cause increased levels of cell adhesion molecules such as VCAM and ICAM? Which other pathways may be involved in the toxicity seen with efavirenz? Can rosiglitazone attenuate oxidative stress generation in the cell lines used?

Another important limitation worth mentioning is that due to university restrictions, no HIV-infected cells were used in this study, which may make it difficult to obtain a realistic picture of the effects of HAART on HIV-positive cells.

7.3 Future perspectives

Future studies may be useful in answering some of the questions highlighted in the previous section. In order to clearly ascertain the role of efavirenz in the generation of oxidative stress in cardiac, endothelial and brain cells, methods such as the DCF assay or the more costly commercially available kits including MitoSOX^{TM} could be carried out. Using western blots, the activation of the different pathways may be investigated further, rather than pharmacological inhibition.

In vivo studies using HIV-infected animal models may be preferable in order to get a more complete picture of the long term effects of Atripla. The following step would of course include the follow-up in clinical trials of patients that have been taking Atripla long term with regular monitoring and assessment of cardiovascular factors.

7.4 Implications

Besides introducing adjuvant therapies such as rosiglitazone to counteract the cardiovascular side effects of Atripla, important measures, albeit costly for screening and monitoring HIV patients on Atripla may include echocardiography, electrocardiography, stress testing, ultrafast electron beam computerised tomography, brachial artery reactivity, intima medial thickness, nuclear cardiology, catheterization and biopsy, pericardiocentesis, tests for treatable nutritional and biochemical causes of heart failure, serum and plasma markers of myocardial injury and Left ventricular dysfunction, blood inflammatory markers, lipid profiles for preventive cardiology, genetic testing, traditional cardiovascular risk profiling, hypertension screening.

When prevention and treatment of cardiovascular disease are necessary, therapeutic strategies may comprise cytokine antagonist therapy, immunomodulatory therapy, anti-infective therapy, heart failure therapy, primary prevention of coronary heart disease involving modulation of factors such as exercise, diet, smoking, hypertension, cholesterol, triglycerides, anticoagulation (Lipshultz *et al.*, 2001).

While this thesis focuses on the side effects of HAART, one needs to consider several important factors that may play a role in the cardiovascular symptoms experienced by the individual patient. The overall picture of a patient may include elements such as compliance, diet, symptom perception, symptom reporting, genetics and comorbidities.

Traditional cardiovascular risk factors including age, gender, tobacco smoking, alcohol consumption, cholesterol, family history and Diabetes mellitus, regardless of HAART play a significant role in the development and progression of cardiovascular complications when on HAART.

Another important aspect to consider is certainly the cardiovascular complications caused by HIV *per se*, irrespective of HAART. These HIV-related cardiovascular abnormalities include dilated cardiomyopathy, coronary heart disease, hypertension and pericardial effusion (Barbaro *et al.*, 2001), all of which may overlap with HAART-related cardiovascular problems.

In addition, a number of reports have shown that the HIV protein Tat may induce oxidative stress by itself, especially in neurons (Kruman *et al.*, 1999; Shi *et al.*, 1998). Interestingly, it was found that supplementing HIV patients with the antioxidants Vitamin C and E could reduce HIV-induced oxidative stress and possibly even reduce viral load (Allard *et al.*, 1998).

7.5 Conclusions

In conclusion, the results of this thesis highlight the detrimental effects of the Atripla pill and suggest one possible class of drug as well as pharmacological inhibition of PARP or antioxidants that may be used as an adjuvant therapy to counteract the cardiovascular toxicity.

The work proposes a possible mechanism by which efavirenz causes cytotoxicity, which overall is thought to include oxidative stress, ER stress and PARP activation and further research focusing on these will be necessary to develop new therapies that may be useful in preventing HAART-related cardiovascular side effects. Newer drugs such as efavirenz were developed in the hope of being safer than the original antiretrovirals such as AZT, however, long term use of Atripla may be causing significant cardiovascular damage, the drug-related side effects will be more detrimental to HIV-infected patients than HIV infection itself.

There are still many open questions about the mechanism of toxicity of the antiretrovirals and the DNA pol-γ hypothesis may be eliminated as the mode of damage may be far more complex involving several pathways.

Bibliography

Abbott NJ, Patabendige AA, Dolman DE, Yusof SR, Begley DJ (2010). Structure and function of the blood-brain barrier. *Neurobiology of disease* **37**(1)**:** 13-25.

Abbott NJ, Ronnback L, Hansson E (2006). Astrocyte-endothelial interactions at the blood-brain barrier. *Nature reviews. Neuroscience* **7**(1)**:** 41-53.

Adachi M, Kurotani R, Morimura K, Shah Y, Sanford M, Madison BB*, et al.* (2006). Peroxisome proliferator activated receptor gamma in colonic epithelial cells protects against experimental inflammatory bowel disease. *Gut* **55**(8)**:** 1104-1113.

Aguilar-Quesada R, Munoz-Gamez JA, Martin-Oliva D, Peralta-Leal A, Quiles-Perez R, Rodriguez-Vargas JM*, et al.* (2007). Modulation of transcription by PARP-1: consequences in carcinogenesis and inflammation. *Current medicinal chemistry* **14**(11)**:** 1179-1187.

Ahn K, Pan SM, Zientek MA, Guy PM, Sisneros AM (1996). Characterization of endothelin converting enzyme from intact cells of a permanent human endothelial cell line, EA.hy926. *Biochemistry and molecular biology international* **39**(3)**:** 573-580.

AIDSinfo (2006). Aidsinfo drug database (Atripla) Vol. 2012.

Alimonti JB, Ball TB, Fowke KR (2003). Mechanisms of CD4+ T lymphocyte cell death in human immunodeficiency virus infection and AIDS. *The Journal of general virology* **84**(Pt 7)**:** 1649-1661.

Allard JP, Aghdassi E, Chau J, Tam C, Kovacs CM, Salit IE*, et al.* (1998). Effects of vitamin E and C supplementation on oxidative stress and viral load in HIV-infected subjects. *Aids* **12**(13)**:** 1653-1659.

Anand P, Springer SA, Copenhaver MM, Altice FL (2010). Neurocognitive impairment and HIV risk factors: a reciprocal relationship. *AIDS and behavior* **14**(6)**:** 1213-1226.

Andersen JK (2004). Oxidative stress in neurodegeneration: cause or consequence? *Nature medicine* **10 Suppl:** S18-25.

Andreone T, Meares GP, Hughes KJ, Hansen PA, Corbett JA (2012). Cytokine-mediated beta-cell damage in PARP-1-deficient islets. *American journal of physiology. Endocrinology and metabolism* **303**(2)**:** E172-179.

Apostolova N, Blas-Garcia A, Esplugues JV (2011). Mitochondrial interference by anti-HIV drugs: mechanisms beyond Pol-gamma inhibition. *Trends in pharmacological sciences* **32**(12)**:** 715-725.

Apostolova N, Gomez-Sucerquia LJ, Moran A, Alvarez A, Blas-Garcia A, Esplugues JV (2010). Enhanced oxidative stress and increased mitochondrial mass during efavirenz-induced apoptosis in human hepatic cells. *British journal of pharmacology* **160**(8)**:** 2069-2084.

Aragones G, Pardo-Reche P, Fernandez-Sender L, Rull A, Beltran-Debon R, Rodriguez-Gallego E*, et al.* (2012). The deleterious influence of tenofovir-based therapies on the progression of atherosclerosis in HIV-infected patients. *Mediators of inflammation* **2012:** 372305.

Araujo CV, Estato V, Tibirica E, Bozza PT, Castro-Faria-Neto HC, Silva AR (2012). PPAR gamma activation protects the brain against microvascular dysfunction in sepsis. *Microvascular research* **84**(2)**:** 218-221.

Ariumi Y, Turelli P, Masutani M, Trono D (2005). DNA damage sensors ATM, ATR, DNA-PKcs, and PARP-1 are dispensable for human immunodeficiency virus type 1 integration. *Journal of virology* **79**(5)**:** 2973-2978.

Aubuchon M, Santoro N (2004). Lessons learned from the WHI: HRT requires a cautious and individualized approach. *Geriatrics* **59**(11)**:** 22-26.

Aveleira CA, Lin CM, Abcouwer SF, Ambrosio AF, Antonetti DA (2010). TNF-alpha signals through PKCzeta/NF-kappaB to alter the tight junction complex and increase retinal endothelial cell permeability. *Diabetes* **59**(11)**:** 2872-2882.

Badley AD, Roumier T, Lum JJ, Kroemer G (2003). Mitochondrion-mediated apoptosis in HIV-1 infection. *Trends in pharmacological sciences* **24**(6)**:** 298-305.

Bakondi E, Bai P, Szabo EE, Hunyadi J, Gergely P, Szabo C*, et al.* (2002). Detection of poly(ADP-ribose) polymerase activation in oxidatively stressed cells and tissues using biotinylated NAD substrate. *The journal of histochemistry and cytochemistry : official journal of the Histochemistry Society* **50**(1)**:** 91-98.

Barbaro G (2002). Cardiovascular manifestations of HIV infection. *Circulation* **106**(11)**:** 1420-1425.

Barbaro G (2003). Pathogenesis of HIV-associated cardiovascular disease. *Advances in cardiology* **40:** 49-70.

Barbaro G, Barbarini G (2007). HIV infection and cancer in the era of highly active antiretroviral therapy (Review). *Oncology reports* **17**(5)**:** 1121-1126.

Barbaro G, Fisher SD, Lipshultz SE (2001). Pathogenesis of HIV-associated cardiovascular complications. *The Lancet infectious diseases* **1**(2)**:** 115-124.

Barbaro G, Silva EF (2009). Cardiovascular complications in the acquired immunodeficiency syndrome. *Revista da Associacao Medica Brasileira* **55**(5)**:** 621-630.

Bernhard D, Wang XL (2007). Smoking, oxidative stress and cardiovascular diseases--do anti-oxidative therapies fail? *Current medicinal chemistry* **14**(16)**:** 1703-1712.

Betz B, Schneider R, Kress T, Schick MA, Wanner C, Sauvant C (2012). Rosiglitazone affects nitric oxide synthases and improves renal outcome in a rat model of severe ischemia/reperfusion injury. *PPAR research* **2012:** 219319.

Blanquicett C, Kang BY, Ritzenthaler JD, Jones DP, Hart CM (2010). Oxidative stress modulates PPAR gamma in vascular endothelial cells. *Free radical biology & medicine* **48**(12)**:** 1618-1625.

Blas-Garcia A, Apostolova N, Ballesteros D, Monleon D, Morales JM, Rocha M*, et al.* (2010). Inhibition of mitochondrial function by efavirenz increases lipid content in hepatic cells. *Hepatology* **52**(1)**:** 115-125.

BNF 61 (2011). *Antiretroviral agents*.

Bonetti PO, Lerman LO, Lerman A (2003). Endothelial dysfunction: a marker of atherosclerotic risk. *Arteriosclerosis, thrombosis, and vascular biology* **23**(2)**:** 168-175.

Bowes J, McDonald MC, Piper J, Thiemermann C (1999). Inhibitors of poly (ADP-ribose) synthetase protect rat cardiomyocytes against oxidant stress. *Cardiovascular research* **41**(1)**:** 126-134.

Boyle JG, Logan PJ, Ewart MA, Reihill JA, Ritchie SA, Connell JM*, et al.* (2008). Rosiglitazone stimulates nitric oxide synthesis in human aortic endothelial cells via AMP-activated protein kinase. *The Journal of biological chemistry* **283**(17)**:** 11210-11217.

Brandmann M, Tulpule K, Schmidt MM, Dringen R (2012). The antiretroviral protease inhibitors indinavir and nelfinavir stimulate Mrp1-mediated GSH export from cultured brain astrocytes. *Journal of neurochemistry* **120**(1)**:** 78-92.

Bruemmer D, Blaschke F, Law RE (2005). New targets for PPARgamma in the vessel wall: implications for restenosis. *International journal of obesity* **29 Suppl 1:** S26-30.

Bulhak AA, Jung C, Ostenson CG, Lundberg JO, Sjoquist PO, Pernow J (2009). PPAR-alpha activation protects the type 2 diabetic myocardium against ischemia-reperfusion injury: involvement of the PI3-Kinase/Akt and NO pathway. *American journal of physiology. Heart and circulatory physiology* **296**(3)**:** H719-727.

Bumpus NN (2011). Efavirenz and 8-hydroxyefavirenz induce cell death via a JNK- and BimEL-dependent mechanism in primary human hepatocytes. *Toxicology and applied pharmacology* **257**(2)**:** 227-234.

Burger D, van der Heiden I, la Porte C, van der Ende M, Groeneveld P, Richter C*, et al.* (2006). Interpatient variability in the pharmacokinetics of the HIV non-nucleoside reverse transcriptase inhibitor efavirenz: the effect of gender, race, and CYP2B6 polymorphism. *British journal of clinical pharmacology* **61**(2)**:** 148-154.

Burgoyne RW, Tan DH (2008). Prolongation and quality of life for HIV-infected adults treated with highly active antiretroviral therapy (HAART): a balancing act. *The Journal of antimicrobial chemotherapy* **61**(3)**:** 469-473.

Cadogan M, Dalgleish AG (2008). HIV immunopathogenesis and strategies for intervention. *The Lancet infectious diseases* **8**(11)**:** 675-684.

Cai H, Harrison DG (2000). Endothelial dysfunction in cardiovascular diseases: the role of oxidant stress. *Circulation research* **87**(10)**:** 840-844.

Cao R, Hu Y, Wang Y, Gurley EC, Studer EJ, Wang X*, et al.* (2010). Prevention of HIV protease inhibitor-induced dysregulation of hepatic lipid metabolism by raltegravir via endoplasmic reticulum stress signaling pathways. *The Journal of pharmacology and experimental therapeutics* **334**(2)**:** 530-539.

Cattelan AM, Trevenzoli M, Sasset L, Rinaldi L, Balasso V, Cadrobbi P (2001). Indinavir and systemic hypertension. *Aids* **15**(6)**:** 805-807.

Ceolotto G, Gallo A, Papparella I, Franco L, Murphy E, Iori E*, et al.* (2007). Rosiglitazone reduces glucose-induced oxidative stress mediated by NAD(P)H oxidase via AMPK-dependent mechanism. *Arteriosclerosis, thrombosis, and vascular biology* **27**(12)**:** 2627-2633.

Chandra J, Samali A, Orrenius S (2000). Triggering and modulation of apoptosis by oxidative stress. *Free radical biology & medicine* **29**(3-4)**:** 323-333.

Chesney M (2003). Adherence to HAART regimens. *AIDS patient care and STDs* **17**(4)**:** 169-177.

Choi AI, Vittinghoff E, Deeks SG, Weekley CC, Li Y, Shlipak MG (2011). Cardiovascular risks associated with abacavir and tenofovir exposure in HIV-infected persons. *Aids* **25**(10)**:** 1289-1298.

Chow DC, Souza SA, Chen R, Richmond-Crum SM, Grandinetti A, Shikuma C (2003). Elevated blood pressure in HIV-infected individuals receiving highly active antiretroviral therapy. *HIV clinical trials* **4**(6)**:** 411-416.

Chu C, Selwyn PA (2010). Diagnosis and initial management of acute HIV infection. *American family physician* **81**(10)**:** 1239-1244.

Cihlar T, Ray AS (2010). Nucleoside and nucleotide HIV reverse transcriptase inhibitors: 25 years after zidovudine. *Antiviral research* **85**(1)**:** 39-58.

Clifford DB, Evans S, Yang Y, Acosta EP, Goodkin K, Tashima K*, et al.* (2005). Impact of efavirenz on neuropsychological performance and symptoms in HIV-infected individuals. *Annals of internal medicine* **143**(10)**:** 714-721.

Cohen D (2010). Rosiglitazone: what went wrong? *Bmj* **341:** c4848.

Conklin BS, Fu W, Lin PH, Lumsden AB, Yao Q, Chen C (2004). HIV protease inhibitor ritonavir decreases endothelium-dependent vasorelaxation and increases superoxide in porcine arteries. *Cardiovascular research* **63**(1)**:** 168-175.

Crane HM, Van Rompaey SE, Kitahata MM (2006). Antiretroviral medications associated with elevated blood pressure among patients receiving highly active antiretroviral therapy. *Aids* **20**(7)**:** 1019-1026.

Csiszar A, Wang M, Lakatta EG, Ungvari Z (2008). Inflammation and endothelial dysfunction during aging: role of NF-kappaB. *Journal of applied physiology* **105**(4)**:** 1333-1341.

Cullinan SB, Diehl JA (2006). Coordination of ER and oxidative stress signaling: the PERK/Nrf2 signaling pathway. *The international journal of biochemistry & cell biology* **38**(3)**:** 317-332.

Currier JS (2009). Update on cardiovascular complications in HIV infection. *Topics in HIV medicine : a publication of the International AIDS Society, USA* **17**(3)**:** 98-103.

Currier JS, Havlir DV (2009). Complications of HIV disease and antiretroviral therapy. *Topics in HIV medicine : a publication of the International AIDS Society, USA* **17**(2)**:** 57-67.

Cuzzocrea S (2005). Shock, inflammation and PARP. *Pharmacological research : the official journal of the Italian Pharmacological Society* **52**(1)**:** 72-82.

Cuzzocrea S, Pisano B, Dugo L, Ianaro A, Maffia P, Patel NS*, et al.* (2004). Rosiglitazone, a ligand of the peroxisome proliferator-activated receptor-gamma, reduces acute inflammation. *European journal of pharmacology* **483**(1)**:** 79-93.

Czaja MJ, Liu H, Wang Y (2003). Oxidant-induced hepatocyte injury from menadione is regulated by ERK and AP-1 signaling. *Hepatology* **37**(6)**:** 1405-1413.

Daar ES, Pilcher CD, Hecht FM (2008). Clinical presentation and diagnosis of primary HIV-1 infection. *Current opinion in HIV and AIDS* **3**(1)**:** 10-15.

Davis ME, Grumbach IM, Fukai T, Cutchins A, Harrison DG (2004). Shear stress regulates endothelial nitric-oxide synthase promoter activity through nuclear factor kappaB binding. *The Journal of biological chemistry* **279**(1)**:** 163-168.

Day BJ, Lewis W (2004). Oxidative stress in NRTI-induced toxicity: evidence from clinical experience and experiments in vitro and in vivo. *Cardiovascular toxicology* **4**(3)**:** 207-216.

de Bethune MP (2010). Non-nucleoside reverse transcriptase inhibitors (NNRTIs), their discovery, development, and use in the treatment of HIV-1 infection: a review of the last 20 years (1989-2009). *Antiviral research* **85**(1)**:** 75-90.

De Clercq E (2009). Anti-HIV drugs: 25 compounds approved within 25 years after the discovery of HIV. *International journal of antimicrobial agents* **33**(4)**:** 307-320.

de Gaetano G, Donati MB, Cerletti C (2003). Prevention of thrombosis and vascular inflammation: benefits and limitations of selective or combined COX-1, COX-2 and 5-LOX inhibitors. *Trends in pharmacological sciences* **24**(5)**:** 245-252.

De Smaele E, Zazzeroni F, Papa S, Nguyen DU, Jin R, Jones J*, et al.* (2001). Induction of gadd45beta by NF-kappaB downregulates pro-apoptotic JNK signalling. *Nature* **414**(6861)**:** 308-313.

Denninger JW, Marletta MA (1999). Guanylate cyclase and the .NO/cGMP signaling pathway. *Biochimica et biophysica acta* **1411**(2-3)**:** 334-350.

Diaz-Delfin J, del Mar Gutierrez M, Gallego-Escuredo JM, Domingo JC, Gracia Mateo M, Villarroya F*, et al.* (2011). Effects of nevirapine and efavirenz on human adipocyte differentiation, gene expression, and release of adipokines and cytokines. *Antiviral research* **91**(2)**:** 112-119.

Ding G, Qin Q, He N, Francis-David SC, Hou J, Liu J*, et al.* (2007). Adiponectin and its receptors are expressed in adult ventricular cardiomyocytes and upregulated by activation of peroxisome proliferator-activated receptor gamma. *Journal of molecular and cellular cardiology* **43**(1)**:** 73-84.

Donato AJ, Pierce GL, Lesniewski LA, Seals DR (2009). Role of NFkappaB in age-related vascular endothelial dysfunction in humans. *Aging* **1**(8)**:** 678-680.

Dong C, Davis RJ, Flavell RA (2002). MAP kinases in the immune response. *Annual review of immunology* **20:** 55-72.

Duan SZ, Usher MG, Mortensen RM (2008). Peroxisome proliferator-activated receptor-gamma-mediated effects in the vasculature. *Circulation research* **102**(3)**:** 283-294.

Dube MP, Lipshultz SE, Fichtenbaum CJ, Greenberg R, Schecter AD, Fisher SD*, et al.* (2008). Effects of HIV infection and antiretroviral therapy on the heart and vasculature. *Circulation* **118**(2)**:** e36-40.

Duez H, Fruchart JC, Staels B (2001). PPARS in inflammation, atherosclerosis and thrombosis. *Journal of cardiovascular risk* **8**(4)**:** 187-194.

Ehrlich BE, Cserr HF (1978). Comparative aspects of brain barrier systems for iodide. *The American journal of physiology* **234**(1)**:** R61-65.

El-Bassossy HM, El-Fawal R, Fahmy A (2012). Arginase inhibition alleviates hypertension associated with diabetes: effect on endothelial dependent relaxation and NO production. *Vascular pharmacology* **57**(5-6)**:** 194-200.

Elens L, Vandercam B, Yombi JC, Lison D, Wallemacq P, Haufroid V (2010). Influence of host genetic factors on efavirenz plasma and intracellular pharmacokinetics in HIV-1-infected patients. *Pharmacogenomics* **11**(9)**:** 1223-1234.

EMA (2007). *EMA* assessment report (Atripla approval).

EMA (2010). *EMA* press release (rosiglitazone suspension).

Este JA, Cihlar T (2010). Current status and challenges of antiretroviral research and therapy. *Antiviral research* **85**(1)**:** 25-33.

Eu JP, Liu L, Zeng M, Stamler JS (2000). An apoptotic model for nitrosative stress. *Biochemistry* **39**(5)**:** 1040-1047.

Fanales-Belasio E, Raimondo M, Suligoi B, Butto S (2010). HIV virology and pathogenetic mechanisms of infection: a brief overview. *Annali dell'Istituto superiore di sanita* **46**(1)**:** 5-14.

Farrow B, Evers BM (2003). Activation of PPARgamma increases PTEN expression in pancreatic cancer cells. *Biochemical and biophysical research communications* **301**(1)**:** 50-53.

FDA (2012). Fast Track, Accelerated Approval and Priority Review Vol. 2012. www.fda.gov

FDA (2006). FDA press release (Atripla approval).

FDA (1995). FDA press release (saquinavir approval).

FDA (1992). FDA press release (zalcitabine approval).

Fiala M, Popik W, Qiao JH, Lossinsky AS, Alce T, Tran K*, et al.* (2004). HIV-1 induces cardiomyopathyby cardiomyocyte invasion and gp120, Tat, and cytokine apoptotic signaling. *Cardiovascular toxicology* **4**(2)**:** 97-107.

Fiorillo C, Ponziani V, Giannini L, Cecchi C, Celli A, Nassi N*, et al.* (2006). Protective effects of the PARP-1 inhibitor PJ34 in hypoxic-reoxygenated cardiomyoblasts. *Cellular and molecular life sciences : CMLS* **63**(24)**:** 3061-3071.

Ford ES, Puronen CE, Sereti I (2009). Immunopathogenesis of asymptomatic chronic HIV Infection: the calm before the storm. *Current opinion in HIV and AIDS* **4**(3)**:** 206-214.

Francisci D, Giannini S, Baldelli F, Leone M, Belfiori B, Guglielmini G*, et al.* (2009). HIV type 1 infection, and not short-term HAART, induces endothelial dysfunction. *Aids* **23**(5)**:** 589-596.

Friis-Moller N, Reiss P, Sabin CA, Weber R, Monforte A, El-Sadr W*, et al.* (2007). Class of antiretroviral drugs and the risk of myocardial infarction. *The New England journal of medicine* **356**(17)**:** 1723-1735.

Friis-Moller N, Weber R, Reiss P, Thiebaut R, Kirk O, d'Arminio Monforte A*, et al.* (2003). Cardiovascular disease risk factors in HIV patients--association with antiretroviral therapy. Results from the DAD study. *Aids* **17**(8)**:** 1179-1193.

Fryer LG, Parbu-Patel A, Carling D (2002). The Anti-diabetic drugs rosiglitazone and metformin stimulate AMP-activated protein kinase through distinct signaling pathways. *The Journal of biological chemistry* **277**(28)**:** 25226-25232.

Furchgott RF, Zawadzki JV (1980). The obligatory role of endothelial cells in the relaxation of arterial smooth muscle by acetylcholine. *Nature* **288**(5789)**:** 373-376.

Gamble LJ, Matthews QL (2010). Current progress in the development of a prophylactic vaccine for HIV-1. *Drug design, development and therapy* **5:** 9-26.

Garcia S, Bodano A, Gonzalez A, Forteza J, Gomez-Reino JJ, Conde C (2006). Partial protection against collagen antibody-induced arthritis in PARP-1 deficient mice. *Arthritis research & therapy* **8**(1)**:** R14.

Gareus R, Kotsaki E, Xanthoulea S, van der Made I, Gijbels MJ, Kardakaris R*, et al.* (2008). Endothelial cell-specific NF-kappaB inhibition protects mice from atherosclerosis. *Cell metabolism* **8**(5)**:** 372-383.

Garrido C, Soriano V, de Mendoza C (2010). New therapeutic strategies for raltegravir. *The Journal of antimicrobial chemotherapy* **65**(2)**:** 218-223.

Gazzard BG, Anderson J, Babiker A, Boffito M, Brook G, Brough G*, et al.* (2008). British HIV Association Guidelines for the treatment of HIV-1-infected adults with antiretroviral therapy 2008. *HIV medicine* **9**(8)**:** 563-608.

Gerschenson M, Nguyen VT, St Claire MC, Harbaugh SW, Harbaugh JW, Proia LA*, et al.* (2001). Chronic stavudine exposure induces hepatic mitochondrial toxicity in adult Erythrocebus patas monkeys. *J Hum Virol* **4**(6)**:** 335-342.

Getahun H, Gunneberg C, Granich R, Nunn P (2010). HIV infection-associated tuberculosis: the epidemiology and the response. *Clinical infectious diseases : an official publication of the Infectious Diseases Society of America* **50 Suppl 3:** S201-207.

Giddings JC (2005). Soluble adhesion molecules in inflammatory and vascular diseases. *Biochemical Society transactions* **33**(Pt 2)**:** 406-408.

Gilliam BL, Riedel DJ, Redfield RR (2011). Clinical use of CCR5 inhibitors in HIV and beyond. *Journal of translational medicine* **9 Suppl 1:** S9.

Glynn SL, Yazdanian M (1998). In vitro blood-brain barrier permeability of nevirapine compared to other HIV antiretroviral agents. *Journal of pharmaceutical sciences* **87**(3)**:** 306-310.

Gomez-Sucerquia LJ, Blas-Garcia A, Marti-Cabrera M, Esplugues JV, Apostolova N (2012). Profile of stress and toxicity gene expression in human hepatic cells treated with Efavirenz. *Antiviral research* **94**(3)**:** 232-241.

Gonzalo T, Garcia Goni M, Munoz-Fernandez MA (2009). Socio-economic impact of antiretroviral treatment in HIV patients. An economic review of cost savings after introduction of HAART. *AIDS reviews* **11**(2)**:** 79-90.

Griendling KK, Sorescu D, Ushio-Fukai M (2000). NAD(P)H oxidase: role in cardiovascular biology and disease. *Circulation research* **86**(5)**:** 494-501.

Gupta GR, Parkhurst JO, Ogden JA, Aggleton P, Mahal A (2008). Structural approaches to HIV prevention. *Lancet* **372**(9640)**:** 764-775.

Gupta SK, Shen C, Moe SM, Kamendulis LM, Goldman M, Dube MP (2012). Worsening endothelial function with efavirenz compared to protease inhibitors: a 12-month prospective study. *PloS one* **7**(9)**:** e45716.

Guzik TJ, Mussa S, Gastaldi D, Sadowski J, Ratnatunga C, Pillai R*, et al.* (2002). Mechanisms of increased vascular superoxide production in human diabetes mellitus: role of NAD(P)H oxidase and endothelial nitric oxide synthase. *Circulation* **105**(14)**:** 1656-1662.

Ha HC, Snyder SH (1999). Poly(ADP-ribose) polymerase is a mediator of necrotic cell death by ATP depletion. *Proceedings of the National Academy of Sciences of the United States of America* **96**(24)**:** 13978-13982.

Han L, Yu Y, Sun X, Wang B (2012). Exendin-4 directly improves endothelial dysfunction in isolated aortas from obese rats through the cAMP or AMPK-eNOS pathways. *Diabetes research and clinical practice* **97**(3)**:** 453-460.

Hans CP, Zerfaoui M, Naura AS, Troxclair D, Strong JP, Matrougui K*, et al.* (2009). Thieno[2,3-c]isoquinolin-5-one, a potent poly(ADP-ribose) polymerase inhibitor, promotes atherosclerotic plaque regression in high-fat diet-fed apolipoprotein E-deficient mice: effects on inflammatory markers and lipid content. *The Journal of pharmacology and experimental therapeutics* **329**(1)**:** 150-158.

Hardie DG (2008). Role of AMP-activated protein kinase in the metabolic syndrome and in heart disease. *FEBS letters* **582**(1)**:** 81-89.

Hayashi T, Fukuto JM, Ignarro LJ, Chaudhuri G (1992). Basal release of nitric oxide from aortic rings is greater in female rabbits than in male rabbits: implications for atherosclerosis. *Proceedings of the National Academy of Sciences of the United States of America* **89**(23)**:** 11259-11263.

Haynes CM, Titus EA, Cooper AA (2004). Degradation of misfolded proteins prevents ER-derived oxidative stress and cell death. *Molecular cell* **15**(5)**:** 767-776.

Heaton RK, Clifford DB, Franklin DR, Jr., Woods SP, Ake C, Vaida F*, et al.* (2010). HIV-associated neurocognitive disorders persist in the era of potent antiretroviral therapy: CHARTER Study. *Neurology* **75**(23)**:** 2087-2096.

Heitzer T, Schlinzig T, Krohn K, Meinertz T, Munzel T (2001). Endothelial dysfunction, oxidative stress, and risk of cardiovascular events in patients with coronary artery disease. *Circulation* **104**(22)**:** 2673-2678.

Helyar SG, Patel B, Headington K, El Assal M, Chatterjee PK, Pacher P*, et al.* (2009). PCB-induced endothelial cell dysfunction: role of poly(ADP-ribose) polymerase. *Biochemical pharmacology* **78**(8)**:** 959-965.

Herceg Z, Wang ZQ (2001). Functions of poly(ADP-ribose) polymerase (PARP) in DNA repair, genomic integrity and cell death. *Mutation research* **477**(1-2)**:** 97-110.

Hetzel J, Balletshofer B, Rittig K, Walcher D, Kratzer W, Hombach V*, et al.* (2005). Rapid effects of rosiglitazone treatment on endothelial function and inflammatory biomarkers. *Arteriosclerosis, thrombosis, and vascular biology* **25**(9)**:** 1804-1809.

Higuchi A, Ohashi K, Shibata R, Sono-Romanelli S, Walsh K, Ouchi N (2010). Thiazolidinediones reduce pathological neovascularization in ischemic retina via an adiponectin-dependent mechanism. *Arteriosclerosis, thrombosis, and vascular biology* **30**(1)**:** 46-53.

Huang SH, Xiong M, Chen XP, Xiao ZY, Zhao YF, Huang ZY (2008). PJ34, an inhibitor of PARP-1, suppresses cell growth and enhances the suppressive effects of cisplatin in liver cancer cells. *Oncology reports* **20**(3)**:** 567-572.

Huang W, Eum SY, Andras IE, Hennig B, Toborek M (2009). PPARalpha and PPARgamma attenuate HIV-induced dysregulation of tight junction proteins by modulations of matrix metalloproteinase and proteasome activities. *FASEB journal : official publication of the Federation of American Societies for Experimental Biology* **23**(5)**:** 1596-1606.

Huang Y, Zhang H, Shao Z, O'Hara KA, Kopilas MA, Yu L*, et al.* (2011). Suppression of endothelin-1-induced cardiac myocyte hypertrophy by PPAR agonists: role of diacylglycerol kinase zeta. *Cardiovascular research* **90**(2)**:** 267-275.

Hulgan T, Morrow J, D'Aquila RT, Raffanti S, Morgan M, Rebeiro P*, et al.* (2003). Oxidant stress is increased during treatment of human immunodeficiency virus infection. *Clinical infectious diseases : an official publication of the Infectious Diseases Society of America* **37**(12)**:** 1711-1717.

Hurwitz BE, Klimas NG, Llabre MM, Maher KJ, Skyler JS, Bilsker MS*, et al.* (2004). HIV, metabolic syndrome X, inflammation, oxidative stress, and coronary heart disease risk : role of protease inhibitor exposure. *Cardiovascular toxicology* **4**(3)**:** 303-316.

Hwang J, Kleinhenz DJ, Lassegue B, Griendling KK, Dikalov S, Hart CM (2005). Peroxisome proliferator-activated receptor-gamma ligands regulate endothelial membrane superoxide production. *American journal of physiology. Cell physiology* **288**(4)**:** C899-905.

Hwang J, Kleinhenz DJ, Rupnow HL, Campbell AG, Thule PM, Sutliff RL*, et al.* (2007). The PPARgamma ligand, rosiglitazone, reduces vascular oxidative stress and NADPH oxidase expression in diabetic mice. *Vascular pharmacology* **46**(6)**:** 456-462.

Igbigbi AA (2012). Oxidative stress induced by chronic administration of Efavirenz on the intracranial visual relay centers of adult Wistar rats. *Biology and Medicine* **3**(5)**:** 16-24.

Jamaluddin MS, Lin PH, Yao Q, Chen C (2010). Non-nucleoside reverse transcriptase inhibitor efavirenz increases monolayer permeability of human coronary artery endothelial cells. *Atherosclerosis* **208**(1)**:** 104-111.

Jiang B, Hebert VY, Li Y, Mathis JM, Alexander JS, Dugas TR (2007). HIV antiretroviral drug combination induces endothelial mitochondrial dysfunction and reactive oxygen species production, but not apoptosis. *Toxicology and applied pharmacology* **224**(1)**:** 60-71.

Jiang B, Hebert VY, Zavecz JH, Dugas TR (2006). Antiretrovirals induce direct endothelial dysfunction in vivo. *Journal of acquired immune deficiency syndromes* **42**(4)**:** 391-395.

Johnson VA, Brun-Vezinet F, Clotet B, Gunthard HF, Kuritzkes DR, Pillay D*, et al.* (2010). Update of the drug resistance mutations in HIV-1: December 2010. *Topics in HIV medicine : a publication of the International AIDS Society, USA* **18**(5)**:** 156-163.

Julg B, Bogner JR (2008). Atriplatrade mark - HIV therapy in one pill. *Therapeutics and clinical risk management* **4**(3)**:** 573-577.

Kakuda TN (2000). Pharmacology of nucleoside and nucleotide reverse transcriptase inhibitor-induced mitochondrial toxicity. *Clinical therapeutics* **22**(6)**:** 685-708.

Kanmogne GD, Primeaux C, Grammas P (2005). HIV-1 gp120 proteins alter tight junction protein expression and brain endothelial cell permeability: implications for the pathogenesis of HIV-associated dementia. *Journal of neuropathology and experimental neurology* **64**(6)**:** 498-505.

Karin M (1999). How NF-kappaB is activated: the role of the IkappaB kinase (IKK) complex. *Oncogene* **18**(49)**:** 6867-6874.

Kaufman RJ (1999). Stress signaling from the lumen of the endoplasmic reticulum: coordination of gene transcriptional and translational controls. *Genes & development* **13**(10)**:** 1211-1233.

Kernohan AF, Spiers A, Sattar N, Hillier C, Cleland SJ, Small M*, et al.* (2004). Effects of low-dose continuous combined HRT on vascular function in women with type 2 diabetes. *Diabetes & vascular disease research : official journal of the International Society of Diabetes and Vascular Disease* **1**(2)**:** 82-88.

Khan NA, Di Cello F, Nath A, Kim KS (2003). Human immunodeficiency virus type 1 tat-mediated cytotoxicity of human brain microvascular endothelial cells. *Journal of neurovirology* **9**(6)**:** 584-593.

Kher N, Marsh JD (2004). Pathobiology of atherosclerosis--a brief review. *Seminars in thrombosis and hemostasis* **30**(6)**:** 665-672.

Kim MG, Yang HN, Kim HW, Jo SK, Cho WY, Kim HK (2010). IL-10 mediates rosiglitazone-induced kidney protection in cisplatin nephrotoxicity. *Journal of Korean medical science* **25**(4)**:** 557-563.

Kimes BW, Brandt BL (1976). Properties of a clonal muscle cell line from rat heart. *Experimental cell research* **98**(2)**:** 367-381.

Kitahata MM (2010). When to start antiretroviral therapy. *Topics in HIV medicine : a publication of the International AIDS Society, USA* **18**(3)**:** 121-126.

Kleemann R, Zadelaar S, Kooistra T (2008). Cytokines and atherosclerosis: a comprehensive review of studies in mice. *Cardiovascular research* **79**(3)**:** 360-376.

Kleinbongard P, Heusch G, Schulz R (2010). TNFalpha in atherosclerosis, myocardial ischemia/reperfusion and heart failure. *Pharmacology & therapeutics* **127**(3)**:** 295-314.

Kline ER, Sutliff RL (2008). The roles of HIV-1 proteins and antiretroviral drug therapy in HIV-1-associated endothelial dysfunction. *Journal of investigative medicine : the official publication of the American Federation for Clinical Research* **56**(5)**:** 752-769.

Kniesel U, Wolburg H (2000). Tight junctions of the blood-brain barrier. *Cellular and molecular neurobiology* **20**(1)**:** 57-76.

Koh DW, Dawson TM, Dawson VL (2005). Mediation of cell death by poly(ADP-ribose) polymerase-1. *Pharmacological research : the official journal of the Italian Pharmacological Society* **52**(1)**:** 5-14.

Kowaltowski AJ, Vercesi AE (1999). Mitochondrial damage induced by conditions of oxidative stress. *Free radical biology & medicine* **26**(3-4)**:** 463-471.

Kraus WL, Lis JT (2003). PARP goes transcription. *Cell* **113**(6)**:** 677-683.

Kruman, II, Nath A, Maragos WF, Chan SL, Jones M, Rangnekar VM*, et al.* (1999). Evidence that Par-4 participates in the pathogenesis of HIV encephalitis. *The American journal of pathology* **155**(1)**:** 39-46.

Kwok HH, Ng WY, Yang MS, Mak NK, Wong RN, Yue PY (2010). The ginsenoside protopanaxatriol protects endothelial cells from hydrogen peroxide-induced cell injury and cell death by modulating intracellular redox status. *Free radical biology & medicine* **48**(3)**:** 437-445.

L'Ecuyer T, Horenstein MS, Thomas R, Vander Heide R (2001). Anthracycline-induced cardiac injury using a cardiac cell line: potential for gene therapy studies. *Molecular genetics and metabolism* **74**(3)**:** 370-379.

L'Ecuyer T, Sanjeev S, Thomas R, Novak R, Das L, Campbell W*, et al.* (2006). DNA damage is an early event in doxorubicin-induced cardiac myocyte death. *American journal of physiology. Heart and circulatory physiology* **291**(3)**:** H1273-1280.

Lane HC (2010). Pathogenesis of HIV infection: total CD4+ T-cell pool, immune activation, and inflammation. *Topics in HIV medicine : a publication of the International AIDS Society, USA* **18**(1)**:** 2-6.

Lee S, Kim W, Moon SO, Sung MJ, Kim DH, Kang KP*, et al.* (2006). Rosiglitazone ameliorates cisplatin-induced renal injury in mice. *Nephrology, dialysis, transplantation : official publication of the European Dialysis and Transplant Association - European Renal Association* **21**(8)**:** 2096-2105.

Lee WK, Chakraborty PK, Roussa E, Wolff NA, Thevenod F (2012). ERK1/2-dependent bestrophin-3 expression prevents ER-stress-induced cell death in renal epithelial cells by reducing CHOP. *Biochimica et biophysica acta* **1823**(10)**:** 1864-1876.

Lee YW, Hirani AA, Kyprianou N, Toborek M (2005). Human immunodeficiency virus-1 Tat protein up-regulates interleukin-6 and interleukin-8 expression in human breast cancer cells. *Inflammation research : official journal of the European Histamine Research Society ... [et al.]* **54**(9)**:** 380-389.

Lenzser G, Kis B, Snipes JA, Gaspar T, Sandor P, Komjati K*, et al.* (2007). Contribution of poly(ADP-ribose) polymerase to postischemic blood-brain barrier damage in rats. *Journal of cerebral blood flow and metabolism : official journal of the International Society of Cerebral Blood Flow and Metabolism* **27**(7)**:** 1318-1326.

Letendre SL, Ellis RJ, Ances BM, McCutchan JA (2010). Neurologic complications of HIV disease and their treatment. *Topics in HIV medicine : a publication of the International AIDS Society, USA* **18**(2)**:** 45-55.

Lewis W, Copeland WC, Day BJ (2001). Mitochondrial dna depletion, oxidative stress, and mutation: mechanisms of dysfunction from nucleoside reverse transcriptase inhibitors. *Laboratory investigation; a journal of technical methods and pathology* **81**(6)**:** 777-790.

Lewis W, Day BJ, Copeland WC (2003). Mitochondrial toxicity of NRTI antiviral drugs: an integrated cellular perspective. *Nature reviews. Drug discovery* **2**(10)**:** 812-822.

Lewis W, Kohler JJ, Hosseini SH, Haase CP, Copeland WC, Bienstock RJ*, et al.* (2006). Antiretroviral nucleosides, deoxynucleotide carrier and mitochondrial DNA: evidence supporting the DNA pol gamma hypothesis. *Aids* **20**(5)**:** 675-684.

Libby P, Sukhova G, Lee RT, Galis ZS (1995). Cytokines regulate vascular functions related to stability of the atherosclerotic plaque. *Journal of cardiovascular pharmacology* **25 Suppl 2:** S9-12.

Lindl KA, Marks DR, Kolson DL, Jordan-Sciutto KL (2010). HIV-associated neurocognitive disorder: pathogenesis and therapeutic opportunities. *Journal of neuroimmune pharmacology : the official journal of the Society on NeuroImmune Pharmacology* **5**(3)**:** 294-309.

Lipshultz SE, Fisher SD, Lai WW, Miller TL (2001). Cardiovascular monitoring and therapy for HIV-infected patients. *Annals of the New York Academy of Sciences* **946:** 236-273.

Liu N, Liu JT, Ji YY, Lu PP (2011). Rosiglitazone regulates c-reactive protein-induced inflammatory responses via glucocorticoid receptor-mediated inhibition of p38 mitogen-activated protein kinase-toll-like receptor 4 signal pathway in vascular smooth muscle cells. *Journal of cardiovascular pharmacology* **57**(3)**:** 348-356.

Lombardi A, Cantini G, Piscitelli E, Gelmini S, Francalanci M, Mello T*, et al.* (2008). A new mechanism involving ERK contributes to rosiglitazone inhibition of tumor necrosis factor-alpha and interferon-gamma inflammatory effects in human endothelial cells. *Arteriosclerosis, thrombosis, and vascular biology* **28**(4)**:** 718-724.

Loubiere S, Moatti JP (2010). Economic evaluation of point-of-care diagnostic technologies for infectious diseases. *Clinical microbiology and infection : the official publication of the European Society of Clinical Microbiology and Infectious Diseases* **16**(8)**:** 1070-1076.

Lund LH, Ljungberg K, Wahren B, Hinkula J (2004). Primary murine cells as a model for HIV-1 infection. *Aids* **18**(7)**:** 1067-1069.

Lyles CM, Kay LS, Crepaz N, Herbst JH, Passin WF, Kim AS*, et al.* (2007). Best-evidence interventions: findings from a systematic review of HIV behavioral interventions for US populations at high risk, 2000-2004. *American journal of public health* **97**(1)**:** 133-143.

Mabley JG, Horvath EM, Murthy KG, Zsengeller Z, Vaslin A, Benko R*, et al.* (2005). Gender differences in the endotoxin-induced inflammatory and vascular responses: potential role of poly(ADP-ribose) polymerase activation. *The Journal of pharmacology and experimental therapeutics* **315**(2)**:** 812-820.

Mabley JG, Soriano FG (2005). Role of nitrosative stress and poly(ADP-ribose) polymerase activation in diabetic vascular dysfunction. *Current vascular pharmacology* **3**(3)**:** 247-252.

Mabley JG, Suarez-Pinzon WL, Hasko G, Salzman AL, Rabinovitch A, Kun E*, et al.* (2001). Inhibition of poly (ADP-ribose) synthetase by gene disruption or inhibition with 5-iodo-6-amino-1,2-benzopyrone protects mice from multiple-low-dose-streptozotocin-induced diabetes. *Br J Pharmacol* **133**(6)**:** 909-919.

Madden E, Lee G, Kotler DP, Wanke C, Lewis CE, Tracy R*, et al.* (2008). Association of antiretroviral therapy with fibrinogen levels in HIV-infection. *Aids* **22**(6)**:** 707-715.

Maggi P, Bellacosa C, Carito V, Perilli F, Lillo A, Volpe A*, et al.* (2011). Cardiovascular risk factors in patients on long-term treatment with nevirapine- or efavirenz-based regimens. *The Journal of antimicrobial chemotherapy* **66**(4)**:** 896-900.

Majno G, Joris I (1995). Apoptosis, oncosis, and necrosis. An overview of cell death. *The American journal of pathology* **146**(1)**:** 3-15.

Mako V, Czucz J, Weiszhar Z, Herczenik E, Matko J, Prohaszka Z*, et al.* (2010). Proinflammatory activation pattern of human umbilical vein endothelial cells induced by IL-1beta, TNF-alpha, and LPS. *Cytometry. Part A : the journal of the International Society for Analytical Cytology* **77**(10)**:** 962-970.

Malhotra JD, Kaufman RJ (2007). The endoplasmic reticulum and the unfolded protein response. *Seminars in cell & developmental biology* **18**(6)**:** 716-731.

Malvestutto CD, Aberg JA (2010). Coronary heart disease in people infected with HIV. *Cleveland Clinic journal of medicine* **77**(8)**:** 547-556.

Mariani SA, Vicenzi E, Poli G (2011). Asymmetric HIV-1 co-receptor use and replication in CD4(+) T lymphocytes. *Journal of translational medicine* **9 Suppl 1:** S8.

Martin HL, Mounsey RB, Mustafa S, Sathe K, Teismann P (2012). Pharmacological manipulation of peroxisome proliferator-activated receptor gamma (PPARgamma) reveals a role for anti-oxidant protection in a model of Parkinson's disease. *Experimental neurology* **235**(2)**:** 528-538.

Martinez E, Larrousse M, Gatell JM (2009). Cardiovascular disease and HIV infection: host, virus, or drugs? *Current opinion in infectious diseases* **22**(1)**:** 28-34.

Marx N, Froehlich J, Siam L, Ittner J, Wierse G, Schmidt A*, et al.* (2003). Antidiabetic PPAR gamma-activator rosiglitazone reduces MMP-9 serum levels in type 2 diabetic patients with coronary artery disease. *Arteriosclerosis, thrombosis, and vascular biology* **23**(2)**:** 283-288.

Marzolini C, Telenti A, Decosterd LA, Greub G, Biollaz J, Buclin T (2001). Efavirenz plasma levels can predict treatment failure and central nervous system side effects in HIV-1-infected patients. *Aids* **15**(1)**:** 71-75.

McNeil JG, Johnston MI, Birx DL, Tramont EC (2004). Policy rebuttal. HIV vaccine trial justified. *Science* **303**(5660)**:** 961.

Merson MH, O'Malley J, Serwadda D, Apisuk C (2008). The history and challenge of HIV prevention. *Lancet* **372**(9637)**:** 475-488.

Michel T, Feron O (1997). Nitric oxide synthases: which, where, how, and why? *The Journal of clinical investigation* **100**(9)**:** 2146-2152.

Mitchelhill KI, Michell BJ, House CM, Stapleton D, Dyck J, Gamble J*, et al.* (1997). Posttranslational modifications of the 5'-AMP-activated protein kinase beta1 subunit. *The Journal of biological chemistry* **272**(39)**:** 24475-24479.

Monaco C, Paleolog E (2004). Nuclear factor kappaB: a potential therapeutic target in atherosclerosis and thrombosis. *Cardiovascular research* **61**(4)**:** 671-682.

Mondal D, Liu K, Hamblin M, Lasky JA, Agrawal KC (2013). Nelfinavir suppresses insulin signaling and nitric oxide production by human aortic endothelial cells: protective effects of thiazolidinediones. *The Ochsner journal* **13**(1)**:** 76-90.

Mondal D, Pradhan L, Ali M, Agrawal KC (2004). HAART drugs induce oxidative stress in human endothelial cells and increase endothelial recruitment of mononuclear cells: exacerbation by inflammatory cytokines and amelioration by antioxidants. *Cardiovascular toxicology* **4**(3)**:** 287-302.

Monsuez JJ, Escaut L, Teicher E, Charniot JC, Vittecoq D (2007). Cytokines in HIV-associated cardiomyopathy. *International journal of cardiology* **120**(2)**:** 150-157.

Moreno S, Lopez Aldeguer J, Arribas JR, Domingo P, Iribarren JA, Ribera E*, et al.* (2010). The future of antiretroviral therapy: challenges and needs. *The Journal of antimicrobial chemotherapy* **65**(5)**:** 827-835.

Mun L, Jun MS, Kim YM, Lee YS, Kim HJ, Seo HG*, et al.* (2011). 7,8-didehydrocimigenol from Cimicifugae rhizoma inhibits TNF-alpha-induced VCAM-1 but not ICAM-1expression through upregulation of PPAR-gamma in human endothelial cells. *Food and chemical toxicology : an international journal published for the British Industrial Biological Research Association* **49**(1)**:** 166-172.

Munro JM, Cotran RS (1988). The pathogenesis of atherosclerosis: atherogenesis and inflammation. *Laboratory investigation; a journal of technical methods and pathology* **58**(3)**:** 249-261.

Naggie S, Hicks C (2010). Protease inhibitor-based antiretroviral therapy in treatment-naive HIV-1-infected patients: the evidence behind the options. *The Journal of antimicrobial chemotherapy* **65**(6)**:** 1094-1099.

Nakajima A, Wada K, Miki H, Kubota N, Nakajima N, Terauchi Y*, et al.* (2001). Endogenous PPAR gamma mediates anti-inflammatory activity in murine ischemia-reperfusion injury. *Gastroenterology* **120**(2)**:** 460-469.

Negredo E, Bonjoch A, Clotet B (2006). Benefits and concerns of simplification strategies in HIV-infected patients. *The Journal of antimicrobial chemotherapy* **58**(2)**:** 235-242.

Neumann T, Woiwod T, Neumann A, Ross B, Von Birgelen C, Volbracht L*, et al.* (2004). Cardiovascular risk factors and probability for cardiovascular events in HIV-infected patients. Part II: gender differences. *European journal of medical research* **9**(2)**:** 55-60.

Nicholls SJ, Uno K (2012). Peroxisome proliferator-activated receptor (PPAR alpha/gamma) agonists as a potential target to reduce cardiovascular risk in diabetes. *Diabetes & vascular disease research : official journal of the International Society of Diabetes and Vascular Disease* **9**(2)**:** 89-94.

Obrosova IG, Drel VR, Pacher P, Ilnytska O, Wang ZQ, Stevens MJ*, et al.* (2005). Oxidative-nitrosative stress and poly(ADP-ribose) polymerase (PARP) activation in experimental diabetic neuropathy: the relation is revisited. *Diabetes* **54**(12)**:** 3435-3441.

Ogita H, Liao J (2004). Endothelial function and oxidative stress. *Endothelium : journal of endothelial cell research* **11**(2)**:** 123-132.

Oliver FJ, Menissier-de Murcia J, Nacci C, Decker P, Andriantsitohaina R, Muller S*, et al.* (1999). Resistance to endotoxic shock as a consequence of defective NF-kappaB activation in poly (ADP-ribose) polymerase-1 deficient mice. *The EMBO journal* **18**(16)**:** 4446-4454.

Oumouna-Benachour K, Hans CP, Suzuki Y, Naura A, Datta R, Belmadani S*, et al.* (2007). Poly(ADP-ribose) polymerase inhibition reduces atherosclerotic plaque size and promotes factors of plaque stability in apolipoprotein E-deficient mice: effects on macrophage recruitment, nuclear factor-kappaB nuclear translocation, and foam cell death. *Circulation* **115**(18)**:** 2442-2450.

Oyadomari S, Mori M (2004). Roles of CHOP/GADD153 in endoplasmic reticulum stress. *Cell death and differentiation* **11**(4)**:** 381-389.

Pacher P, Liaudet L, Mabley J, Komjati K, Szabo C (2002a). Pharmacologic inhibition of poly(adenosine diphosphate-ribose) polymerase may represent a novel therapeutic approach in chronic heart failure. *Journal of the American College of Cardiology* **40**(5)**:** 1006-1016.

Pacher P, Mabley JG, Soriano FG, Liaudet L, Komjati K, Szabo C (2002b). Endothelial dysfunction in aging animals: the role of poly(ADP-ribose) polymerase activation. *British journal of pharmacology* **135**(6)**:** 1347-1350.

Pacher P, Szabo C (2007). Role of poly(ADP-ribose) polymerase 1 (PARP-1) in cardiovascular diseases: the therapeutic potential of PARP inhibitors. *Cardiovascular drug reviews* **25**(3)**:** 235-260.

Palee S, Chattipakorn S, Phrommintikul A, Chattipakorn N (2011). PPARgamma activator, rosiglitazone: Is it beneficial or harmful to the cardiovascular system? *World journal of cardiology* **3**(5)**:** 144-152.

Parkin JM, Murphy M, Anderson J, El-Gadi S, Forster G, Pinching AJ (2000). Tolerability and side-effects of post-exposure prophylaxis for HIV infection. *Lancet* **355**(9205)**:** 722-723.

Patel AK, Patel KK (2006). Future implications: compliance and failure with antiretroviral treatment. *Journal of postgraduate medicine* **52**(3)**:** 197-200.

Pernerstorfer-Schoen H, Jilma B, Perschler A, Wichlas S, Schindler K, Schindl A*, et al.* (2001). Sex differences in HAART-associated dyslipidaemia. *Aids* **15**(6)**:** 725-734.

Petroll AE, Hare CB, Pinkerton SD (2008). The essentials of HIV: a review for nurses. *Journal of infusion nursing : the official publication of the Infusion Nurses Society* **31**(4)**:** 228-235.

Piconi L, Quagliaro L, Da Ros R, Assaloni R, Giugliano D, Esposito K*, et al.* (2004). Intermittent high glucose enhances ICAM-1, VCAM-1, E-selectin and interleukin-6 expression in human umbilical endothelial cells in culture: the role of poly(ADP-ribose) polymerase. *Journal of thrombosis and haemostasis : JTH* **2**(8)**:** 1453-1459.

Pieper AA, Verma A, Zhang J, Snyder SH (1999). Poly (ADP-ribose) polymerase, nitric oxide and cell death. *Trends in pharmacological sciences* **20**(4)**:** 171-181.

Pilon AA, Lum JJ, Sanchez-Dardon J, Phenix BN, Douglas R, Badley AD (2002). Induction of apoptosis by a nonnucleoside human immunodeficiency virus type 1 reverse transcriptase inhibitor. *Antimicrobial agents and chemotherapy* **46**(8)**:** 2687-2691.

Pistrosch F, Passauer J, Fischer S, Fuecker K, Hanefeld M, Gross P (2004). In type 2 diabetes, rosiglitazone therapy for insulin resistance ameliorates endothelial dysfunction independent of glucose control. *Diabetes care* **27**(2)**:** 484-490.

Polikandriotis JA, Mazzella LJ, Rupnow HL, Hart CM (2005). Peroxisome proliferator-activated receptor gamma ligands stimulate endothelial nitric oxide production through distinct peroxisome proliferator-activated receptor gamma-dependent mechanisms. *Arteriosclerosis, thrombosis, and vascular biology* **25**(9)**:** 1810-1816.

Pyke KE, Tschakovsky ME (2005). The relationship between shear stress and flow-mediated dilatation: implications for the assessment of endothelial function. *The Journal of physiology* **568**(Pt 2)**:** 357-369.

Qu C, Tang L, Zhu Y (2012). Effect of fenofibrate on the secretion of endothelium-derived contracting factors in hypertensive rats. *Zhongguo yi xue ke xue yuan xue bao. Acta Academiae Medicinae Sinicae* **34**(3)**:** 239-243.

Quinn TC (2008). HIV epidemiology and the effects of antiviral therapy on long-term consequences. *Aids* **22 Suppl 3:** S7-12.

Racz B, Hanto K, Tapodi A, Solti I, Kalman N, Jakus P*, et al.* (2010). Regulation of MKP-1 expression and MAPK activation by PARP-1 in oxidative stress: a new mechanism for the cytoplasmic effect of PARP-1 activation. *Free radical biology & medicine* **49**(12)**:** 1978-1988.

Reape TJ, Groot PH (1999). Chemokines and atherosclerosis. *Atherosclerosis* **147**(2)**:** 213-225.

Rodriguez de la Concepcion ML, Yubero P, Domingo JC, Iglesias R, Domingo P, Villarroya F*, et al.* (2005). Reverse transcriptase inhibitors alter uncoupling protein-1 and mitochondrial biogenesis in brown adipocytes. *Antiviral therapy* **10**(4)**:** 515-526.

Russell RR, 3rd, Li J, Coven DL, Pypaert M, Zechner C, Palmeri M*, et al.* (2004). AMP-activated protein kinase mediates ischemic glucose uptake and prevents postischemic cardiac dysfunction, apoptosis, and injury. *The Journal of clinical investigation* **114**(4)**:** 495-503.

Ryan MJ, Didion SP, Mathur S, Faraci FM, Sigmund CD (2004). PPAR(gamma) agonist rosiglitazone improves vascular function and lowers blood pressure in hypertensive transgenic mice. *Hypertension* **43**(3)**:** 661-666.

Samsioe G (2003). HRT and cardiovascular disease. *Annals of the New York Academy of Sciences* **997:** 358-372.

Satoh H, Tsukamoto K, Hashimoto Y, Hashimoto N, Togo M, Hara M*, et al.* (1999). Thiazolidinediones suppress endothelin-1 secretion from bovine vascular endothelial cells: a new possible role of PPARgamma on vascular endothelial function. *Biochemical and biophysical research communications* **254**(3)**:** 757-763.

Schackman BR, Gebo KA, Walensky RP, Losina E, Muccio T, Sax PE*, et al.* (2006). The lifetime cost of current human immunodeficiency virus care in the United States. *Medical care* **44**(11)**:** 990-997.

Schecter AD, Berman AB, Yi L, Mosoian A, McManus CM, Berman JW*, et al.* (2001). HIV envelope gp120 activates human arterial smooth muscle cells. *Proceedings of the National Academy of Sciences of the United States of America* **98**(18)**:** 10142-10147.

Schneider C, Jick SS, Meier CR (2009). Risk of cardiovascular outcomes in users of estradiol/dydrogesterone or other HRT preparations. *Climacteric : the journal of the International Menopause Society* **12**(5)**:** 445-453.

Scoditti E, Massaro M, Carluccio MA, Distante A, Storelli C, De Caterina R (2010). PPARgamma agonists inhibit angiogenesis by suppressing PKCalpha- and CREB-mediated COX-2 expression in the human endothelium. *Cardiovascular research* **86**(2)**:** 302-310.

Seaberg EC, Munoz A, Lu M, Detels R, Margolick JB, Riddler SA*, et al.* (2005). Association between highly active antiretroviral therapy and hypertension in a large cohort of men followed from 1984 to 2003. *Aids* **19**(9)**:** 953-960.

Shete A, Thakar M, Abraham PR, Paranjape R (2010). A review on peripheral blood CD4+ T lymphocyte counts in healthy adult Indians. *Indian J Med Res* **132**(6)**:** 667-675.

Shi B, Raina J, Lorenzo A, Busciglio J, Gabuzda D (1998). Neuronal apoptosis induced by HIV-1 Tat protein and TNF-alpha: potentiation of neurotoxicity mediated by oxidative stress and implications for HIV-1 dementia. *Journal of neurovirology* **4**(3)**:** 281-290.

Shimokawa H (1999). Primary endothelial dysfunction: atherosclerosis. *Journal of molecular and cellular cardiology* **31**(1)**:** 23-37.

Sies H (1997). Oxidative stress: oxidants and antioxidants. *Experimental physiology* **82**(2)**:** 291-295.

Simon V, Ho DD, Abdool Karim Q (2006). HIV/AIDS epidemiology, pathogenesis, prevention, and treatment. *Lancet* **368**(9534)**:** 489-504.

Siva AC, Bushman F (2002). Poly(ADP-ribose) polymerase 1 is not strictly required for infection of murine cells by retroviruses. *Journal of virology* **76**(23)**:** 11904-11910.

Sivarajah A, Chatterjee PK, Patel NS, Todorovic Z, Hattori Y, Brown PA*, et al.* (2003). Agonists of peroxisome-proliferator activated receptor-gamma reduce renal ischemia/reperfusion injury. *American journal of nephrology* **23**(4)**:** 267-276.

Soriano FG, Virag L, Szabo C (2001). Diabetic endothelial dysfunction: role of reactive oxygen and nitrogen species production and poly(ADP-ribose) polymerase activation. *Journal of molecular medicine* **79**(8)**:** 437-448.

Stevenson JC, Hodis HN, Pickar JH, Lobo RA (2009). Coronary heart disease and menopause management: the swinging pendulum of HRT. *Atherosclerosis* **207**(2)**:** 336-340.

Stuck BJ, Lenski M, Bohm M, Laufs U (2008). Metabolic switch and hypertrophy of cardiomyocytes following treatment with angiotensin II are prevented by AMP-activated protein kinase. *The Journal of biological chemistry* **283**(47)**:** 32562-32569.

Sudano I, Spieker LE, Noll G, Corti R, Weber R, Luscher TF (2006). Cardiovascular disease in HIV infection. *American heart journal* **151**(6)**:** 1147-1155.

Sumpio BE, Riley JT, Dardik A (2002). Cells in focus: endothelial cell. *The international journal of biochemistry & cell biology* **34**(12)**:** 1508-1512.

Sutliff RL, Dikalov S, Weiss D, Parker J, Raidel S, Racine AK*, et al.* (2002). Nucleoside reverse transcriptase inhibitors impair endothelium-dependent relaxation by increasing superoxide. *American journal of physiology. Heart and circulatory physiology* **283**(6)**:** H2363-2370.

Szabados E, Fischer GM, Toth K, Csete B, Nemeti B, Trombitas K*, et al.* (1999). Role of reactive oxygen species and poly-ADP-ribose polymerase in the development of AZT-induced cardiomyopathy in rat. *Free radical biology & medicine* **26**(3-4)**:** 309-317.

Szabo C (2005). Cardioprotective effects of poly(ADP-ribose) polymerase inhibition. *Pharmacological research : the official journal of the Italian Pharmacological Society* **52**(1)**:** 34-43.

Szabo C (2002). PARP as a Drug Target for the Therapy of Diabetic Cardiovascular Dysfunction. *Drug news & perspectives* **15**(4)**:** 197-205.

Szabo C (1997). Role of poly(ADP-ribose) synthetase activation in the suppression of cellular energetics in response to nitric oxide and peroxynitrite. *Biochemical Society transactions* **25**(3)**:** 919-924.

Szabo C, Pacher P, Zsengeller Z, Vaslin A, Komjati K, Benko R*, et al.* (2004). Angiotensin II-mediated endothelial dysfunction: role of poly(ADP-ribose) polymerase activation. *Molecular medicine* **10**(1-6)**:** 28-35.

Szegezdi E, Logue SE, Gorman AM, Samali A (2006). Mediators of endoplasmic reticulum stress-induced apoptosis. *EMBO reports* **7**(9)**:** 880-885.

Tan JJ, Cong XJ, Hu LM, Wang CX, Jia L, Liang XJ (2010). Therapeutic strategies underpinning the development of novel techniques for the treatment of HIV infection. *Drug discovery today* **15**(5-6)**:** 186-197.

Tasatargil A, Dalaklioglu S, Sadan G (2005). Inhibition of poly(ADP-ribose) polymerase prevents vascular hyporesponsiveness induced by lipopolysaccharide in isolated rat aorta. *Pharmacological research : the official journal of the Italian Pharmacological Society* **51**(6)**:** 581-586.

Teixeira C, Gomes JR, Gomes P, Maurel F, Barbault F (2011). Viral surface glycoproteins, gp120 and gp41, as potential drug targets against HIV-1: brief overview one quarter of a century past the approval of zidovudine, the first anti-retroviral drug. *European journal of medicinal chemistry* **46**(4)**:** 979-992.

Tentori L, Portarena I, Graziani G (2002). Potential clinical applications of poly(ADP-ribose) polymerase (PARP) inhibitors. *Pharmacological research : the official journal of the Italian Pharmacological Society* **45**(2)**:** 73-85.

Thorne C, Newell ML (2005). Treatment options for the prevention of mother-to-child transmission of HIV. *Current opinion in investigational drugs* **6**(8)**:** 804-811.

Toledo EM, Inestrosa NC (2010). Activation of Wnt signaling by lithium and rosiglitazone reduced spatial memory impairment and neurodegeneration in brains of an APPswe/PSEN1DeltaE9 mouse model of Alzheimer's disease. *Molecular psychiatry* **15**(3)**:** 272-285, 228.

Tovar-y-Romo LB, Bumpus NN, Pomerantz D, Avery LB, Sacktor N, McArthur JC*, et al.* (2012). Dendritic spine injury induced by the 8-hydroxy metabolite of efavirenz. *The Journal of pharmacology and experimental therapeutics* **343**(3)**:** 696-703.

Triant VA, Lee H, Hadigan C, Grinspoon SK (2007). Increased acute myocardial infarction rates and cardiovascular risk factors among patients with human immunodeficiency virus disease. *The Journal of clinical endocrinology and metabolism* **92**(7)**:** 2506-2512.

Tripathi P, Agrawal S (2007). Immunobiology of human imunodeficiency virus infection. *Indian journal of medical microbiology* **25**(4)**:** 311-322.

Tsibris AM, Hirsch MS (2010). Antiretroviral therapy in the clinic. *Journal of virology* **84**(11)**:** 5458-5464.

Tsou TC, Tsai FY, Wu MC, Chang LW (2003). The protective role of NF-kappaB and AP-1 in arsenite-induced apoptosis in aortic endothelial cells. *Toxicology and applied pharmacology* **191**(2)**:** 177-187.

Ungvari Z, Gupte SA, Recchia FA, Batkai S, Pacher P (2005). Role of oxidative-nitrosative stress and downstream pathways in various forms of cardiomyopathy and heart failure. *Current vascular pharmacology* **3**(3)**:** 221-229.

Vahlne A (2009). A historical reflection on the discovery of human retroviruses. *Retrovirology* **6:** 40.

Valcour V, Sithinamsuwan P, Letendre S, Ances B (2011). Pathogenesis of HIV in the central nervous system. *Current HIV/AIDS reports* **8**(1)**:** 54-61.

van Wijk SJ, Hageman GJ (2005). Poly(ADP-ribose) polymerase-1 mediated caspase-independent cell death after ischemia/reperfusion. *Free radical biology & medicine* **39**(1)**:** 81-90.

Virag L (2005). Structure and function of poly(ADP-ribose) polymerase-1: role in oxidative stress-related pathologies. *Current vascular pharmacology* **3**(3)**:** 209-214.

Virag L, Szabo C (2002). The therapeutic potential of poly(ADP-ribose) polymerase inhibitors. *Pharmacological reviews* **54**(3)**:** 375-429.

Vitoria M, Granich R, Gilks CF, Gunneberg C, Hosseini M, Were W*, et al.* (2009). The global fight against HIV/AIDS, tuberculosis, and malaria: current status and future perspectives. *American journal of clinical pathology* **131**(6)**:** 844-848.

Vogel M, Schwarze-Zander C, Wasmuth JC, Spengler U, Sauerbruch T, Rockstroh JK (2010). The treatment of patients with HIV. *Deutsches Arzteblatt international* **107**(28-29)**:** 507-515; quiz 516.

Wainberg MA, Jeang KT (2008). 25 years of HIV-1 research - progress and perspectives. *BMC medicine* **6:** 31.

Wang H, Sun J, Goldstein H (2008). Human immunodeficiency virus type 1 infection increases the in vivo capacity of peripheral monocytes to cross the blood-brain barrier into the brain and the in vivo sensitivity of the blood-brain barrier to disruption by lipopolysaccharide. *Journal of virology* **82**(15)**:** 7591-7600.

Widlansky ME, Gokce N, Keaney JF, Jr., Vita JA (2003). The clinical implications of endothelial dysfunction. *Journal of the American College of Cardiology* **42**(7)**:** 1149-1160.

Wong CM, Yung LM, Leung FP, Tsang SY, Au CL, Chen ZY*, et al.* (2008). Raloxifene protects endothelial cell function against oxidative stress. *British journal of pharmacology* **155**(3)**:** 326-334.

Woodcock J, Sharfstein JM, Hamburg M (2010). Regulatory action on rosiglitazone by the U.S. Food and Drug Administration. *The New England journal of medicine* **363**(16)**:** 1489-1491.

Wu CW, Chu ES, Lam CN, Cheng AS, Lee CW, Wong VW*, et al.* (2010). PPARgamma is essential for protection against nonalcoholic steatohepatitis. *Gene therapy* **17**(6)**:** 790-798.

Xie JJ, Yu X, Liao YH, Chen J, Yao R, Chen Y*, et al.* (2009). Poly (ADP-Ribose) polymerase inhibition attenuates atherosclerotic plaque development in ApoE-/- mice with hyperhomocysteinemia. *Journal of atherosclerosis and thrombosis* **16**(5)**:** 641-653.

Xin X, Yang S, Kowalski J, Gerritsen ME (1999). Peroxisome proliferator-activated receptor gamma ligands are potent inhibitors of angiogenesis in vitro and in vivo. *The Journal of biological chemistry* **274**(13)**:** 9116-9121.

Xu S, Zhao Y, Yu L, Shen X, Ding F, Fu G (2011). Rosiglitazone attenuates endothelial progenitor cell apoptosis induced by TNF-alpha via ERK/MAPK and NF-kappaB signal pathways. *Journal of pharmacological sciences* **117**(4)**:** 265-274.

Yen CH, Lau YT (2004). 17beta-Oestradiol enhances aortic endothelium function and smooth muscle contraction in male spontaneously hypertensive rats. *Clinical science* **106**(5)**:** 541-546.

Yoshida H (2007). ER stress and diseases. *The FEBS journal* **274**(3)**:** 630-658.

Yu SW, Wang Y, Frydenlund DS, Ottersen OP, Dawson VL, Dawson TM (2009). Outer mitochondrial membrane localization of apoptosis-inducing factor: mechanistic implications for release. *ASN neuro* **1**(5).

Yu Z, Kuncewicz T, Dubinsky WP, Kone BC (2006). Nitric oxide-dependent negative feedback of PARP-1 trans-activation of the inducible nitric-oxide synthase gene. *The Journal of biological chemistry* **281**(14)**:** 9101-9109.

Yue TL, Nerurkar SS, Bao W, Jucker BM, Sarov-Blat L, Steplewski K*, et al.* (2008). In vivo activation of peroxisome proliferator-activated receptor-delta protects the heart from ischemia/reperfusion injury in Zucker fatty rats. *The Journal of pharmacology and experimental therapeutics* **325**(2)**:** 466-474.

Zalba G, Beaumont J, San Jose G, Fortuno A, Fortuno MA, Diez J (2000). Vascular oxidant stress: molecular mechanisms and pathophysiological implications. *Journal of physiology and biochemistry* **56**(1)**:** 57-64.

Zaremba T, Thomas HD, Cole M, Coulthard SA, Plummer ER, Curtin NJ (2011). Poly(ADP-ribose) polymerase-1 (PARP-1) pharmacogenetics, activity and expression analysis in cancer patients and healthy volunteers. *The Biochemical journal* **436**(3)**:** 671-679.

Zhang K (2010). Integration of ER stress, oxidative stress and the inflammatory response in health and disease. *International journal of clinical and experimental medicine* **3**(1)**:** 33-40.

Zhu M, Flynt L, Ghosh S, Mellema M, Banerjee A, Williams E*, et al.* (2011). Anti-inflammatory effects of thiazolidinediones in human airway smooth muscle cells. *American journal of respiratory cell and molecular biology* **45**(1)**:** 111-119.